EUROPEAN ORGANISATION FOR NUCLEAR RESEARCH (CERN)

Submitted to: JHEP

CERN-EP-2016-194
25th October 2016

Measurement of the ZZ production cross section in proton–proton collisions at $\sqrt{s} = 8$ TeV using the $ZZ \to \ell^-\ell^+\ell'^-\ell'^+$ and $ZZ \to \ell^-\ell^+\nu\bar{\nu}$ decay channels with the ATLAS detector

The ATLAS Collaboration

A measurement of the ZZ production cross section in the $\ell^-\ell^+\ell'^-\ell'^+$ and $\ell^-\ell^+\nu\bar{\nu}$ channels ($\ell = e, \mu$) in proton–proton collisions at $\sqrt{s} = 8$ TeV at the Large Hadron Collider at CERN, using data corresponding to an integrated luminosity of 20.3 fb^{-1} collected by the ATLAS experiment in 2012 is presented. The fiducial cross sections for $ZZ \to \ell^-\ell^+\ell'^-\ell'^+$ and $ZZ \to \ell^-\ell^+\nu\bar{\nu}$ are measured in selected phase-space regions. The total cross section for ZZ events produced with both Z bosons in the mass range 66 to 116 GeV is measured from the combination of the two channels to be 7.3 ± 0.4 (stat) ± 0.3 (syst) $^{+0.2}_{-0.1}$ (lumi) pb, which is consistent with the Standard Model prediction of $6.6^{+0.7}_{-0.6}$ pb. The differential cross sections in bins of various kinematic variables are presented. The differential event yield as a function of the transverse momentum of the leading Z boson is used to set limits on anomalous neutral triple gauge boson couplings in ZZ production.

Contents

1 Introduction

The underlying structure of the Standard Model (SM) in the electroweak sector is the non-abelian $SU(2)_L \times U(1)_Y$ gauge group [1–3] that has been successful in describing features such as the masses of the vector bosons and their couplings to fermions. The production of electroweak gauge boson pairs provides an opportunity to perform precision studies of the electroweak sector by looking for deviations from the predicted total and differential production cross sections, which could be an indication of new resonances or couplings not included in the SM.

In the SM, Z boson pairs may be produced at lowest order via quark–antiquark ($q\bar{q}$) annihilation, as well as through gluon–gluon fusion via a quark loop. In $\sqrt{s} = 8$ TeV proton–proton (pp) collisions, approximately 6% of the predicted total cross section is due to gluon–gluon fusion [4]. A pair of Z bosons may also be produced by the decay of a Higgs boson. Lowest-order Feynman diagrams for SM production of ZZ dibosons are given in Figures 1(a), 1(b) and 1(d) to 1(f). These represent the dominant mechanisms for ZZ diboson production at the Large Hadron Collider (LHC). The self-couplings of the electroweak gauge bosons are fixed by the form of the SM Lagrangian. Consequently, neutral triple gauge couplings such as ZZZ and $ZZ\gamma$ are not present in the SM, making the contribution from the s-channel diagram zero (Figure 1(c)).

In addition to precision tests of the electroweak sector of the SM, ZZ diboson measurements motivate higher-order calculations in perturbative quantum chromodynamics (pQCD) and allow for in-depth tests of pQCD. Production of ZZ dibosons is a background to the SM Higgs boson process and to many searches for physics beyond the SM, and precise knowledge of the cross section is necessary to observe deviations relative to SM predictions.

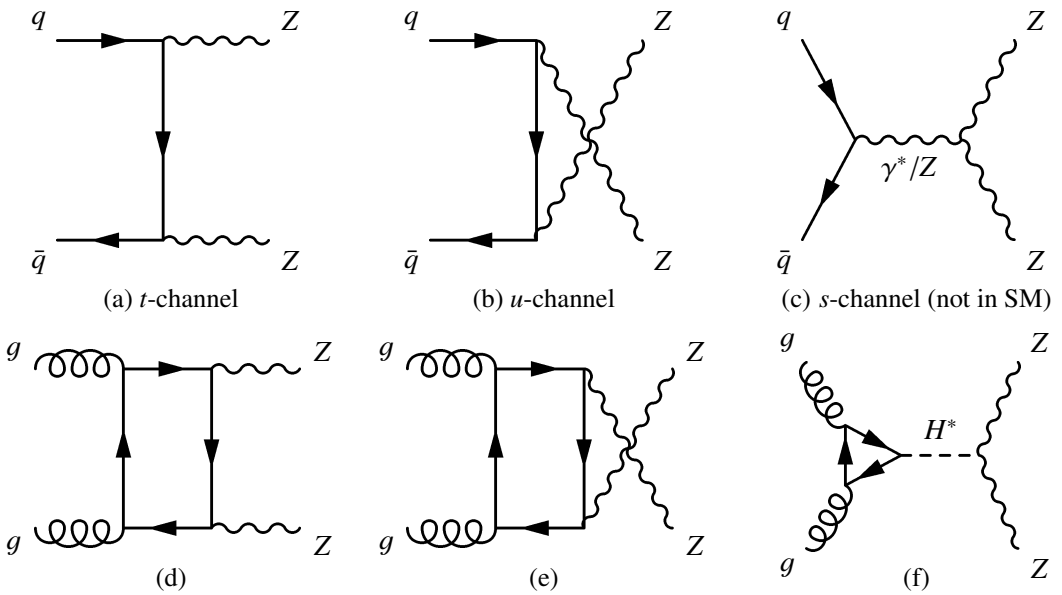

(a) t-channel (b) u-channel (c) s-channel (not in SM)

(d) (e) (f)

Figure 1: Lowest-order Feynman diagrams for ZZ production. The (a) t-channel and (b) u-channel diagrams contribute to ZZ production cross section, while the (c) s-channel diagram is not present in the SM, as it contains a neutral ZZZ or $ZZ\gamma$ vertex. Examples of one-loop contributions to ZZ production via gluon pairs are shown in (d), (e) and (f).

Many extensions to the SM predict new scalar, vector, or tensor particles, which can decay to pairs of electroweak bosons. For example, diboson resonances are predicted in technicolour models [5–8], models with warped extra dimensions [9–11], extended gauge models [12, 13], and grand unified theories [14]. Furthermore, extensions to the SM such as supersymmetry or extra dimensions predict new particles, which can either produce boson pairs directly, in cascade decays, or indirectly via loops. At higher orders, loop contributions involving new particles can lead to effective anomalous neutral triple gauge couplings (aTGCS) as large as 10^{-3} [15]. Any significant deviation in the observed production cross section relative to the SM predictions can indicate a potential source of new physics. Thus, ZZ production is important not only for precision tests of the electroweak sector and pQCD, but also for searches for new physics processes.

This paper presents measurements of the fiducial, total and differential cross sections for ZZ production in pp collisions at a centre-of-mass energy of $\sqrt{s} = 8$ TeV using 20.3 fb^{-1} of data. These have been measured by both the ATLAS [16] and CMS [17] Collaborations at 7 TeV. Recently, the ATLAS Collaboration has measured the fiducial and total cross section for ZZ production at a centre-of-mass energy of $\sqrt{s} = 13$ TeV [18] and the cross section as a function of the invariant mass of the four-lepton system at a centre-of-mass energy of $\sqrt{s} = 8$ TeV [19]. The CMS Collaboration has recently measured the ZZ production cross section at 8 TeV [20].

This paper also presents limits on ZZZ and $ZZ\gamma$ aTGCs within the context of an effective Lagrangian framework [21]. The limits obtained by both ATLAS [16] and CMS [17] using the full 7 TeV data sets are approximately 10 to 20 times stricter than limits set at LEP2 [22] and the Tevatron [23]. More recently, limits on aTGCs have been set by the CMS Collaboration using the full 8 TeV data set of 19.6 fb^{-1} in the $ZZ \to \ell^-\ell^+\ell'^-\ell'^+$ channel ($\ell = e, \mu, \tau$) [20]. CMS has also measured the ZZ production cross section using the $ZZ \to \ell^-\ell^+\nu\bar{\nu}$ decay mode and set limits on aTGCs using the combination of 5 fb^{-1} of data at 7 TeV and 19.6 fb^{-1} of data at 8 TeV [24].

The paper is organized as follows. An overview of the ATLAS detector is given in Section 2. Section 3 defines the phase space in which the cross sections are measured, while Section 4 gives the SM predictions. The simulated signal and background samples used for this analysis are given in Section 5. Data samples, reconstruction of leptons, jets and $E_{\mathrm{T}}^{\mathrm{miss}}$, and event selection for each final state are presented in Section 6. The estimation of background contributions to the $ZZ \to \ell^-\ell^+\ell'^-\ell'^+$ and $ZZ \to \ell^-\ell^+\nu\bar{\nu}$ channels, using a combination of simulation-based and data-driven techniques, is discussed in Section 7. The observed and expected event yields are presented in Section 8, while Section 9 describes the correction factors and detector acceptance for this measurement. Section 10 describes the experimental and theoretical systematic uncertainties considered. Section 11 presents the results of the total and differential cross-section measurements. Limits on aTGCs are discussed in Section 12 in the context of an effective Lagrangian framework. Finally, Section 13 presents the conclusions.

2 The ATLAS detector

The ATLAS detector [25] is a multi-purpose particle physics detector with a forward-backward symmetric cylindrical geometry. It consists of inner tracking devices surrounded by a superconducting solenoid, which provides a 2 T axial magnetic field, electromagnetic and hadronic sampling calorimeters and a muon spectrometer (MS) with a toroidal magnetic field.

The inner detector (ID) provides tracking of charged particles in the pseudorapidity[1] range $|\eta| < 2.5$. It consists of three layers of silicon pixel detectors and eight layers of silicon microstrip detectors surrounded by a straw-tube transition radiation tracker in the region $|\eta| < 2.0$, which contributes to electron identification.

The high-granularity electromagnetic (EM) calorimeter utilizes liquid argon (LAr) as the sampling medium and lead as an absorber, covering the pseudorapidity range $|\eta| < 3.2$. A steel/scintillator-tile calorimeter provides hadronic coverage for $|\eta| < 1.7$. The endcap and forward regions of the calorimeter system, extending to $|\eta| = 4.9$, are instrumented with copper/LAr and tungsten/LAr modules for both the EM and hadronic measurements.

The MS consists of three large superconducting toroids, each comprising eight coils, and a system of trigger chambers and tracking chambers that provide triggering and tracking capabilities in the ranges $|\eta| < 2.4$ and $|\eta| < 2.7$, respectively.

The ATLAS trigger system [26] consists of a hardware-based Level-1 trigger followed by a software-based High-Level Trigger (HLT). It selects events to be recorded for offline analysis, reducing their rate to about 400 Hz.

3 Phase-space definitions

This analysis measures the cross section of ZZ diboson production in a region of kinematic phase space very close to the geometric acceptance of the full detector. Fiducial cross sections are measured for the $e^-e^+e^-e^+$, $e^-e^+\mu^-\mu^+$ and $\mu^-\mu^+\mu^-\mu^+$ final states in the $ZZ \to \ell^-\ell^+\ell'^-\ell'^+$ channel and for the $e^-e^+\nu\bar{\nu}$ and $\mu^-\mu^+\nu\bar{\nu}$ final states in the $ZZ \to \ell^-\ell^+\nu\bar{\nu}$ channel. Final states with leptonic τ decays are not included as signal in any of the final states considered.

The information from each final state in both channels is combined to measure the total ZZ production cross section in a kinematic phase space, referred to as the total phase space, defined by $66 < m_{\ell^-\ell^+} < 116$ GeV, where $m_{\ell^-\ell^+}$ is the invariant mass of each charged lepton pair. Where there is ambiguity in the choice of lepton pairs, the pairing procedure described in Section 6.3.1 is used.

The kinematic properties of final-state electrons and muons include the contributions from final-state radiated photons within a distance in the (η, ϕ) plane of $\Delta R = 0.1$ around the direction of the charged lepton.[2]

3.1 $ZZ \to \ell^-\ell^+\ell'^-\ell'^+$ channel

Three different fiducial phase-space regions are used for the $ZZ \to \ell^-\ell^+\ell'^-\ell'^+$ channel of the analysis, one for each decay mode, and selected to increase the geometric acceptance by using the forward regions of the detector while controlling backgrounds. The Z boson pairs are required to decay to $e^-e^+e^-e^+$, $e^-e^+\mu^-\mu^+$, or $\mu^-\mu^+\mu^-\mu^+$, where the invariant mass of each opposite-sign, same-flavour lepton pair is

[1] ATLAS uses a right-handed coordinate system with its origin at the nominal interaction point (IP) in the centre of the detector and the z-axis along the beam pipe. The x-axis points from the IP to the centre of the LHC ring and the y-axis points upward. Cylindrical coordinates (r,ϕ) are used in the transverse plane, ϕ being the azimuthal angle around the beam pipe. The pseudorapidity is defined in terms of the polar angle θ as $\eta = -\ln[\tan(\theta/2)]$.

[2] Angular separations between particles or reconstructed objects are measured in the (η, ϕ) plane using $\Delta R = \sqrt{(\Delta\phi)^2 + (\Delta\eta)^2}$.

required to be within $66 < m_{\ell^-\ell^+} < 116$ GeV. The transverse momentum, p_{T}, of each lepton must be at least 7 GeV. In the $\mu^-\mu^+\mu^-\mu^+$ decay mode, the muons must fall within a pseudorapidity range $|\eta| < 2.7$. In the $e^-e^+e^-e^+$ decay mode, three electrons are required to have $|\eta| < 2.5$ and the fourth electron is required to lie in the pseudorapidity range $|\eta| < 4.9$. In the $e^-e^+\mu^-\mu^+$ decay mode, both muons are required to be within $|\eta| < 2.7$, while for the electrons, one electron must be central ($|\eta| < 2.5$), while the second must fall within $|\eta| < 4.9$. The minimum angular separation between any two of the four charged leptons must be $\Delta R > 0.2$.

3.2 $ZZ \to \ell^-\ell^+\nu\bar{\nu}$ channel

The fiducial phase space for the $ZZ \to \ell^-\ell^+\nu\bar{\nu}$ channel is defined by requiring one Z boson to decay to neutrinos (invisible) and one Z boson to decay to an e^-e^+ or $\mu^-\mu^+$ pair. The invariant mass of the charged lepton pair must lie within $76 < m_{\ell^-\ell^+} < 106$ GeV. Each charged lepton used to form Z candidates must have transverse momentum $p_{\mathrm{T}} > 25$ GeV and $|\eta| < 2.5$. The charged leptons must be separated by more than $\Delta R = 0.3$. The axial missing transverse momentum in the event (axial-$E_{\mathrm{T}}^{\mathrm{miss}}$), which expresses the projection of the transverse momentum of the neutrino pair of the invisibly decaying Z boson ($\vec{p}_{\mathrm{T}}^{\,\nu\bar{\nu}}$) onto the direction of the transverse momentum of the Z boson decaying to charged leptons ($\vec{p}_{\mathrm{T}}^{\,Z}$), is defined as $-p_{\mathrm{T}}^{\nu\bar{\nu}} \cdot \cos(\Delta\phi(\vec{p}_{\mathrm{T}}^{\,\nu\bar{\nu}}, \vec{p}_{\mathrm{T}}^{\,Z}))$. The axial-$E_{\mathrm{T}}^{\mathrm{miss}}$ is required to be greater than 90 GeV. The p_{T}-balance between the two Z bosons, defined as $|p_{\mathrm{T}}^{\nu\bar{\nu}} - p_{\mathrm{T}}^{Z}|/p_{\mathrm{T}}^{Z}$, must be less than 0.4. There must be no particle-level jets with $p_{\mathrm{T}} > 25$ GeV, $|\eta| < 4.5$ and each jet must have a minimum distance of $\Delta R = 0.3$ from any prompt electron. Particle-level jets are constructed from stable particles with a lifetime of $\tau > 30$ ps, excluding muons and neutrinos, using the anti-k_t algorithm [27] with a radius parameter of $R = 0.4$.

The definitions of the fiducial phase space for each of the five ZZ final states under study are summarized in Table 1.

Fiducial Phase Space					
Selection	$e^-e^+e^-e^+$	$\mu^-\mu^+\mu^-\mu^+$	$e^-e^+\mu^-\mu^+$	$e^-e^+\nu\bar{\nu}$	$\mu^-\mu^+\nu\bar{\nu}$
Lepton p_{T}	> 7 GeV			> 25 GeV	
Lepton $\|\eta\|$	$\|\eta\|_{e_1,e_2,e_3} < 2.5$ $\|\eta\|_{e_4} < 4.9$	$\|\eta\|_{\mu} < 2.7$	$\|\eta\|_{e_1} < 2.5$, $\|\eta\|_{e_2} < 4.9$ $\|\eta\|_{\mu} < 2.7$	$\|\eta\|_{e} < 2.5$	$\|\eta\|_{\mu} < 2.5$
$\Delta R(\ell, \ell')$	> 0.2			> 0.3	
$m_{\ell^-\ell^+}$	$66 < m_{\ell^-\ell^+} < 116$ GeV			$76 < m_{\ell^-\ell^+} < 106$ GeV	
Axial-$E_{\mathrm{T}}^{\mathrm{miss}}$	-			> 90 GeV	
p_{T}-balance	-			< 0.4	
Jet veto	-			$p_{\mathrm{Tjet}} > 25$ GeV, $\|\eta\|_{\mathrm{jet}} < 4.5$, and $\Delta R(e, \mathrm{jet}) > 0.3$	

Table 1: Fiducial phase-space definitions for each of the five ZZ final states under study.

4 Standard Model predictions

The fiducial and total cross-section predictions for SM ZZ production reported in this paper are evaluated with PowHegBox [28, 29] at next-to-leading order (NLO) in QCD and are supplemented with predictions from `gg2VV` [30, 31] to account for ZZ production via gluon–gluon fusion at leading order (LO) in the

gluon-induced process. Interference effects with SM Higgs boson production via gluon–gluon fusion as well as off-shell Higgs boson production effects are considered, based on recent calculations [31]. The contribution of the gluon–gluon initial state to the fiducial cross sections is about 6% for the $ZZ \to \ell^-\ell^+\ell'^-\ell'^+$ channel and about 3% for the $ZZ \to \ell^-\ell^+\nu\bar{\nu}$ channel. All computations are performed using dynamic renormalization and factorization scales (μ_R and μ_F) equal to the invariant mass of the ZZ system (m_{ZZ}) as the baseline, and the CT10 parton distribution function (PDF) set [32].

The results from PowHegBox are corrected for virtual NLO electroweak (EW) effects [33], applied as reweighting factors on an event-by-event basis, following the method described in Ref. [34]. As a result, the fiducial cross-section predictions for the $ZZ \to \ell^-\ell^+\ell'^-\ell'^+$ and $ZZ \to \ell^-\ell^+\nu\bar{\nu}$ channels are reduced by 4% and 9% respectively.

$\sigma^{\text{fid}}_{ZZ\to e^-e^+e^-e^+}$	=	$6.2\ ^{+0.6}_{-0.5}$	fb
$\sigma^{\text{fid}}_{ZZ\to e^-e^+\mu^-\mu^+}$	=	$10.8\ ^{+1.1}_{-1.0}$	fb
$\sigma^{\text{fid}}_{ZZ\to \mu^-\mu^+\mu^-\mu^+}$	=	$4.9\ ^{+0.5}_{-0.4}$	fb
$\sigma^{\text{fid}}_{ZZ\to e^-e^+\nu\bar{\nu}}$	=	3.7 ± 0.3	fb
$\sigma^{\text{fid}}_{ZZ\to \mu^-\mu^+\nu\bar{\nu}}$	=	3.5 ± 0.3	fb
$\sigma^{\text{total}}_{pp\to ZZ}$	=	$6.6\ ^{+0.7}_{-0.6}$	pb

Table 2: Predicted fiducial and total ZZ production cross sections. The considered systematic uncertainties and the accuracy in pertubation theory are detailed in the text.

The SM predictions for the fiducial and total ZZ production cross sections in the regions defined in Section 3 and including the EW corrections are summarized in Table 2. The systematic uncertainties shown in the table include a PDF uncertainty of $^{+4.2\%}_{-3.3\%}$ [35] applied to the results from both the PowHegBox and `gg2VV` generators. For the PowHegBox contribution, a scale uncertainty of $^{+3.1\%}_{-2.3\%}$ [35] is included. For the gluon–gluon fusion contribution, recent publications [36–38] suggest an increase of the ZZ production cross section by up to a factor of about two, when the calculation is performed at higher orders in QCD. This calculation is sensitive to the choice of PDF set and even more to the μ_R and μ_F scales. As this correction is not available differentially for all distributions and all final states analysed in this paper, no reweighting is applied to the prediction of `gg2VV`. In order to account for these higher-order QCD effects, the scale uncertainty for `gg2VV` is set to ±60%. PDF and scale uncertainties are added linearly following the recommendation of Ref. [39]. The jet veto uncertainty obtained using the Stewart and Tackmann method [40] is shown in Table 8 and is added in quadrature to the systematic uncertainty of the fiducial cross sections for each $ZZ \to \ell^-\ell^+\nu\bar{\nu}$ final state. This approach is conservative and it covers further uncertainties from higher-order QCD effects.

The contribution to the cross section predicted with PowHegBox is known to increase by approximately 5% when considering NNLO QCD effects [41, 42]. This enhancement is not considered in the theoretical prediction used in this paper.

5 Simulated event samples

Simulated samples [43] are used to correct the measured distributions for detector effects and acceptance and to determine or validate some background contributions. Production and subsequent decays of ZZ pairs are simulated using PowhegBox at NLO in the $q\bar{q}$ process, and `gg2VV` at LO in the gluon-induced process, both interfaced to Pythia 8 [44] for parton showering and underlying-event modelling, with the CT10 PDF set. In each case, the simulation includes the interference terms between the Z and γ^* diagrams. The NLO EW corrections are applied to the PowhegBox predictions as explained in the previous section.

Moreover, the PowhegBox generator interfaced to Herwig [45] and Jimmy [46] is used to estimate systematic uncertainties due to the choice of parton shower and underlying-event modelling. The LO multi-leg generator Sherpa [47] with the CT10 PDF set is used to assign systematic uncertainties due to the choice of event generator as well as to generate signal samples with ZZZ and $ZZ\gamma$ aTGCs.

The LO generator Alpgen [48] using the CTEQ6L1 PDFs [49] and interfaced to Pythia [50] is used to simulate Z+jets and W+jets background samples. The same generator interfaced to Herwig is used to model the $W\gamma$ process. The diboson production processes WW and WZ are generated with PowhegBox interfaced to Pythia 8 using the CT10 PDFs. Top quark pair production ($t\bar{t}$) is simulated with MC@NLO [51] using the CT10 PDFs. Single-top production, including Wt production, is modelled with MC@NLO [52], interfaced to Herwig, and AcerMC [53] using the CTEQ6L1 PDFs. The LO generator MadGraph [54] using the CTEQ6L1 PDFs is used to model the ZZZ^*, ZWW^* and $t\bar{t}Z$ processes. Events with two hard interactions in a pp collision (double proton interactions, DPI) that each produce a Z boson decaying to leptons are simulated using Pythia 8 with the CTEQ6L1 PDF set.

The signal and background generated Monte Carlo (MC) samples are passed through the ATLAS detector simulation [43] based on GEANT4 [55]. Additional inelastic pp interactions (pile-up) are included in the simulation. The MC events are reweighted to reproduce the distribution of the mean number of interactions per bunch crossing observed in data.

6 Data samples, reconstruction of leptons, jets, and $E_{\mathrm{T}}^{\mathrm{miss}}$ and event selections

6.1 Data samples

The measurement presented in this paper uses the full data set of pp collisions at a centre-of-mass energy of $\sqrt{s} = 8$ TeV collected with the ATLAS detector at the LHC in 2012. The data corresponds to a total integrated luminosity of $20.3\,\mathrm{fb}^{-1}$, with an uncertainty of 1.9% [56]. The absolute luminosity scale and its uncertainty are derived from beam-separation scans performed in November 2012. All events were required to satisfy basic quality criteria indicating stable beams and good operating characteristics of the detector during data taking. The data analysed were selected using single-lepton triggers [57, 58] with isolation requirements and thresholds of 24 GeV for the transverse momentum (energy) of muons (electrons).

During each bunch crossing, several pp collisions take place, which results in multiple vertices being reconstructed. To ensure that the objects analysed originate from the products of the hard-scattered pp

collision, and to reduce contamination from cosmic rays, the primary vertex is chosen to be the vertex with the highest sum of the squared transverse momenta of the associated ID tracks.

6.2 Reconstruction of leptons, jets, and $E_{\mathrm{T}}^{\mathrm{miss}}$

Muon candidates are identified by tracks, or track segments, reconstructed in the MS and matched to tracks reconstructed in the ID [59]. Muons within $|\eta| < 2.5$ are referred to as "central muons". Muons within $2.5 < |\eta| < 2.7$, where there is no ID coverage and they are reconstructed only in the MS, are referred to as "forward muons". In order to recover efficiency at $|\eta| < 0.1$ where ϕ coverage in the MS is reduced due to mechanical supports and services, "calorimeter-tagged" muons are reconstructed using calorimeter energy deposits to tag ID tracks. In the $ZZ \to \ell^-\ell^+\ell'^-\ell'^+$ channel all three types of muons, "central" with $p_{\mathrm{T}} > 7$ GeV, "forward" with $p_{\mathrm{T}} > 10$ GeV and "calorimeter-tagged" with $p_{\mathrm{T}} > 20$ GeV are used, while in the $ZZ \to \ell^-\ell^+\nu\bar{\nu}$ channel, only "central" muons with $p_{\mathrm{T}} > 25$ GeV are used. For muons with a track in the ID ("central" and "calorimeter-tagged" muons), the ratio of the transverse impact parameter, d_0, with respect to the primary vertex, to its uncertainty (d_0 significance), must be smaller than 3.0 and the longitudinal impact parameter, $|z_0| \times \sin\theta$, must be less than 0.5 mm. Isolated muons are then selected based on track or calorimeter requirements. Track isolation is imposed on "central" and "calorimeter-tagged" muons, by requiring the scalar sum of the p_{T} of the tracks originating from the primary vertex inside a cone of size $\Delta R = 0.2$ around the muon to be less than 15% of the muon p_{T}. Similarly, calorimeter isolation requires the sum of the calorimeter transverse energy in a cone of size $\Delta R = 0.2$ around the muon candidate to be less than 15% of the muon p_{T}. For the $ZZ \to \ell^-\ell^+\nu\bar{\nu}$ channel, both track and calorimeter isolation are imposed on muons, while for the $ZZ \to \ell^-\ell^+\ell'^-\ell'^+$ channel, for "central" muons, calorimeter isolation is not required, as it does not offer any extra background rejection, and for "forward" muons, where track isolation is not possible, only calorimeter isolation is required.

Electron candidates in the central region are reconstructed from energy clusters in the calorimeter matched to an ID track [60]. The lateral and transverse shapes of the cluster must be consistent with those of an electromagnetic shower. The transverse energy of the electron, E_{T}, must be greater than 7 GeV for the $ZZ \to \ell^-\ell^+\ell'^-\ell'^+$ channel and greater than 25 GeV for the $ZZ \to \ell^-\ell^+\nu\bar{\nu}$ channel, while the pseudorapidity of the electromagnetic cluster for both channels must be $|\eta| < 2.47$. To ensure that electron candidates originate from the primary vertex, the d_0 significance of the electron must be smaller than 6.0 and the longitudinal impact parameter, $|z_0| \times \sin\theta$, must be less than 0.5 mm. The electron candidates must be isolated; therefore, the scalar sum of the transverse momentum of all the tracks inside a cone of size $\Delta R = 0.2$ around the electron must be less than 15% of the p_{T} of the electron. Calorimeter isolation requires the total transverse energy, E_{T}, corrected for pile-up effects in an isolation cone of size $\Delta R = 0.2$ to be less than 15% of the electron p_{T} and is required only for the $ZZ \to \ell^-\ell^+\nu\bar{\nu}$ channel.

To further increase the detector acceptance in the $ZZ \to \ell^-\ell^+\ell'^-\ell'^+$ channel, "forward" electrons are used, extending the pseudorapidity coverage to $2.50 < |\eta| < 3.16$ and $3.35 < |\eta| < 4.90$ [61]. These "forward" electrons have $E_{\mathrm{T}} > 20$ GeV, without any track or calorimeter isolation requirements. Beyond $|\eta| = 2.5$ there is no ID coverage for tracking, so these electrons are reconstructed from calorimeter information alone. No calorimeter isolation is used for electrons in this region as the calorimeter segmentation is too coarse.

The missing transverse momentum, with magnitude $E_{\mathrm{T}}^{\mathrm{miss}}$, is defined as the negative vector sum of the transverse momenta of reconstructed muons, electrons, and jets as well as calorimeter cells not associated

to objects. Calorimeter cells are calibrated to the jet energy scale (JES) if they are associated with a jet and to the electromagnetic energy scale otherwise [62].

Jets are reconstructed using the anti-k_t algorithm [27] with a radius parameter $R = 0.4$, using topological clusters of energy deposition in the calorimeter. Jets arising from detector noise or non-collision events are rejected. The jet energy is corrected to account for detector and pile-up effects and is calibrated to account for the different response of the calorimeters to electrons and hadrons, using a combination of simulations and in situ techniques [63–65]. In order to reject jets from pile-up, the summed scalar p_{T} of tracks associated with both the jet and the primary vertex is required to be greater than 50% of the summed scalar p_{T} of all tracks associated with the jet. This criterion is only applied to jets with $p_{\mathrm{T}} < 50$ GeV and $|\eta| < 2.4$. Jets used in this analysis are required to have $|\eta| < 4.5$ and $p_{\mathrm{T}} > 25$ GeV. Jets that are within $\Delta R = 0.3$ to an electron or muon that passes the selection requirements are not considered in the analysis.

6.3 Event selection

6.3.1 $ZZ \to \ell^-\ell^+\ell'^-\ell'^+$ selection

The $ZZ \to \ell^-\ell^+\ell'^-\ell'^+$ events are characterized by two pairs of oppositely charged, same-flavour leptons. Events fall into three categories: $e^-e^+e^-e^+$, $e^-e^+\mu^-\mu^+$ and $\mu^-\mu^+\mu^-\mu^+$. Selected events are required to have exactly four isolated leptons above the p_{T} threshold. At least one lepton with $p_{\mathrm{T}} > 25$ GeV must be matched to a trigger object. In the $e^-e^+e^-e^+$ and $\mu^-\mu^+\mu^-\mu^+$ decay modes, there is an ambiguity when pairing leptons to form Z candidates. A pairing procedure to form the candidates is used, which minimizes the quantity $|m_{\ell^-\ell^+} - m_Z| + |m_{\ell'^-\ell'^+} - m_Z|$, where $m_{\ell^-\ell^+}$, and $m_{\ell'^-\ell'^+}$ are the invariant masses of the two lepton pairs of a given pairing from the quadruplet, and m_Z is the Z mass [66]. The two Z candidates must have masses in the range $66 < m_{\ell^-\ell^+} < 116$ GeV. All leptons are required to be separated by $\Delta R > 0.2$. Each event is allowed to have a maximum of one extension lepton per category (forward electron, forward muon, or calorimeter-tagged muon) and each lepton pair may only have one extension lepton. In this way, an event must contain at least two central leptons and may contain two extension leptons of different types, as long as they are each paired with a central lepton. Events with a forward electron have the additional requirement that the central electron that is paired with the forward electron must have a transverse momentum of at least 20 GeV instead of 7 GeV.

6.3.2 $ZZ \to \ell^-\ell^+\nu\bar{\nu}$ selection

In the $ZZ \to \ell^-\ell^+\nu\bar{\nu}$ channel, final states with electron or muon pairs and large $E_{\mathrm{T}}^{\mathrm{miss}}$ are considered. Candidate events must have exactly two opposite-sign, same-flavour isolated leptons of $p_{\mathrm{T}} > 25$ GeV. At least one of the two leptons must be matched to a trigger object. The invariant mass of the leptons must be in the range $76 < m_{\ell^-\ell^+} < 106$ GeV. The mass-window requirement is stricter than in the $ZZ \to \ell^-\ell^+\ell'^-\ell'^+$ channel in order to suppress backgrounds, which could produce real or fake lepton pairs close to the Z mass. Leptons are also required to have an angular separation of $\Delta R > 0.3$. The selection of $ZZ \to \ell^-\ell^+\nu\bar{\nu}$ candidate events requires that the $\vec{E}_{\mathrm{T}}^{\mathrm{miss}}$ be highly anti-collinear with the $\vec{p}_{\mathrm{T}}$ of the Z candidate decaying to charged leptons. The quantity used is referred to as axial-$E_{\mathrm{T}}^{\mathrm{miss}}$ and is given by $-E_{\mathrm{T}}^{\mathrm{miss}} \cdot \cos(\Delta\phi(\vec{E}_{\mathrm{T}}^{\mathrm{miss}}, \vec{p}_{\mathrm{T}}^{Z}))$, where $\vec{p}_{\mathrm{T}}^{Z}$ is the transverse momentum of the Z candidate. The axial-$E_{\mathrm{T}}^{\mathrm{miss}}$ is required to be above 90 GeV. This requirement is particularly effective in removing Z +jets background,

as mismeasured $E_{\mathrm{T}}^{\mathrm{miss}}$ would in general not have the $\vec{E}_{\mathrm{T}}^{\mathrm{miss}}$ anti-parallel to the $\vec{p}_{\mathrm{T}}$ of the Z candidate. The p_{T}-balance, defined by $|E_{\mathrm{T}}^{\mathrm{miss}} - p_{\mathrm{T}}^{Z}|/p_{\mathrm{T}}^{Z}$, is required to be less than 0.4 in order to distinguish the signal $ZZ \to \ell^-\ell^+\nu\bar{\nu}$ from the background, such as Z + jets. In order to suppress the $t\bar{t}$ and single-top-quark backgrounds, events are required not to have any reconstructed jet with $p_{\mathrm{T}} > 25$ GeV and $|\eta| < 4.5$. This requirement is referred to as the "jet veto". Finally, to suppress WZ background, a veto on a third electron (muon) with $p_{\mathrm{T}} > 7$ GeV (6 GeV) is applied.

7 Background estimation

7.1 $ZZ \to \ell^-\ell^+\ell'^-\ell'^+$ backgrounds

Backgrounds to the $ZZ \to \ell^-\ell^+\ell'^-\ell'^+$ channel are events in which four objects identified as isolated, prompt leptons have paired-lepton invariant masses in the signal region $66 < m_{\ell^-\ell^+} < 116$. The leptons of background events in the $ZZ \to \ell^-\ell^+\ell'^-\ell'^+$ channel can either be "true" leptons from the decays of Z bosons, $W^{\pm}$ bosons, or top quarks or they can be "fake" leptons that are defined as jets which are misidentified as leptons or leptons that come from hadronic decays. Background events in which all four leptons are true leptons are called the "irreducible background" as these events have the same signature as the signal events in this channel. In the SM, there are few final states with significant cross sections that can produce four true leptons. The largest sources of irreducible backgrounds are $t\bar{t}Z$ and ZZZ^*/ZWW^* production and events with DPI that separately produce Z bosons that each decay to two leptons. The contributions from each of these background sources are estimated from MC simulations that have been scaled to 20.3 fb^{-1} and can be found in Table 3. The systematic uncertainty for the irreducible background is neglected. The cross sections for these processes are much smaller than for the signal, and their overall contribution to the total background is small.

Source	$e^-e^+e^-e^+$	$\mu^-\mu^+\mu^-\mu^+$	$e^-e^+\mu^-\mu^+$	$\ell^-\ell^+\ell'^-\ell'^+$
ZZZ^*/ZWW^*	0.12 ± 0.01	0.19 ± 0.01	0.28 ± 0.02	0.58 ± 0.02
DPI	0.13 ± 0.01	0.15 ± 0.01	0.29 ± 0.01	0.57 ± 0.02
$t\bar{t}\,Z$	0.15 ± 0.03	0.16 ± 0.03	0.35 ± 0.05	0.66 ± 0.07
Total irreducible background	0.40 ± 0.04	0.50 ± 0.04	0.93 ± 0.05	1.82 ± 0.08

Table 3: Number of events from the irreducible background SM sources that can produce four true leptons scaled to 20.3 fb^{-1}. The full event selection is applied along with all corrections and scale factors. The errors shown are statistical only.

Background events containing one or more fake leptons, constitute the "reducible background". The dominant reducible background contributions to $ZZ \to \ell^-\ell^+\ell'^-\ell'^+$ production are Z + jets, WW + jets, and top quark ($t\bar{t}$ and single-top quark) events in which two prompt leptons are paired with two jets or leptons from a heavy-flavour decay which are misidentified as isolated leptons. Additional background arises from WZ+jets events containing three true leptons and one fake lepton. To estimate backgrounds containing fake leptons, the data-driven method employed in the ATLAS measurement at 7 TeV [16] is used and only a summary of the relevant parameters is given here.

The data-driven background estimate requires identifying events with two or three selected leptons, with the remaining leptons satisfying a relaxed set of criteria. The relaxed set of criteria is defined for each

Ingredients in Eq. 1	$e^-e^+e^-e^+$	$\mu^-\mu^+\mu^-\mu^+$	$e^-e^+\mu^-\mu^+$	Combined ($\ell^-\ell^+\ell'^-\ell'^+$)
$(+)N_{\text{data}}(\ell\ell\ell j) \times f$	8.6 ± 0.7	4.8 ± 2.4	16.0 ± 3.5	29.3 ± 4.3
$(-)N_{ZZ}(\ell\ell\ell j) \times f$	0.58 ± 0.01	1.96 ± 0.02	2.82 ± 0.02	5.36 ± 0.03
$(-)N_{\text{data}}(\ell\ell jj) \times f^2$	3.6 ± 0.1	1.0 ± 0.4	4.1 ± 0.6	8.8 ± 0.8
$(+)N_{ZZ}(\ell\ell jj) \times f^2$	0.00 ± 0.01	0.02 ± 0.08	0.02 ± 0.02	0.04 ± 0.02
Background estimate, N(BG)	4.4 ± 0.7 (stat) ± 2.8 (syst)	1.8 ± 2.4 (stat) ± 0.9 (syst)	9.0 ± 3.6 (stat) ± 3.9 (syst)	15.2 ± 4.4 (stat) ± 7.1 (syst)

Table 4: The number of ZZ background events from sources with fake leptons estimated using the data-driven fake-factor method in 20.3 fb^{-1} of data. The uncertainties quoted are statistical only, unless otherwise indicated, and combine the statistical uncertainty in the number of observed events of each type and the statistical uncertainty in the associated fake factor. The systematic uncertainty is shown for the background estimate in each final state.

lepton type. For muons, the relaxed criteria give fully selected muons except that they either fail the isolation requirement or fail the impact parameter requirement but not both. For electrons with $|\eta| < 2.47$, the relaxed criteria give clusters in the electromagnetic calorimeter matched to ID tracks that fail either the strict identification requirement or the isolation requirement but not both. For electrons with $|\eta| > 2.5$, the relaxed criteria give electromagnetic clusters that are reconstructed as electrons but fail the identification requirement. All events are otherwise required to satisfy the full event selection.

The expected number of reducible background $\ell^-\ell^+\ell'^-\ell'^+$ events, N(BG), is calculated as:

$$N(\text{ BG}) = [N_{\text{data}}(\ell\ell\ell j) - N_{ZZ}(\ell\ell\ell j)] \times f - [N_{\text{data}}(\ell\ell jj) - N_{ZZ}(\ell\ell jj)] \times f^2 \quad (1)$$

where double counting from $\ell\ell\ell j$ and $\ell\ell jj$ events is accounted for, and the terms $N_{ZZ}(\ell\ell\ell j)$ and $N_{ZZ}(\ell\ell jj)$ are MC estimates correcting for contributions from signal $ZZ \to \ell^-\ell^+\ell'^-\ell'^+$ events having one or two real leptons that instead satisfy the relaxed lepton selection criteria (j).

The factor f is calculated as a function of the p_{T} and η of the fake lepton and is the ratio of the probability for a fake lepton to satisfy the full lepton selection criteria to the probability of the fake lepton only satisfying the relaxed lepton criteria. It is measured in a control sample of data events that contains a Z boson candidate consisting of a pair of isolated same-flavour opposite-sign electrons or muons. In these events, f is measured using the leptons and relaxed leptons not assigned to the Z boson and is found to vary from 0.082 ± 0.001 (0.33 ± 0.01) for $p_{\text{T}} < 10$ GeV to 0.027 ± 0.001 (0.72 ± 0.11) for $p_{\text{T}} > 40$ GeV for electrons (muons). The quoted uncertainties are statistical. The weighted number of data events for each of the ingredients in Equation (1) can be found in Table 4.

The systematic uncertainty in the reducible background is estimated using two additional and independent methods. The maximum difference between each additional estimate and the nominal estimate is taken as the systematic uncertainty. The first additional method is to count the number of events in data with one pair of opposite-sign, same-flavour leptons and another pair of same-sign, same-flavour leptons ($\ell^+\ell^-\ell'^\pm\ell'^\pm$) that satisfy the complete selection criteria while subtracting the number of ZZ events that have one lepton with misidentified charge from MC simulation. The second additional method removes the parameterization of the factor f in p_{T} and η and uses Equation (1) to recalculate the background estimate. The systematic uncertainty is estimated to be ±2.8 events (63%) in the $e^-e^+e^-e^+$final state, ±0.9 events (48%) in the $\mu^-\mu^+\mu^-\mu^+$final state, ±3.9 events (43%) in the $e^-e^+\mu^-\mu^+$final state and ±7.1 events (46%) in the combined $\ell^-\ell^+\ell'^-\ell'^+$channel.

7.2 $ZZ \to \ell^-\ell^+\nu\bar{\nu}$ backgrounds

The main background sources for the $ZZ \to \ell^-\ell^+\nu\bar{\nu}$ channel are processes with two true isolated leptons and $E_{\mathrm{T}}^{\mathrm{miss}}$ in the event. Such processes can be diboson WZ events, as well as $ZZ \to \ell^-\ell^+\ell'^-\ell'^+$, $t\bar{t}$, W^-W^+, Wt, $ZZ \to \tau\tau\nu\nu$ and $Z \to \tau^-\tau^+$. Additionally, processes such as the production of a Z or a W boson in association with jets (Z + jets, W+ jets), as well as multijets, may satisfy the $ZZ \to \ell^-\ell^+\nu\bar{\nu}$ event selection criteria and contribute to the background. The backgrounds from diboson WZ and $ZZ \to \ell^-\ell^+\ell'^-\ell'^+$ production are estimated from MC simulations, while, for all other background sources mentioned above, a combination of data-driven techniques and MC simulation is used for their estimation.

7.2.1 Backgrounds from leptonic WZ decays and $ZZ \to \ell^-\ell^+\ell'^-\ell'^+$ decays

Background events with multiple true isolated leptons may be WZ events in which both bosons decay leptonically and one of the three leptons is not reconstructed in the detector, and $ZZ \to \ell^-\ell^+\ell'^-\ell'^+$ events in which two of the four leptons are not reconstructed. After all selections, the WZ events constitute the dominant background for the $ZZ \to \ell^-\ell^+\nu\bar{\nu}$ channel. Although this background is estimated only from MC simulation, the simulation is validated using events in dedicated control regions, eee, $\mu\mu\mu$, $\mu\mu e$ and $ee\mu$, in which a third lepton is required in addition to the full selection criteria. No significant difference between data and MC simulation is observed in the three-lepton control regions and therefore no scaling is applied to the MC prediction in the signal region. The background due to WZ events is estimated to be 16.7 ± 1.1(stat) ± 1.7(syst) events in the $e^-e^+\nu\bar{\nu}$ final state and 18.5 ± 1.0(stat) ± 1.5(syst) events in the $\mu^-\mu^+\nu\bar{\nu}$ final state, and constitutes more than 50% of the total background. The background due to $ZZ \to \ell^-\ell^+\ell'^-\ell'^+$ is small, contributing less than 2% to the total background as shown in Table 5. The dominant uncertainties of this background source are theoretical, followed by uncertainties in the reconstruction correction factors applied to the simulated events. The dominant theoretical uncertainty is in the choice of QCD scale (about 7%), while the PDF uncertainties are less than 1%.

7.2.2 Backgrounds from $t\bar{t}$, W^-W^+, Wt, $ZZ \to \tau\tau\nu\nu$ and $Z \to \tau^-\tau^+$

The background contribution from these processes is measured by extrapolating from a control region formed by events with one electron and one muon (instead of two electrons or two muons), which otherwise satisfy the full $ZZ \to \ell^-\ell^+\nu\bar{\nu}$ selection. This $e\mu$ region is free from signal events. The extrapolation from the $e\mu$ control region to the ee or $\mu\mu$ signal regions takes into account the relative branching fractions ($2 : 1 : 1$ for $e\mu : ee : \mu\mu$), as well as the ratio of the efficiencies ϵ_{ee} or $\epsilon_{\mu\mu}$, for the ee or $\mu\mu$ selections to the efficiency $\epsilon_{e\mu}$ for the $e\mu$ selection. These efficiency ratios are not equal to unity because of the difference in electron and muon reconstruction and trigger efficiencies [16]. This background is estimated to be 13.3 ± 3.2(stat) ± 0.2(syst) events in the $e^-e^+\nu\bar{\nu}$ final state and 15.4 ± 3.6(stat) ± 0.3(syst) events in the $\mu^-\mu^+\nu\bar{\nu}$ final state, and accounts for the 41% and 46% of the total background in the $e^-e^+\nu\bar{\nu}$ and $\mu^-\mu^+\nu\bar{\nu}$ final states, respectively. The dominant uncertainty for these background contributions is statistical because of the limited number of events in the control region, while additional uncertainties are due to systematic uncertainties in the normalization of the simulated samples used to correct the $e\mu$ contribution in data and the systematic uncertainty in the efficiency correction factors.

7.2.3 W+jets and multijet background

Leptons originating from semileptonic decays of heavy-flavour hadrons may also contribute in the electron or muon final states. However, this background is highly suppressed because of the dilepton mass requirement in the signal selection. The W+jets and multijet background is estimated using the "matrix method" technique [67]. The fraction of events in the signal region that contain at least one fake lepton is estimated by extrapolating from a background-dominated control region to the signal region using factors measured in data. The contribution of this background to the total background is 8% in the $e^-e^+\nu\bar{\nu}$ final state and negligible in the $\mu^-\mu^+\nu\bar{\nu}$ final state. The dominant systematic uncertainty for this background is due to the uncertainty in the extrapolation factors and the limited number of events in the control regions.

7.2.4 Z+jets background

Occasionally, events with one Z boson produced in association with jets or with a photon (Z+jets, or $Z+\gamma$) may mimic signal events if they have large $E_{\mathrm{T}}^{\mathrm{miss}}$ due to the mismeasurement of the jets or the photon. This background of events with a Z boson and jets is estimated by selecting events in data with a high-p_{T} photon and jets, and reweighting these events to account for differences in the Z boson and photon p_{T} spectra and reconstruction efficiencies. These weights are determined in a low-$E_{\mathrm{T}}^{\mathrm{miss}}$ control region. To remove contamination to single-photon events, subtraction of non-(γ + jet) events (e.g. $Z(\rightarrow \nu\bar{\nu}) + \gamma$) is performed. The full signal selection is applied to the single-photon plus jets events, and the background is estimated by reweighting these events using weights determined from the low-$E_{\mathrm{T}}^{\mathrm{miss}}$ control region. The procedure is repeated in bins of p_{T}^{Z} in order to obtain the p_{T} distribution of the Z+jets and $Z + \gamma$ backgrounds. As shown in Table 5, this background is negligible in both the $e^-e^+\nu\bar{\nu}$ and $\mu^-\mu^+\nu\bar{\nu}$ final states. The dominant uncertainty for this background is due to the statistical uncertainty of non-(γ+jet) events, which are subtracted from the γ+ jets sample.

7.2.5 Background summary for $ZZ \rightarrow \ell^-\ell^+\nu\bar{\nu}$

A summary of both the simulation-based and data-driven backgrounds in the $ZZ \rightarrow \ell^-\ell^+\nu\bar{\nu}$ channel is given in Table 5. The largest background contributions come from WZ and $t\bar{t}$, W^-W^+, Wt, $ZZ \rightarrow \tau\tau\nu\nu$, and $Z \rightarrow \tau^-\tau^+$. Several of the techniques used to determine the data-driven backgrounds require subtraction of non-background processes so that negative background estimates may result when extrapolating to the signal region. Background estimates are required to have a minimum value of zero but are allowed to fluctuate positively within their uncertainty bounds during the cross-section extraction.

8 Event yields

The observed $ZZ \rightarrow \ell^-\ell^+\ell'^-\ell'^+$ and $ZZ \rightarrow \ell^-\ell^+\nu\bar{\nu}$ number of candidates in the data, the total background estimates and the expected signal for the individual decay modes, as well as their combinations, are shown in Table 6. The kinematic distributions of the leading lepton pair mass (the pair with the larger transverse momentum of the two pairs of leptons), $m_{\ell^-\ell^+}^{\mathrm{lead}}$, the transverse momentum of the leading Z boson (the Z boson that decays to the leading lepton pair), $p_{\mathrm{T}}^{Z_{\mathrm{lead}}}$, the mass of the four leptons, $m_{\ell^-\ell^+\ell'^-\ell'^-}$, as well as the transverse momentum of the ZZ system, p_{T}^{ZZ}, for the $ZZ \rightarrow \ell^-\ell^+\ell'^-\ell'^+$ candidates in all four-lepton

Source	$e^-e^+\nu\bar{\nu}$	$\mu^-\mu^+\nu\bar{\nu}$
WZ	$16.7 \pm 1.1 \pm 1.7$	$18.5 \pm 1.0 \pm 1.5$
$ZZ \to \ell^-\ell^+\ell'^-\ell'^+$	$0.6 \pm 0.1 \pm 0.1$	$0.6 \pm 0.1 \pm 0.1$
$t\bar{t}$, W^-W^+, Wt, $ZZ \to \tau\tau\nu\nu$, $Z \to \tau^-\tau^+$	$13.3 \pm 3.2 \pm 0.2$	$15.4 \pm 3.6 \pm 0.3$
W + jets	$2.6 \pm 1.1 \pm 0.5$	$-0.9 \pm 0.7 \pm 1.0$
Z + jets	$-0.7 \pm 3.5 \pm 2.7$	$-0.5 \pm 3.8 \pm 2.9$
Total background	$32.4 \pm 5.5 \pm 3.3$	$33.2 \pm 6.0 \pm 3.4$

Table 5: Number of background events for simulation-based and data-driven estimates in the $ZZ \to \ell^-\ell^+\nu\bar{\nu}$ channel ($e^-e^+\nu\bar{\nu}$ and $\mu^-\mu^+\nu\bar{\nu}$). The first uncertainty is statistical and the second systematic. The exact treatment of background estimates for the cross-section extraction is discussed in the text.

$ZZ \to \ell^-\ell^+\ell'^-\ell'^+$	$e^-e^+e^-e^+$	$\mu^-\mu^+\mu^-\mu^+$	$e^-e^+\mu^-\mu^+$	$\ell^-\ell^+\ell'^-\ell'^+$
Observed data	64	86	171	321
Expected signal	$62.2 \pm 0.3 \pm 2.6$	$83.7 \pm 0.4 \pm 3.2$	$141.6 \pm 0.6 \pm 4.0$	$287.0 \pm 0.8 \pm 8.1$
Expected background	$4.8 \pm 0.7 \pm 2.8$	$2.3 \pm 2.4 \pm 1.0$	$10.0 \pm 3.6 \pm 3.9$	$17.1 \pm 4.4 \pm 7.1$

$ZZ \to \ell^-\ell^+\nu\bar{\nu}$	$e^-e^+\nu\bar{\nu}$	$\mu^-\mu^+\nu\bar{\nu}$	$\ell^-\ell^+\nu\bar{\nu}$
Observed data	102	106	208
Expected signal	$51.1 \pm 0.9 \pm 2.6$	$55.1 \pm 1.0 \pm 2.9$	$106.2 \pm 1.3 \pm 3.9$
Expected background	$32.4 \pm 5.5 \pm 3.3$	$33.2 \pm 6.0 \pm 3.4$	$65.6 \pm 8.1 \pm 4.7$

Table 6: Summary of observed $ZZ \to \ell^-\ell^+\ell'^-\ell'^+$ and $ZZ \to \ell^-\ell^+\nu\bar{\nu}$ candidates in the data, total background estimates and expected signal for the individual decay modes and for their combination (last column). The first uncertainty quoted is statistical, while the second is systematic. The uncertainty in the integrated luminosity (1.9%) is not included.

final states, are shown in Figure 2. Figure 3 shows the mass of the leading lepton pair versus the mass of the subleading lepton pair for the data and predicted signal events in the $ZZ \to \ell^-\ell^+\ell'^-\ell'^+$ channel.

The kinematic distributions of the lepton pair mass, $m_{\ell^-\ell^+}$, the p_{T}^Z, the transverse mass[3] of the ZZ system, m_{T}^{ZZ}, and the azimuthal angle between the two leptons (electrons or muons) originating from the Z boson, $\Delta\phi(\ell^+, \ell^-)$, for the $ZZ \to \ell^-\ell^+\nu\bar{\nu}$ candidates in both lepton final states, are shown in Figure 4.

[3] The transverse mass, m_{T}^{ZZ}, is defined as: $m_{\mathrm{T}}^{ZZ} = \sqrt{\left(\sqrt{p_{\mathrm{T}}^2 + m_Z^2} + \sqrt{E_{\mathrm{T}}^{\mathrm{miss}\,2} + m_Z^2}\right)^2 - (p_{\mathrm{T}} + E_{\mathrm{T}}^{\mathrm{miss}})^2}$, where p_{T} is the transverse momentum of the dilepton pair and $m_Z = 91.1876$ GeV, the mass of the Z boson [66].

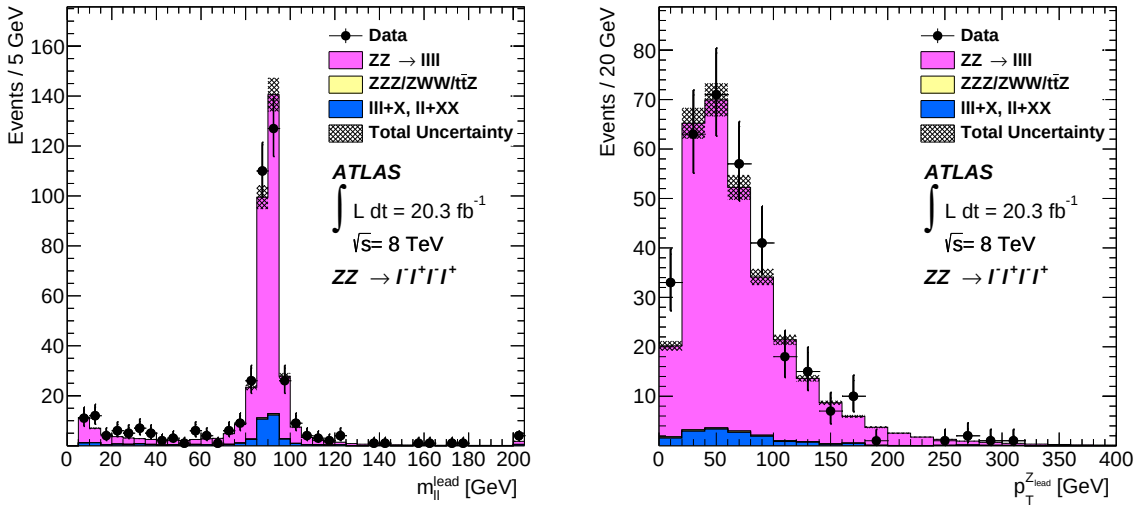

(a) (b)

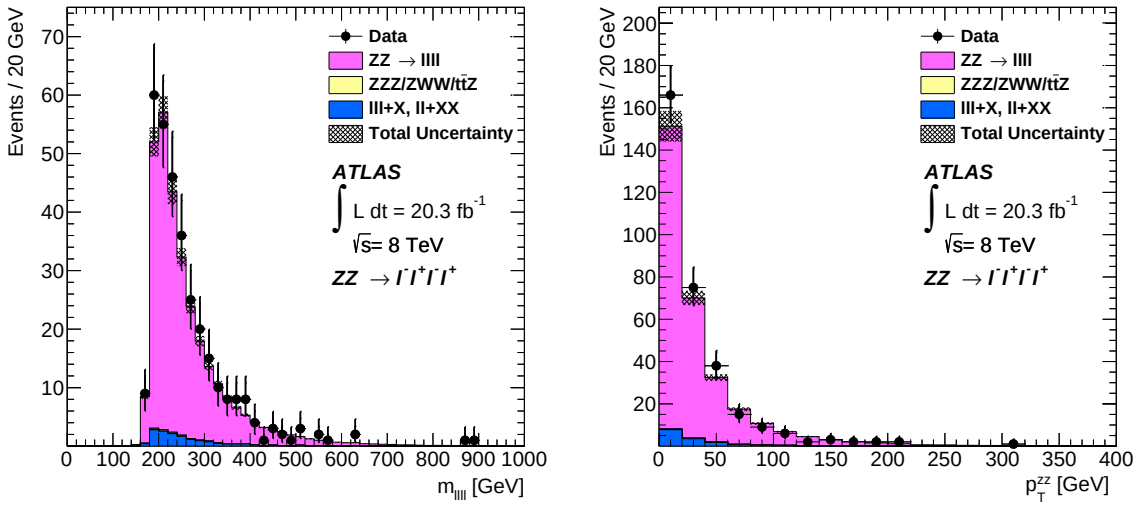

(c) (d)

Figure 2: Kinematic distributions for $ZZ \to \ell^-\ell^+\ell'^-\ell'^+$ candidates in all four-lepton final states: (a) $m^{\text{lead}}_{\ell^-\ell^+}$, (b) $p_{\text{T}}^{Z_{\text{lead}}}$, (c) $m_{\ell^-\ell^+\ell'^-\ell'^-}$ and (d) p_{T}^{ZZ}. The points represent the observed data and the histograms show the expected number of ZZ signal events and the background estimate. The shaded band shows the combined statistical and systematic uncertainties in the prediction and the background. No selection on the leading lepton pair mass is required for (a), while the full selection is applied for the other distributions.

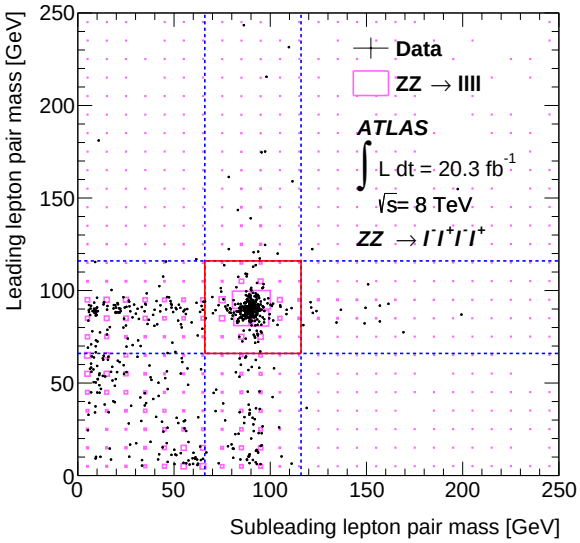

Figure 3: The mass of the leading lepton pair versus the mass of the subleading lepton pair. The events observed in the data are shown as solid circles and the $ZZ \to \ell^-\ell^+\ell'^-\ell'^+$ signal prediction from simulation, normalized to the luminosity of the data, as pink boxes. The size of each box is proportional to the number of events in each bin. The region enclosed in the solid red box indicates the signal region defined by the requirements on the lepton pair masses for ZZ events.

9 Correction factors and detector acceptance

The fiducial cross section as measured in a given phase space for a given final state, $ZZ \to \ell^-\ell^+\ell'^-\ell'^+$ or $ZZ \to \ell^-\ell^+\nu\bar{\nu}$, where ℓ and ℓ' are either an electron or a muon, may be expressed as:

$$\sigma^{\text{fid}} = \frac{N_{\text{data}} - N_{\text{bkg}}}{\mathcal{L} \cdot C_{ZZ}}, \tag{2}$$

where N_{data} is the number of observed candidate events in data passing the full selection, N_{bkg} is the estimated number of background events, $\mathcal{L}$ is the integrated luminosity, and C_{ZZ} is the correction factor applied to the measured cross section to account for detector effects. This factor corrects for detector inefficiencies and resolution and is defined as:

$$C_{ZZ} = \frac{N_{ZZ}^{\text{reco}}}{N_{ZZ}^{\text{fid}}}, \tag{3}$$

where the numerator, N_{ZZ}^{reco}, is the expected yield of reconstructed ZZ events in the signal region after the full selection is applied, and the denominator, N_{ZZ}^{fid}, is the generated yield of ZZ events in the fiducial phase space defined for a given final state. It is determined using simulated ZZ production samples. The numbers of events N_{ZZ}^{reco} and N_{ZZ}^{fid} found in each sample (PowHegBox and `gg2VV`) are weighted by the relative cross sections of the two samples in order to combine them in the ratio. In the calculation of C_{ZZ} for $ZZ \to \ell^-\ell^+\ell'^-\ell'^+$ final states, pairs of oppositely charged leptons produced from decays of $Z \to \tau^+\tau^- \to \ell^+\ell^-\nu\bar{\nu}\nu\bar{\nu}$ are included in N_{ZZ}^{reco}, as those decays have the same final state as the signal and are not subtracted as background but are excluded from N_{ZZ}^{fid} because the fiducial regions are defined only with ZZ decays directly to electrons, muons or neutrinos, depending on the channel.

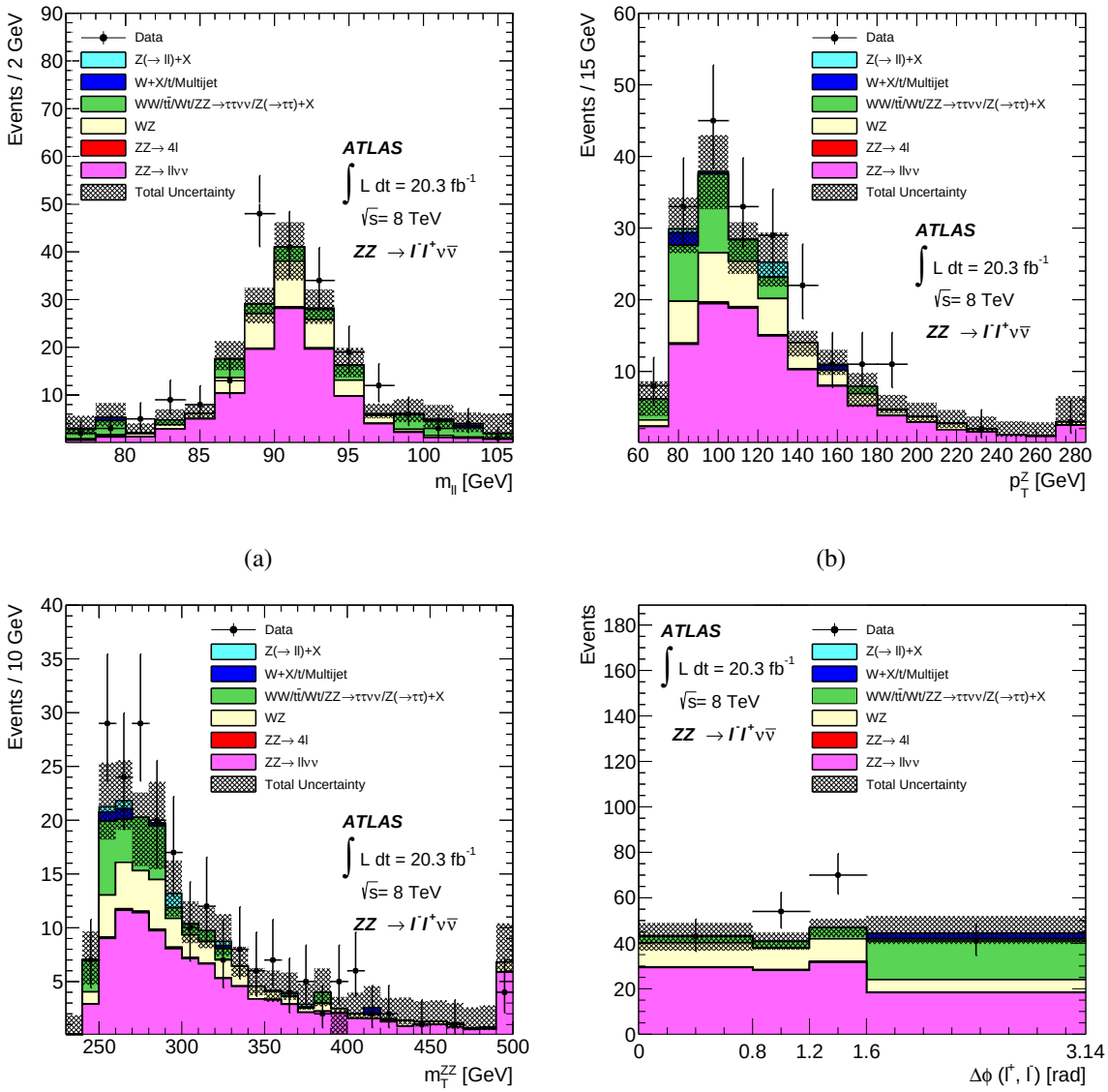

Figure 4: Kinematic distributions for $ZZ \to \ell^-\ell^+\nu\bar{\nu}$ candidates in both lepton final states: (a) $m_{\ell^-\ell^+}$, (b) p_{T}^{Z}, (c) m_{T}^{ZZ} and (d) $\Delta\phi(\ell^+,\ell^-)$. The points represent the observed data and the histograms show the expected number of ZZ signal events and the background estimate. The shaded band shows the combined statistical and systematic uncertainties in the prediction and the background. The last bin in (b) and (c) distributions, contains the overflow events.

Channel	C_{ZZ}	A_{ZZ}
$e^-e^+e^-e^+$	0.495±0.023	0.817±0.017
$e^-e^+\mu^-\mu^+$	0.643±0.021	0.725±0.017
$\mu^-\mu^+\mu^-\mu^+$	0.846±0.034	0.645±0.020
$e^-e^+\nu\bar{\nu}$	0.678±0.039	0.0413±0.0022
$\mu^-\mu^+\nu\bar{\nu}$	0.752±0.048	0.0400±0.0019

Table 7: The C_{ZZ} and A_{ZZ} factors for each of the $ZZ \to \ell^-\ell^+\ell'^-\ell'^+$ and $ZZ \to \ell^-\ell^+\nu\bar{\nu}$ decay modes. The total uncertainties (statistical and systematic) are shown and a description of the systematic uncertainties can be found in Section 10.

The total cross section as measured in a particular final state may be expressed as:

$$\sigma^{\text{tot}} = \frac{N_{\text{data}} - N_{\text{bkg}}}{\mathcal{L} \cdot C_{ZZ} \cdot A_{ZZ} \cdot \text{BF}} = \frac{\sigma^{\text{fid}}}{A_{ZZ} \cdot \text{BF}}, \tag{4}$$

where BF is the branching fraction of ZZ to a particular final state (0.113% for $e^-e^+e^-e^+$ and $\mu^-\mu^+\mu^-\mu^+$ final states, 0.226% for the $e^-e^+\mu^-\mu^+$ final state and 2.69% for the $\ell^-\ell^+\nu\bar{\nu}$ channel) and A_{ZZ} is the detector acceptance as measured in a particular decay mode and is determined at particle level. The acceptance factor is defined as:

$$A_{ZZ} = \frac{N_{ZZ}^{\text{fid}}}{N_{ZZ}^{\text{tot}}}, \tag{5}$$

where the numerator, N_{ZZ}^{fid}, is again the number of ZZ events predicted in the fiducial phase space, and the denominator, N_{ZZ}^{tot}, is the number of ZZ events predicted in the total phase space.

According to Equation (4), the acceptance for the total phase-space events in the signal region is given by the quantity $C_{ZZ} \cdot A_{ZZ} \cdot \text{BF}$. The purpose of this factorization is to separate the term that is sensitive to theoretical uncertainties (A_{ZZ}) from the term representing primarily detector efficiency (C_{ZZ}).

The C_{ZZ} and A_{ZZ} factors are shown in Table 7 for all decay modes considered here. The acceptance in the $ZZ \to \ell^-\ell^+\nu\bar{\nu}$ channel is much smaller than the one in the $ZZ \to \ell^-\ell^+\ell'^-\ell'^+$ channel mainly due to the axial-$E_{\text{T}}^{\text{miss}}$ and jet veto requirements, which reduce the number of selected events by about 86% and 40% respectively.

10 Systematic uncertainties

Systematic uncertainties arise from theoretical and experimental sources, which affect the correction factor, C_{ZZ}, the detector acceptance, A_{ZZ}, the number of expected background events, and the extracted aTGCs limits. These uncertainties are also propagated through the unfolding procedure (Section 11.2) to obtain the differential distributions. A summary of these uncertainties is shown in Table 8.

The dominant experimental uncertainties depend on both the channel and final state under study. In the $ZZ \to \ell^-\ell^+\ell'^-\ell'^+$ channel, the lepton reconstruction uncertainty along with the isolation and impact

parameter uncertainties have the largest effect, while in the $ZZ \to \ell^-\ell^+\nu\bar{\nu}$ channel, the modelling of the jets and the measurement of the $E_{\mathrm{T}}^{\mathrm{miss}}$ are the dominant uncertainties. The systematic uncertainties due to lepton reconstruction are estimated using the $Z \to \ell^+\ell^-$ and $W \to \ell\nu$ processes as described in Refs. [59, 60, 68]. For final states with electrons, the electron reconstruction uncertainty is about 4.0%, 2.0% and 1.7% in the $ZZ \to e^-e^+e^-e^+$, $ZZ \to e^-e^+\mu^-\mu^+$ and $ZZ \to e^-e^+\nu\bar{\nu}$ final states, respectively. Modelling of the isolation of muons along with their reconstructed impact parameter relative to the reconstructed collision vertex are the dominant effects on C_{ZZ} for final states with muons, having contributions of 3.4% and 3.2% in the $ZZ \to \mu^-\mu^+\mu^-\mu^+$ and $ZZ \to \mu^-\mu^+\nu\bar{\nu}$ final states, respectively.

Uncertainties in the modelling of the jets and $E_{\mathrm{T}}^{\mathrm{miss}}$ are significant in the $ZZ \to \ell^-\ell^+\nu\bar{\nu}$ channel due to the jet veto requirement and the axial-$E_{\mathrm{T}}^{\mathrm{miss}} > 90$ GeV selection. The JES uncertainty[4] corresponding to the local cluster weighting calibration scheme is obtained using data from test-beams, LHC collision data and simulations [69, 70] and is provided in bins of jet p_{T} and $|\eta|$. The jet energy resolution (JER) and its uncertainty are determined using in situ techniques based on the transverse momentum balance in dijet events. The impact due to the uncertainty on the resolution is evaluated by smearing the p_{T} of the jets within its uncertainty. The reconstruction of the $E_{\mathrm{T}}^{\mathrm{miss}}$ is affected by uncertainties associated with the leptons, JES and JER that are propagated to the $E_{\mathrm{T}}^{\mathrm{miss}}$ determination. As there are no requirements on either jet reconstruction or $E_{\mathrm{T}}^{\mathrm{miss}}$ for the $ZZ \to \ell^-\ell^+\ell'^-\ell'^+$ channel, the impact of these uncertainties is negligible for these final states.

The uncertainty in the integrated luminosity is 1.9%. This affects the overall normalization of ZZ production for the total cross-section measurement and the unfolded differential distributions.

In addition to experimental uncertainties, the measurements are subject to sources of theoretical uncertainty. The correction factor and detector acceptance for $ZZ \to \ell^-\ell^+\ell'^-\ell'^+$ and $ZZ \to \ell^-\ell^+\nu\bar{\nu}$ final states are calculated using PowhegBox interfaced to Pythia for the $q\bar{q}$ component, and using `gg2VV` for the $gg \to ZZ$ component. These calculations are sensitive to the choice of μ_{R} and μ_{F} scales, as they are missing higher terms from the perturbative expansion. The uncertainty associated with this choice is estimated by comparing the detector acceptance, A_{ZZ}, when the μ_{R} and μ_{F} scales are increased and decreased by a factor of two, with the nominal. The uncertainty associated with the jet veto in the $ZZ \to \ell^-\ell^+\nu\bar{\nu}$ final state is determined via the Stewart and Tackmann method [40] using the jet veto efficiency for each sample generated with different μ_{R} and μ_{F} scales.

The choice of parton shower and underlying-event modelling is one of the smaller sources of theoretical uncertainty and its effect is estimated in two ways. First, A_{ZZ} is recalculated from MC samples generated with PowhegBox but interfaced with Herwig for the parton showering instead of Pythia as is done for the nominal samples. The uncertainty is estimated from the difference in A_{ZZ} for the Herwig and Pythia showered samples. The second method uses ZZ samples generated using Sherpa to calculate both C_{ZZ} and A_{ZZ}. Sherpa is formally a LO generator with respect to the $q\bar{q}$ process, and does not include the gluon diagrams. However, Sherpa uses its own matrix-element generation and parton shower algorithms, and can be used to provide an estimate of the effects of the uncertainty due to the choice of parton shower. As in the first method, the uncertainty is estimated using the difference in C_{ZZ} and A_{ZZ} calculated using the nominal and Sherpa samples.

As described in Section 4, the predicted cross sections for the ZZ final states are corrected for virtual NLO EW effects by applying a reweighting factor to each event. The uncertainty in this reweighting procedure

[4] The JES uncertainty is fully parameterized by 56 nuisance parameters resulting from various estimation techniques including Z+jets, γ+jets and multijet balance.

is estimated by combining the uncertainty in the theoretical predictions used to estimate the NLO EW effects and the statistical uncertainty from its prediction. These uncertainties are added in quadrature.

The choice of PDF represents an additional source of uncertainty. To estimate this theoretical uncertainty, the eigenvectors of the CT10 PDF set are varied within their $\pm 1\sigma$ uncertainties. The same procedure is followed for the backgrounds estimated from simulation where the CT10 PDF set is used.

Source	$e^-e^+e^-e^+$	$\mu^-\mu^+\mu^-\mu^+$	$e^-e^+\mu^-\mu^+$	$e^-e^+\nu\bar{\nu}$	$\mu^-\mu^+\nu\bar{\nu}$
			C_{ZZ}		
Electron rec. and ID efficiency	4.0 %	–	2.0 %	1.7 %	–
Electron energy/momentum	0.4 %	0.01%	0.2 %	2.0 %	0.1 %
Electron isolation/impact parameter	1.4 %	–	0.7 %	0.3 %	–
Muon rec. and ID efficiency	–	1.8 %	0.9 %	–	0.7 %
Muon energy/momentum	–	0.03%	0.04%	–	0.3 %
Muon isolation/impact parameter	–	3.4 %	1.7 %	–	3.2 %
Jet+$E_{\mathrm{T}}^{\mathrm{miss}}$ modelling	NA	NA	NA	4.7 %	5.3 %
Trigger efficiency	0.1 %	0.2 %	0.1 %	0.1 %	0.5 %
PDF and parton shower	0.2 %	0.1 %	0.1 %	0.9 %	2.2 %
			A_{ZZ}		
Jet veto	NA	NA	NA	1.8 %	1.6 %
Electroweak Corrections	0.03%	0.03%	0.02%	0.9 %	1.0 %
PDF and scale	0.7 %	0.9 %	0.8 %	3.1 %	2.1 %
Generator modelling and parton shower	2.0 %	3.0 %	2.3 %	4.3 %	4.1 %

Table 8: A summary of the systematic uncertainties, as relative percentages of the correction factor C_{ZZ} and the detector acceptance A_{ZZ} is shown. For rows with multiple sources, the uncertainties are added in quadrature. Dashes indicate uncertainties which are smaller than 0.01% and uncertainites with NA are not applicable for that specific final state.

11 Cross-section measurements

11.1 Cross-section extraction

Two types of cross sections, fiducial and total, are extracted using Equations (2) and (4). A fiducial cross section is extracted for every final state in both the $ZZ \to \ell^-\ell^+\ell'^-\ell'^+$ and $ZZ \to \ell^-\ell^+\nu\bar{\nu}$ channels. The information from these final states is combined to measure a single $pp \to ZZ$ total cross section in the total phase space ($66 < m_{\ell^-\ell^+} < 116$ GeV) using the detector acceptance and branching fraction of ZZ to a given four-lepton or dilepton + $\nu\bar{\nu}$ final state. For each measurement, a likelihood method is used to extract the expected ZZ event rate according to a Poisson probability distribution, as described in Ref. [71]. The likelihood is maximized with respect to the cross section. For fiducial (total) cross-section measurements, sources of systematic uncertainties affecting backgrounds, object reconstruction and identification efficiencies, detector acceptance and luminosity are included as nuisance parameters and the affected terms are allowed to fluctuate according to Gaussian probability distributions with widths equal to the uncertainties. The measured cross sections for the $ZZ \to \ell^-\ell^+\ell'^-\ell'^+$ and $ZZ \to \ell^-\ell^+\nu\bar{\nu}$ channels are given in Table 9 and the ratios of these measurements with respect to the SM predictions are shown in Figure 5.

	Measurement	Prediction
$\sigma^{\text{fid}}_{ZZ\to e^-e^+e^-e^+}$	$= 5.9 \pm 0.8\,(\text{stat}) \pm 0.4\,(\text{syst}) \pm 0.1\,(\text{lumi})$ fb	$6.2\ ^{+0.6}_{-0.5}$ fb
$\sigma^{\text{fid}}_{ZZ\to e^-e^+\mu^-\mu^+}$	$= 12.4 \pm 1.0\,(\text{stat})\ ^{+0.6}_{-0.5}\,(\text{syst})\ ^{+0.3}_{-0.2}\,(\text{lumi})$ fb	$10.8\ ^{+1.1}_{-1.0}$ fb
$\sigma^{\text{fid}}_{ZZ\to \mu^-\mu^+\mu^-\mu^+}$	$= 4.9\ ^{+0.6}_{-0.5}\,(\text{stat})\ ^{+0.3}_{-0.2}\,(\text{syst}) \pm 0.1\,(\text{lumi})$ fb	$4.9\ ^{+0.5}_{-0.4}$ fb
$\sigma^{\text{fid}}_{ZZ\to e^-e^+\nu\bar{\nu}}$	$= 5.0\ ^{+0.8}_{-0.7}\,(\text{stat})\ ^{+0.5}_{-0.4}\,(\text{syst}) \pm 0.1\,(\text{lumi})$ fb	3.7 ± 0.3 fb
$\sigma^{\text{fid}}_{ZZ\to \mu^-\mu^+\nu\bar{\nu}}$	$= 4.7 \pm 0.7\,(\text{stat})\ ^{+0.5}_{-0.4}\,(\text{syst}) \pm 0.1\,(\text{lumi})$ fb	3.5 ± 0.3 fb
$\sigma^{\text{total}}_{pp\to ZZ}$	$= 7.3 \pm 0.4\,(\text{stat}) \pm 0.3\,(\text{syst})\ ^{+0.2}_{-0.1}\,(\text{lumi})$ pb	$6.6\ ^{+0.7}_{-0.6}$ pb

Table 9: The measured fiducial cross sections and the combined total cross section compared to the SM predictions. For experimental results, the statistical, systematic, and luminosity uncertainties are shown. For the theoretical predictions, the combined statistical and systematic uncertainty is shown.

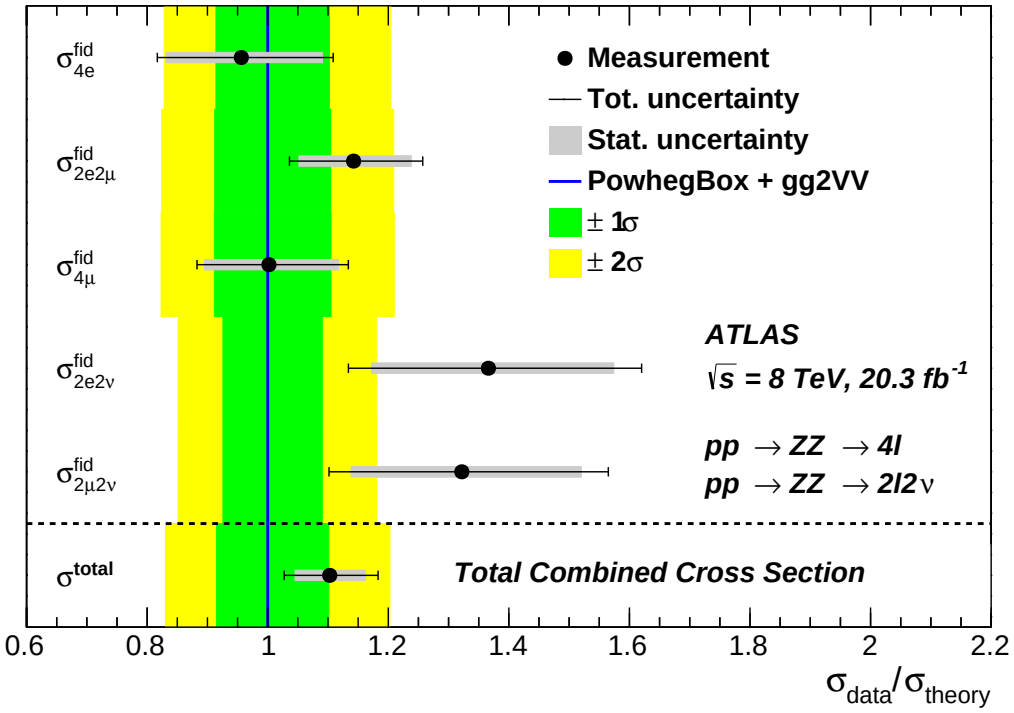

Figure 5: The ratio of the measured ZZ cross sections in the fiducial phase space to the SM prediction from PowHegBox and gg2VV in each of the five decay modes considered. The ratio between the total combined cross section and the SM prediction is also shown. The inner grey error bars on the data points represent the statistical uncertainties, while the outer black error bars represent the total uncertainties. The green and yellow bands represent the 1σ and 2σ uncertainties, respectively, associated with the SM prediction.

11.2 Differential cross sections

The differential cross sections presented in this section allow a more detailed comparison of the measurement to current and future theoretical predictions. The measured kinematic distributions are unfolded back to the underlying distributions, accounting for the effect of detector resolution, efficiency and acceptance. The unfolding as a function of different kinematic variables is performed separately for the two channels. More specifically, it is performed within the fiducial phase space of the $ZZ \to \ell^-\ell^+\nu\bar{\nu}$ measurement and within the total phase space of the $ZZ \to \ell^-\ell^+\ell'^-\ell'^+$ measurement, defined in Section 3. This different approach between the channels is chosen to benefit from the extended fiducial phase space for leptons in the $ZZ \to \ell^-\ell^+\ell'^-\ell'^+$ channel.

The unfolding procedure is based on a Bayesian iterative algorithm [72]. In the unfolding of binned data, the effects of the experimental acceptance and resolution are expressed in terms of a two-dimensional response matrix, A_{ij}, where each element corresponds to the probability of an event in the i-th generator-level bin being reconstructed in the j-th measurement bin. The unfolding algorithm combines the measured spectrum with the response matrix to form a likelihood, takes as input a prior for the specific kinematic variable and iterates using the posterior distribution as prior for the next iteration. The SM prediction calculated using the PowhegBox and `gg2VV` generators is used as the initial prior and three iterations are performed. The number of iterations is optimized to find a balance between too many iterations, causing high statistical uncertainties associated with the unfolded spectra, and too few iterations, which increases the dependency on the MC prior.

The statistical uncertainty of the unfolded distribution is tested via toy-MC tests. Each measured datapoint is Poisson fluctuated and the full nominal unfolding procedure is applied. This is repeated 2000 times and the root mean square of the resulting unfolded values is taken as the unfolded distribution's statistical uncertainty.

The systematic uncertainties are estimated as follows: for each scale, efficiency or resolution systematic uncertainty, a new response matrix is produced reflecting a variation by that systematic uncertainty. The measured data distribution is then unfolded for all instances separately, leading to one distribution for each systematic uncertainty. The difference between each of the distributions that correspond to the different systematic uncertainties and the nominal distribution, where no variation has been applied, is defined as the systematic uncertainty in each bin.

Uncertainties on the unfolding due to imperfect description of the kinematic properties of the data by the MC are evaluated using a data-driven method [73], where the MC differential distribution is corrected to match the data distribution and the resulting weighted MC distribution at reconstruction level is unfolded with the response matrix used in the actual data unfolding. The new unfolded distribution is compared to the weighted MC distribution at generator level and the difference is taken as the systematic uncertainty. Moreover, in the $ZZ \to \ell^-\ell^+\ell'^-\ell'^+$ channel, as the unfolding is performed within the total phase space, theoretical uncertainties due to this extrapolation are also considered. These uncertainties include the choice of μ_R and μ_F scales, which access the impact of higher-order contributions from QCD, the PDF set, and the parton shower modelling. The latter is estimated by comparisons with Sherpa ZZ samples.

The bin limits and bin widths of the differential kinematic distributions are chosen to balance the need of finer bins, in order to provide detailed information, against the limited number of events and bin migration effects. More specifically, the fraction of reconstructed events generated in the same bin (i.e. purity) is higher than 75%.

11.2.1 $ZZ \to \ell^-\ell^+\ell'^-\ell'^+$ channel

The kinematic distributions that are unfolded in this channel are the $p_{\mathrm{T}}^{Z_{\mathrm{lead}}}$, the number of jets in associated production with $ZZ \to \ell^-\ell^+\ell'^-\ell'^+$ (N_{jets}), the azimuthal angle between the two leptons (electrons or muons) originating from the leading Z boson ($\Delta\phi(\ell^+,\ell^-)_{\mathrm{lead}}$) and the difference in rapidity between the two Z bosons of the ZZ system ($\Delta y(Z,Z)$). The differential cross sections and their comparison with the SM predictions (PowHegBox and gg2VV) are shown in Figure 6. The dominant uncertainty is the statistical uncertainty of the data, ranging from 7% to 17% in most bins. The theoretical modelling uncertainties are of the order of 1%–3%. According to Figure 6(b), more than 70% of $ZZ \to \ell^-\ell^+\ell'^-\ell'^+$ events are produced without any associated high-p_{T} jets, and this is well modelled by MC simulation. The measurement is consistent with the SM prediction within 1 σ in most of the bins.

11.2.2 $ZZ \to \ell^-\ell^+\nu\bar{\nu}$ channel

The kinematic distributions that are unfolded in this channel are the p_{T}^{Z} of the Z boson that decays to electrons or muons, the azimuthal angle between the two leptons (electrons or muons) originating from the Z boson ($\Delta\phi(\ell^+,\ell^-)$) and the transverse mass of the ZZ system (m_{T}^{ZZ}).

The differential cross sections are shown in Figure 7. The measured values are compared with the SM predictions (PowHegBox and gg2VV). The theoretical modelling uncertainties, evaluated by the data-driven method described in Section 11.2, are in the order of a few percent (0.7%–1% for p_{T}^{Z} , 0.7%–1.5% for $\Delta\phi(\ell^+,\ell^-)$ and 3%–9% for m_{T}^{ZZ}). While the central values of the unfolded data differ from the prediction by up to 50% in some of the bins, the measurement is consistent with the SM prediction within 1–2σ.

12 Anomalous neutral triple gauge couplings

According to the SM $\mathrm{SU(2)_L \times U(1)_Y}$ gauge symmetry, vertices of the form ZZZ and $ZZ\gamma$ are not present at tree level. Consequently, ZZ production does not receive a contribution from the s-channel resonance diagram (Figure 1(c)). At one-loop level, fermionic triangle loops contribute to the generation of effective neutral aTGCs at the level of 10^{-4} to 10^{-3} [15]. A typical signature of aTGCs is an enhanced cross section at high centre-of-mass energies. Thus, observables which are proportional to the invariant mass of the ZZ diboson system and the gauge boson transverse momentum are particularly sensitive to contributions from aTGCs. Studies of aTGCs have been performed by the LEP Collaborations [22, 74–77], as well as the CDF and D0 Collaborations. More recent studies performed by the ATLAS and CMS Collaborations using data collected during 2011 at 7 TeV indicate that if there are any contributions from new physics at the TeV scale, they are at most of the order of 10^{-3}.

In this paper, an effective Lagrangian framework [78] is used for the aTGCs studies, where the most general ZZV ($V = Z$ or γ) couplings, which respect gauge and Lorentz invariance [21] are considered. Such couplings can be parameterized by two CP-violating (f_4^γ, f_4^Z) and two CP-conserving (f_5^γ, f_5^Z) parameters. The contribution of anomalous couplings to the ZZ production cross section grows with the partonic centre-of-mass energy squared, $\hat{s}$. To avoid violation of unitarity a form factor is introduced to the anomalous couplings of the form:

$$f_i^V(\hat{s}) = f_{i,0}^V\Big(1 + \frac{\hat{s}}{\Lambda^2}\Big)^{-2}, \tag{6}$$

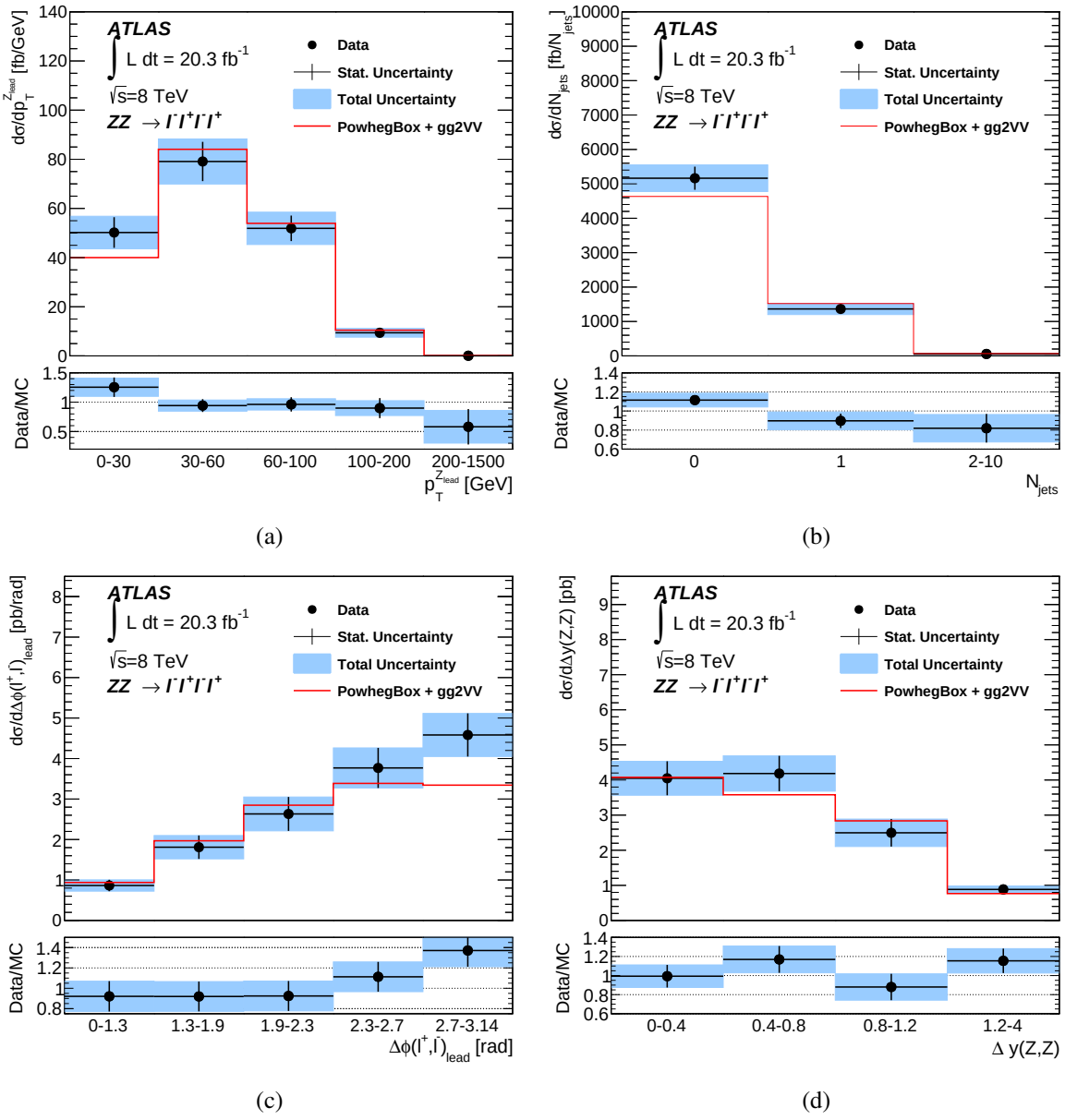

Figure 6: The measured differential cross-section distributions (black points) normalized to the bin width for (a) $p_{\mathrm{T}}^{Z_{\mathrm{lead}}}$, (b) N_{jets}, (c) $\Delta\phi(\ell^+,\ell^-)_{\mathrm{lead}}$ and (d) $\Delta y(Z,Z)$ in the $ZZ \to \ell^-\ell^+\ell'^-\ell'^+$ channel, unfolded within the total phase space, compared to the theory predictions of PowHegBox and `gg2VV` (red line). The vertical error bars show the respective statistical uncertainties, while the light blue error bands express the statistical and systematic uncertainties of the measurements added in quadrature.

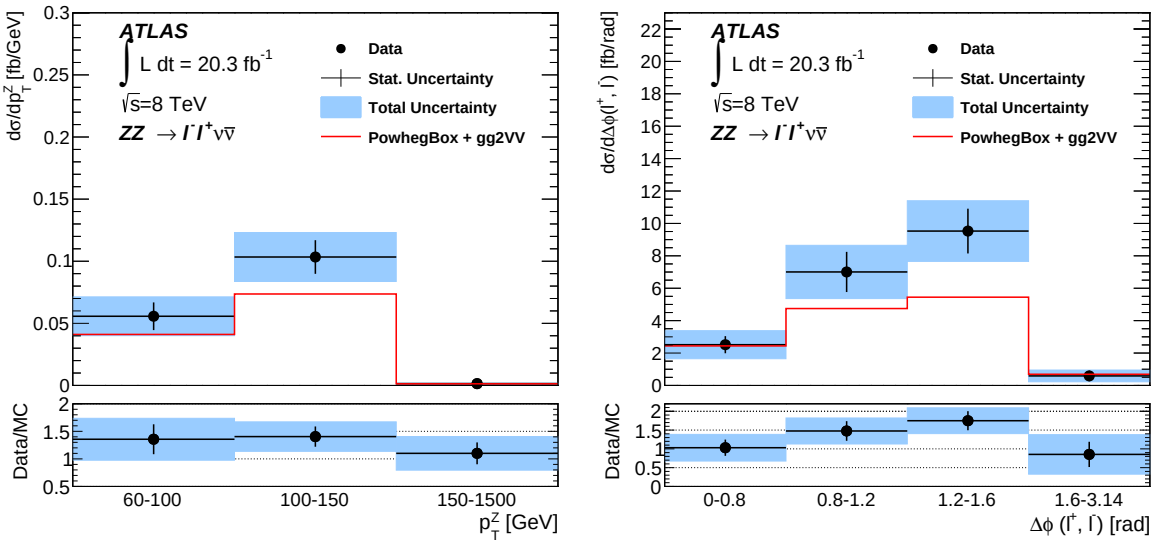

(a) (b)

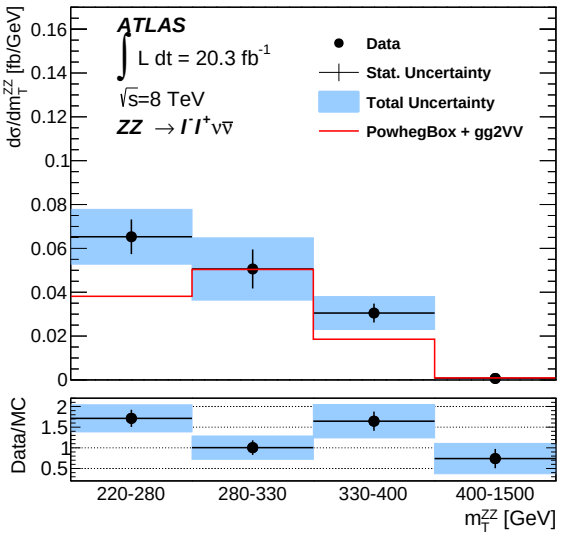

(c)

Figure 7: The measured differential cross-section distributions (black points) normalized to the bin width for (a) p_{T}^{Z}, (b) $\Delta\phi(\ell^+,\ell^-)$ and (c) m_{T}^{ZZ} in the $ZZ \to \ell^-\ell^+\nu\bar{\nu}$ channel, unfolded within the fiducial phase space, compared to the theory predictions of PowHegBox and gg2VV (red line). The vertical error bars show the respective statistical uncertainties, while the light blue error bands express the statistical and systematic uncertainties of the measurements added in quadrature.

where $f_{i,0}^{V}$ is the generic anomalous coupling value (i=4,5) at low energy and Λ is a cutoff scale related to the energy at which the effective field theory breaks down and new physics would be observed. For the results presented, no form factor is used as the current sensitivity is well within the unitarization constraints and Λ is large enough that no energy dependence for the anomalous couplings needs to be considered. The ZZV couplings in ZZ production considered here are distinct from the $Z\gamma V$ couplings probed in $Z\gamma$ production in e^-e^+ and hadronic collisions. Additional anomalous couplings can contribute when the Z bosons are off-shell [79], although these couplings are highly suppressed near the Z boson resonance.

12.1 Parameterization of signal yield

In order to look for the effects of ZZV aTGCs, the signal yield must be parameterized in terms of the coupling strength. Simulated samples are produced using a generator which contains matrix elements with aTGCs at various strengths with one reference sample generated at the SM points of zero for all couplings, and at least two other samples with non-zero couplings in various combinations. The signal yield is obtained as the simulated samples are reweighted from one aTGC point to another using a framework [80] which allows the kinematics properties to be reweighted on an event-by-event basis. The matrix elements used for reweighting are extracted from the Baur, Han and Ohnemus (BHO) [81] generator. The event yields are then expressed as a function of the aTGC parameters, which contains terms both linearly and quadratically proportional to the couplings. The expected number of events generated by Sherpa (only $q\bar{q} \to ZZ$) is then normalized to the prediction of PowhegBox + `gg2VV`.

12.2 Confidence intervals for aTGCs

The $p_{\mathrm{T}}^{Z_{\mathrm{lead}}}$ in the $ZZ \to \ell^-\ell^+\ell^-\ell^+$ channel and the p_{T}^{Z} in the $ZZ \to \ell^-\ell^+\nu\bar{\nu}$ channel are particularly sensitive to aTGCs and therefore these distributions are used to probe them. Given the limited number of events in the selected data sample, especially in the high-p_{T}^{Z} region, all the events of the $e^-e^+e^-e^+$, $e^-e^+\mu^-\mu^+$ and $\mu^-\mu^+\mu^-\mu^+$ final states in the $\ell^-\ell^+\ell'^-\ell'^+$ channel are combined. Likewise, all the events of the $e^-e^+\nu\bar{\nu}$ and $\mu^-\mu^+\nu\bar{\nu}$ final states in the $\ell^-\ell^+\nu\bar{\nu}$ channel are combined. Figure 8 shows the data distribution comparison with the SM predictions, as well as the prediction for a non-zero aTGC parameter point, where the CP-violating parameter f_4^{γ} is set to be equal to 0.01, while all other anomalous couplings are set to zero. The deficit in data versus the MC prediction for bin 2 in (a) is 2.2 σ while for bin 4 in (b) it is 1.9 σ. The data are found to be consistent with the SM predictions, and no indication of aTGCs is observed.

Limits on neutral aTGC parameters are determined using the expected and observed numbers of events in the following p_{T}^{Z} bins: 280–430 GeV and 430–1500 GeV for the $ZZ \to \ell^-\ell^+\ell'^-\ell'^+$ channel, and 270–350 GeV and 350–1500 GeV for the $ZZ \to \ell^-\ell^+\nu\bar{\nu}$ channel. The binning is optimized for maximum sensitivity in the aTGCs. Table 10 shows the expected number of events from non-ZZ backgrounds and from SM ZZ events along with the observed number of events in each bin.

A normalization factor is applied to the expected SM ZZ events, to scale the predicted ZZ fiducial cross section to the measurement. The uncertainty in this normalization factor is propagated to the limit-setting procedure. Apart from the uncertainties described in Section 10, an additional systematic uncertainty in the modelling of the p_{T}^{Z} shape for the $q\bar{q} \to ZZ$ process is taken into account by comparing the predictions from PowhegBox and Sherpa. The difference ranges from 30% to 80% for the $ZZ \to \ell^-\ell^+\nu\bar{\nu}$ channel and from 30% to 40% for the $ZZ \to \ell^-\ell^+\ell'^-\ell'^+$ channel.

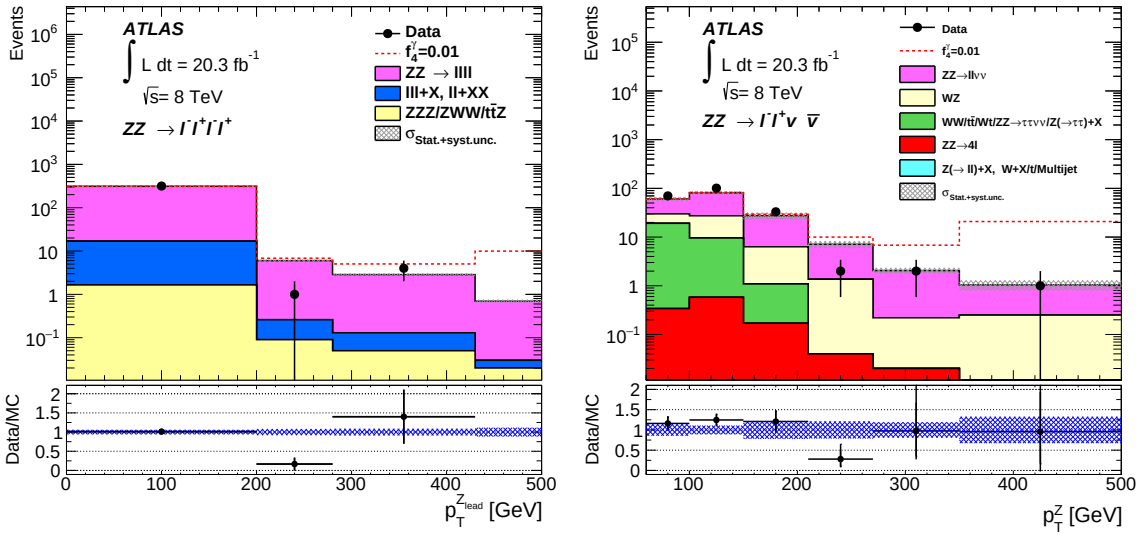

(a) (b)

Figure 8: Data and SM prediction of the p_{T}^{Z} distribution for the (a) $ZZ \to \ell^-\ell^+\ell'^-\ell'^+$ and (b) $ZZ \to \ell^-\ell^+\nu\bar{\nu}$ channels. The expected contribution from the aTGC point with $f_4^{\gamma} = 0.01$ is also shown.

The extraction of the aTGC limits is based on detector-level distributions. A profile-likelihood-ratio test statistic [82] is used to assess whether the predictions with aTGCs are compatible with the data. Then a frequentist method [83] is used to determine the 95% confidence level (CL) intervals for the aTGC parameters. The number of observed data events and the predictions for the aTGC signal and background processes are used to construct the Poissonian probability density functions, in which systematic uncertainties are considered as nuisance parameters constrained with Gaussian functions. The observed intervals are compared with the expected intervals by generating 'Asimov' data sets, which are representative event samples that provide both the median expectation for an experimental result and its expected statistical variation in the asymptotic approximation as described in Ref. [82]. The expected limits calculated with 'Asimov' data sets are cross-checked with limits obtained from 5000 pseudo-experiments generated using the expected number of events at each point in the aTGC parameter space.

	Expected non-ZZ background	Expected SM ZZ events	Observed events
$ZZ \to \ell^-\ell^+\ell'^-\ell'^+$			
$280 < p_{\mathrm{T}}^{Z_{\mathrm{lead}}} < 430$ GeV	$0.13 \pm 0.01 \pm 0.04$	$2.7 \pm 0.1 \pm 0.9$	4
$p_{\mathrm{T}}^{Z_{\mathrm{lead}}} > 430$ GeV	$0.03 \pm 0.01 \pm 0.01$	$0.7 \pm 0.1 \pm 0.3$	0
$ZZ \to \ell^-\ell^+\nu\bar{\nu}$			
$270 < p_{\mathrm{T}}^{Z} < 350$ GeV	$0.22 \pm 0.10 \pm 0.03$	$2.3 \pm 0.20 \pm 1.8$	2
$p_{\mathrm{T}}^{Z} > 350$ GeV	$0.25 \pm 0.12 \pm 0.03$	$1.0 \pm 0.13 \pm 0.4$	1

Table 10: The expected background from non-ZZ events and SM ZZ events, and the number of observed events in the two highest $p_{\mathrm{T}}^{Z_{\mathrm{lead}}}$ and p_{T}^{Z} bins for all final states in each ZZ channel. For the expected background and SM ZZ events, the first uncertainty is statistical and the second is systematic.

Limits are set on each coupling, assuming all of the other couplings are zero (as in the SM), and on

pairs of couplings assuming the remaining two couplings are zero. The observed and expected 95% CL invervals for the four aTGC parameters for the $ZZ \to \ell^-\ell^+\ell'^-\ell'^+$ and $ZZ \to \ell^-\ell^+\nu\bar{\nu}$ channels combined are listed in Table 11. Since the energy scale at which new physics may appear is unknown, no form factor is used when deriving the limits. The two-dimensional 95% CL intervals are shown in Figure 9.

Coupling	Expected (10^{-3})	Observed (10^{-3})
f_4^γ	$[-4.6, 4.8]$	$[-3.8, 3.8]$
f_4^Z	$[-4.0, 4.1]$	$[-3.3, 3.2]$
f_5^γ	$[-4.8, 4.8]$	$[-3.8, 3.8]$
f_5^Z	$[-4.1, 4.1]$	$[-3.3, 3.3]$

Table 11: One-dimensional expected and observed 95% CL limits on the aTGC parameters for both the $ZZ \to \ell^-\ell^+\ell'^-\ell'^+$ and $ZZ \to \ell^-\ell^+\nu\bar{\nu}$ channels combined. The limit for each coupling assumes that the other couplings are fixed at their SM value.

The one-dimensional limits are more stringent than those derived from measurements at LEP [22], the Tevatron [23] and previously by ATLAS [16] and are comparable to the limits set by CMS at 8 TeV [20]. CMS has recently improved the limits on aTGCs by combining measurements at 7 and 8 TeV [24].

13 Conclusion

A measurement of the ZZ production cross section in LHC pp collisions at $\sqrt{s} = 8$ TeV is presented, using data corresponding to an integrated luminosity of 20.3 fb^{-1} collected by the ATLAS detector in 2012. Fiducial cross sections are measured for every final state in the $ZZ \to \ell^-\ell^+\ell'^-\ell'^+$ and $ZZ \to \ell^-\ell^+\nu\bar{\nu}$ ($\ell = e, \mu$) decay channels and the results are compatible with the SM expected cross sections. The combined total ZZ production cross section is measured to be:

$$\sigma^{\text{total}}_{pp\to ZZ} = 7.3 \pm 0.4\,(\text{stat}) \pm 0.3\,(\text{syst})\ ^{+0.2}_{-0.1}\,(\text{lumi})\ \text{pb}$$

The result is consistent with the SM prediction:

$$\sigma^{\text{total}}_{pp\to ZZ} = 6.6^{+0.7}_{-0.6}\ \text{pb}$$

which includes predictions from QCD at NLO for the $q\bar{q}$ process corrected for virtual NLO EW effects and predictions from LO gluon–gluon fusion.

Differential cross sections in the total phase space in the $ZZ \to \ell^-\ell^+\ell'^-\ell'^+$ channel are derived for the transverse momentum of the leading Z boson, the number of jets, the azimuthal angle between the two leptons originating from the leading Z boson and the difference in rapidity between the two Z bosons of the ZZ system. In the $ZZ \to \ell^-\ell^+\nu\bar{\nu}$ channel, the differential cross sections are measured in the fiducial phase space for the transverse momentum of the Z boson, the azimuthal angle between the two leptons originating from the Z and the transverse mass of the ZZ system.

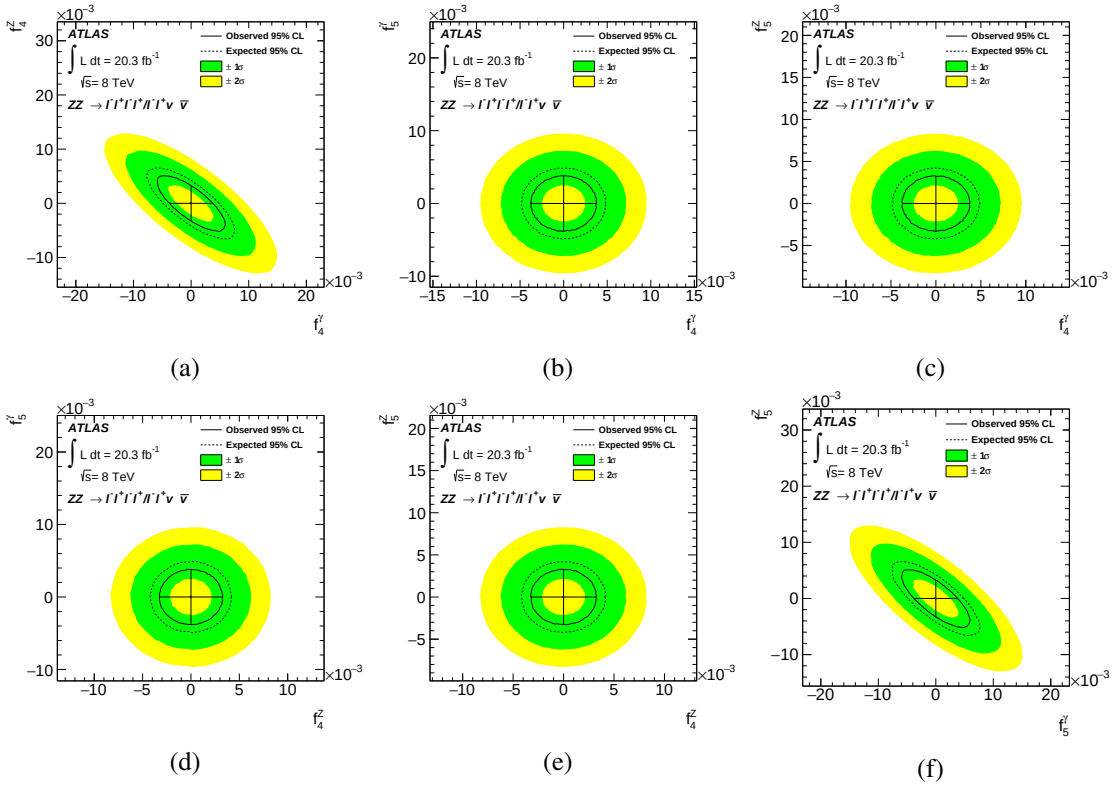

Figure 9: The observed and expected two-dimensional 95% CL contours for limits in the plane of two simultaneously non-zero parameters for the combined $ZZ \to \ell^-\ell^+\ell'^-\ell'^+$ and $ZZ \to \ell^-\ell^+\nu\bar{\nu}$ channels. Except for the two aTGC parameters under study, all others are set to zero. The horizontal and vertical lines correspond to the one-dimensional limits for each aTGC parameter.

The event yields as a function of the p_{T} of the leading Z boson for the $ZZ \to \ell^-\ell^+\ell'^-\ell'^+$ and $ZZ \to \ell^-\ell^+\nu\bar{\nu}$ event selections are used to derive 95% confidence intervals for anomalous neutral triple gauge boson couplings. These limits are more stringent than the previous ATLAS results by approximately a factor of four.

Acknowledgements

We thank CERN for the very successful operation of the LHC, as well as the support staff from our institutions without whom ATLAS could not be operated efficiently.

We acknowledge the support of ANPCyT, Argentina; YerPhI, Armenia; ARC, Australia; BMWFW and FWF, Austria; ANAS, Azerbaijan; SSTC, Belarus; CNPq and FAPESP, Brazil; NSERC, NRC and CFI, Canada; CERN; CONICYT, Chile; CAS, MOST and NSFC, China; COLCIENCIAS, Colombia; MSMT CR, MPO CR and VSC CR, Czech Republic; DNRF and DNSRC, Denmark; IN2P3-CNRS, CEA-DSM/IRFU, France; GNSF, Georgia; BMBF, HGF, and MPG, Germany; GSRT, Greece; RGC, Hong Kong SAR, China; ISF, I-CORE and Benoziyo Center, Israel; INFN, Italy; MEXT and JSPS, Japan; CNRST, Morocco; FOM and NWO, Netherlands; RCN, Norway; MNiSW and NCN, Poland; FCT, Portugal; MNE/IFA, Romania; MES of Russia and NRC KI, Russian Federation; JINR; MESTD, Serbia;

MSSR, Slovakia; ARRS and MIZŠ, Slovenia; DST/NRF, South Africa; MINECO, Spain; SRC and Wallenberg Foundation, Sweden; SERI, SNSF and Cantons of Bern and Geneva, Switzerland; MOST, Taiwan; TAEK, Turkey; STFC, United Kingdom; DOE and NSF, United States of America. In addition, individual groups and members have received support from BCKDF, the Canada Council, CANARIE, CRC, Compute Canada, FQRNT, and the Ontario Innovation Trust, Canada; EPLANET, ERC, FP7, Horizon 2020 and Marie Skłodowska-Curie Actions, European Union; Investissements d'Avenir Labex and Idex, ANR, Région Auvergne and Fondation Partager le Savoir, France; DFG and AvH Foundation, Germany; Herakleitos, Thales and Aristeia programmes co-financed by EU-ESF and the Greek NSRF; BSF, GIF and Minerva, Israel; BRF, Norway; Generalitat de Catalunya, Generalitat Valenciana, Spain; the Royal Society and Leverhulme Trust, United Kingdom.

The crucial computing support from all WLCG partners is acknowledged gratefully, in particular from CERN, the ATLAS Tier-1 facilities at TRIUMF (Canada), NDGF (Denmark, Norway, Sweden), CC-IN2P3 (France), KIT/GridKA (Germany), INFN-CNAF (Italy), NL-T1 (Netherlands), PIC (Spain), ASGC (Taiwan), RAL (UK) and BNL (USA), the Tier-2 facilities worldwide and large non-WLCG resource providers. Major contributors of computing resources are listed in Ref. [84].

References

[1] S. L. Glashow, *Partial Symmetries of Weak Interactions*, Nucl. Phys. **22** (1961) 579–588.

[2] A. Salam and J. C. Ward, *Gauge theory of elementary interactions*, Phys. Rev. **136** (1964) B763–B768.

[3] S. Weinberg, *A Model of Leptons*, Phys. Rev. Lett. **19** (1967) 1264–1266.

[4] J. M. Campbell, R. K. Ellis and C. Williams, *Vector boson pair production at the LHC*, JHEP **07** (2011) 018, arXiv:1105.0020 [hep-ph].

[5] K. Lane and S. Mrenna, *The Collider Phenomenology of Technihadrons in the Technicolor Straw Man Model*, Phys. Rev. D **67** (2003) 115011, arXiv:hep-ph/0210299 [hep-ph].

[6] E. Eichten and K. Lane, *Low-scale technicolor at the Tevatron and LHC*, Phys. Lett. B **669** (2008) 235–238, arXiv:0706.2339 [hep-ph].

[7] F. Sannino and K. Tuominen, *Orientifold theory dynamics and symmetry breaking*, Phys. Rev. D **71** (2005) 051901, arXiv:hep-ph/0405209 [hep-ph].

[8] J. R. Andersen et al., *Discovering Technicolor*, Eur. Phys. J. Plus **126** (2011) 81, arXiv:1104.1255 [hep-ph].

[9] L. Randall and R. Sundrum, *A Large Mass Hierarchy from a Small Extra Dimension*, Phys. Rev. Lett. **83** (1999) 3370–3373, arXiv:hep-ph/9905221 [hep-ph].

[10] L. Randall and R. Sundrum, *An Alternative to Compactification*, Phys. Rev. Lett. **83** (1999) 4690–4693, arXiv:hep-th/9906064 [hep-th].

[11] H. Davoudiasl, J. L. Hewett and T. G. Rizzo, *Experimental probes of localized gravity: On and off the wall*, Phys. Rev. D **63** (2001) 075004, arXiv:hep-ph/0006041 [hep-ph].

[12] G. Altarelli, B. Mele and M. Ruiz-Altaba, *Searching for New Heavy Vector Bosons in $p\bar{p}$ Colliders*, Z. Phys. C **45** (1989) 109, [Erratum: Z. Phys. C 47, 676 (1990)].

[13] E. Eichten et al., *Super Collider Physics*, Rev. Mod. Phys. **56** (1984) 579–707, [Erratum: Rev. Mod. Phys. 58, 1065 (1986)].

[14] H. Georgi and S. L. Glashow, *Unity of All Elementary Particle Forces*, Phys. Rev. Lett. **32** (1974) 438–441.

[15] G. J. Gounaris, J. Layssac and F. M. Renard, *New and standard physics contributions to anomalous Z and γ self-couplings*, Phys. Rev. D **62** (2000) 073013, arXiv:hep-ph/0003143 [hep-ph].

[16] ATLAS Collaboration, *Measurement of ZZ production in pp collisions at $\sqrt{s} = 7$ TeV and limits on anomalous ZZZ and ZZγ couplings with the ATLAS detector*, JHEP **03** (2013) 128, arXiv:1211.6096 [hep-ex].

[17] CMS Collaboration, *Measurement of the ZZ production cross section and search for anomalous couplings in $2\ell 2\ell'$ final states in pp collisions at $\sqrt{s} = 7$ TeV*, JHEP **01** (2013) 063, arXiv:1211.4890 [hep-ex].

[18] ATLAS Collaboration, *Measurement of the ZZ Production Cross Section in pp Collisions at* $\sqrt{s}$ *= 13 TeV with the ATLAS Detector*, Phys. Rev. Lett. **116** (2016) 101801, arXiv:1512.05314 [hep-ex].

[19] ATLAS Collaboration, *Measurements of four-lepton production in pp collisions at* $\sqrt{s}$ *= 8 TeV with the ATLAS detector*, Phys. Lett. B **753** (2016) 552–572, arXiv:1509.07844 [hep-ex].

[20] CMS Collaboration, *Measurement of the* $pp \to ZZ$ *production cross section and constraints on anomalous triple gauge couplings in four-lepton final states at* $\sqrt{s}$ = 8 *TeV*, Phys. Lett. B **740** (2015) 250–272, arXiv:1406.0113 [hep-ex].

[21] K. Hagiwara et al., *Probing the Weak Boson Sector in* $e^+e^- \to W^+W^-$, Nucl. Phys. B **282** (1987) 253.

[22] The LEP Collaborations: ALEPH, DELPHI, L3, OPAL and the LEP Electroweak Working Group, *A Combination of Preliminary Electroweak Measurements and Constraints on the Standard Model*, (2006), arXiv:hep-ex/0612034 [hep-ex].

[23] DØ Collaboration, V. M. Abazov et al., *Search for ZZ and* $Z\gamma^*$ *production in* $p\bar{p}$ *collisions at* $\sqrt{s}$ = 1.96 *TeV and limits on anomalous ZZZ and* $ZZ\gamma^*$ *couplings*, Phys. Rev. Lett. **100** (2008) 131801, arXiv:0712.0599 [hep-ex].

[24] CMS Collaboration, *Measurements of the ZZ production cross sections in the* $2\ell 2\nu$ *channel in proton–proton collisions at* $\sqrt{s}$ = 7 *and* 8 *TeV and combined constraints on triple gauge couplings*, Eur. Phys. J. C **75** (2015) 511, arXiv:1503.05467 [hep-ex].

[25] ATLAS Collaboration, *The ATLAS Experiment at the CERN Large Hadron Collider*, JINST **3** (2008) S08003.

[26] ATLAS Collaboration, *Performance of the ATLAS Trigger System in 2010*, Eur. Phys. J. C **72** (2012) 1849, arXiv:1110.1530 [hep-ex].

[27] M. Cacciari, G. P. Salam and G. Soyez, *The anti-*k_t *jet clustering algorithm*, JHEP **04** (2008) 063, arXiv:0802.1189 [hep-ph].

[28] S. Alioli et al., *A general framework for implementing NLO calculations in shower Monte Carlo programs: the* POWHEGBox, JHEP **06** (2010) 043, arXiv:1002.2581 [hep-ph].

[29] T. Melia et al., W^+W^-*, WZ and ZZ production in the* POWHEGBox, JHEP **11** (2011) 078, arXiv:1107.5051 [hep-ph].

[30] N. Kauer and G. Passarino, *Inadequacy of zero-width approximation for a light Higgs boson signal*, JHEP **08** (2012) 116, arXiv:1206.4803 [hep-ph].

[31] N. Kauer, *Interference effects for* $H \to WW/ZZ \to \ell\bar{\nu}_\ell\bar{\ell}\nu_\ell$ *searches in gluon fusion at the LHC*, JHEP **12** (2013) 082, arXiv:1310.7011 [hep-ph].

[32] H.-L. Lai et al., *New parton distributions for collider physics*, Phys. Rev. D **82** (2010) 074024, arXiv:1007.2241 [hep-ph].

[33] A. Bierweiler, T. Kasprzik and J. H. Kühn, *Vector-boson pair production at the LHC to* $O(\alpha^3)$ *accuracy*, JHEP **12** (2013) 071, arXiv:1305.5402 [hep-ph].

[34] S. Gieseke, T. Kasprzik and J. H. Kühn,
Vector-boson pair production and electroweak corrections in HERWIG++,
Eur. Phys. J. C **74** (2014) 2988, arXiv:1401.3964 [hep-ph].

[35] J. Baglio, L. D. Ninh and M. M. Weber,
Massive gauge boson pair production at the LHC: a next-to-leading order story,
Phys. Rev. D **88** (2013) 113005, arXiv:1307.4331 [hep-ph].

[36] C. S. Li et al.,
Soft gluon resummation in the signal-background interference process of $gg(\to h^*) \to ZZ$,
JHEP **08** (2015) 065, arXiv:1504.02388 [hep-ph].

[37] F. Caola et al., *QCD corrections to ZZ production in gluon fusion at the LHC*,
Phys. Rev. D **92** (2015) 094028, arXiv:1509.06734 [hep-ph].

[38] G. Passarino, *Higgs CAT*, Eur. Phys. J. C **74** (2014) 2866, arXiv:1312.2397 [hep-ph].

[39] S. Dittmaier et al., *Handbook of LHC Higgs Cross Sections: 1. Inclusive Observables*, (2011),
arXiv:1101.0593 [hep-ph].

[40] I. W. Stewart and F. J. Tackmann,
Theory Uncertainties for Higgs and Other Searches Using Jet Bins,
Phys. Rev. D **85** (2012) 034011, arXiv:1107.2117 [hep-ph].

[41] M. Grazzini, S. Kallweit and D. Rathlev,
ZZ production at the LHC: fiducial cross sections and distributions in NNLO QCD,
Phys. Lett. B **750** (2015) 407–410, arXiv:1507.06257 [hep-ph].

[42] F. Cascioli et al., *ZZ production at hadron colliders in NNLO QCD*,
Phys. Lett. B **735** (2014) 311–313, arXiv:1405.2219 [hep-ph].

[43] ATLAS Collaboration, *The ATLAS Simulation Infrastructure*, Eur. Phys. J. C **70** (2010) 823–874,
arXiv:1005.4568 [physics.ins-det].

[44] T. Sjöstrand, S. Mrenna and P. Z. Skands, *A Brief Introduction to PYTHIA 8.1*,
Comput. Phys. Commun. **178** (2008) 852–867, arXiv:0710.3820 [hep-ph].

[45] G. Corcella et al., *HERWIG 6: An Event generator for hadron emission reactions with interfering gluons (including supersymmetric processes)*, JHEP **01** (2001) 010,
arXiv:hep-ph/0011363 [hep-ph].

[46] J. M. Butterworth, J. R. Forshaw and M. H. Seymour,
Multiparton interactions in photoproduction at HERA, Z. Phys. C **72** (1996) 637–646,
arXiv:hep-ph/9601371 [hep-ph].

[47] T. Gleisberg et al., *Event generation with* Sherpa *1.1*, JHEP **02** (2009) 007,
arXiv:0811.4622 [hep-ph].

[48] M. L. Mangano et al.,
ALPGEN, a generator for hard multiparton processes in hadronic collisions,
JHEP **07** (2003) 001, arXiv:hep-ph/0206293 [hep-ph].

[49] J. Pumplin et al.,
New generation of parton distributions with uncertainties from global QCD analysis,
JHEP **07** (2002) 012, arXiv:hep-ph/0201195 [hep-ph].

[50] T. Sjöstrand, S. Mrenna and P. Z. Skands, *PYTHIA 6.4 Physics and Manual*, JHEP **05** (2006) 026,
arXiv:hep-ph/0603175 [hep-ph].

[51] S. Frixione and B. R. Webber, *Matching NLO QCD computations and parton shower simulations*, JHEP **06** (2002) 029, arXiv:hep-ph/0204244 [hep-ph].

[52] S. Frixione et al., *Single-top production in MC@NLO*, JHEP **03** (2006) 092, arXiv:hep-ph/0512250 [hep-ph].

[53] B. P. Kersevan and E. Richter-Was, *The Monte Carlo event generator AcerMC versions 2.0 to 3.8 with interfaces to PYTHIA 6.4, HERWIG 6.5 and ARIADNE 4.1*, Comput. Phys. Commun. **184** (2013) 919–985, arXiv:hep-ph/0405247 [hep-ph].

[54] T. Stelzer and W. F. Long, *Automatic generation of tree level helicity amplitudes*, Comput. Phys. Commun. **81** (1994) 357–371, arXiv:hep-ph/9401258 [hep-ph].

[55] S. Agostinelli et al., *GEANT4: A Simulation Toolkit*, Nucl. Instrum. Meth. A **506** (2003) 250–303.

[56] ATLAS Collaboration, *Luminosity determination in pp collisions at $\sqrt{s}$= 8 TeV using the ATLAS detector at the LHC*, (2016), arXiv:1608.03953 [hep-ex].

[57] ATLAS Collaboration, *Performance of the ATLAS muon trigger in pp collisions at $\sqrt{s}$ = 8 TeV*, Eur. Phys. J. C **75** (2015) 120, arXiv:1408.3179 [hep-ex].

[58] ATLAS Collaboration, *Performance of the ATLAS Electron and Photon Trigger in pp Collisions at $\sqrt{s}$ = 7 TeV in 2011*, ATLAS-CONF-2012-048, 2012, URL: https://cds.cern.ch/record/1450089.

[59] ATLAS Collaboration, *Measurement of the muon reconstruction performance of the ATLAS detector using 2011 and 2012 LHC proton–proton collision data*, Eur. Phys. J. C **74** (2014) 3130, arXiv:1407.3935 [hep-ex].

[60] ATLAS Collaboration, *Electron efficiency measurements with the ATLAS detector using the 2012 LHC proton–proton collision data*, ATLAS-CONF-2014-032, 2014, URL: https://cds.cern.ch/record/1706245.

[61] ATLAS Collaboration, *Electron reconstruction and identification efficiency measurements with the ATLAS detector using the 2011 LHC proton–proton collision data*, Eur. Phys. J. C **74** (2014) 2941, arXiv:1404.2240 [hep-ex].

[62] ATLAS Collaboration, *Performance of Missing Transverse Momentum Reconstruction in ATLAS studied in Proton–Proton Collisions recorded in 2012 at $\sqrt{s}$ = 8 TeV*, ATLAS-CONF-2013-082, 2013, URL: https://cds.cern.ch/record/1570993.

[63] ATLAS Collaboration, *Jet energy measurement and its systematic uncertainty in proton–proton collisions at $\sqrt{s}$ = 7 TeV with the ATLAS detector*, Eur. Phys. J. C **75** (2015) 17, arXiv:1406.0076 [hep-ex].

[64] M. Cacciari and G. P. Salam, *Pileup subtraction using jet areas*, Phys. Lett. B **659** (2008) 119, arXiv:0707.1378 [hep-ph].

[65] ATLAS Collaboration, *Pile-up subtraction and suppression for jets in ATLAS*, ATLAS-CONF-2013-083, 2013, URL: https://cds.cern.ch/record/1570994.

[66] K. A. Olive et al., *Review of Particle Physics*, Chin. Phys. C **38** (2014) 090001.

[67] ATLAS Collaboration, *Measurement of the top quark pair cross section with ATLAS in pp collisions at $\sqrt{s}$ = 7 TeV using final states with an electron or a muon and a hadronically decaying τ lepton*, Phys. Lett. B **717** (2012) 89–108, arXiv:1205.2067 [hep-ex].

[68] ATLAS Collaboration,
Electron and photon energy calibration with the ATLAS detector using LHC Run 1 data,
Eur. Phys. J. C **74** (2014) 3071, arXiv:1407.5063 [hep-ex].

[69] ATLAS Collaboration, *Monte Carlo Calibration and Combination of In-situ Measurements of Jet Energy Scale, Jet Energy Resolution and Jet Mass in ATLAS*, ATLAS-CONF-2015-037, 2015, URL: https://cds.cern.ch/record/2044941.

[70] ATLAS Collaboration, *Data-driven determination of the energy scale and resolution of jets reconstructed in the ATLAS calorimeters using dijet and multijet events at* $\sqrt{s} = 8$ *TeV*, ATLAS-CONF-2015-017, 2015, URL: https://cds.cern.ch/record/2008678.

[71] ATLAS Collaboration,
Measurements of four-lepton production in pp collisions at $\sqrt{s} = 8$ *TeV with the ATLAS detector*,
Phys. Lett. B **753** (2016) 552–572, arXiv:1509.07844 [hep-ex].

[72] G.D'Agostini, *Improved iterative Bayesian unfolding*, (2010),
arXiv:1010.0632 [physics.data-an].

[73] B. Malaescu, *An Iterative, Dynamically Stabilized (IDS) Method for Data Unfolding*, (2011),
arXiv:1106.3107 [physics.data-an].

[74] R. Barate et al., *Measurement of the* $e^+e^- \to ZZ$ *production cross-section at center-of-mass energies of 183 GeV and 189 GeV*, Phys. Lett. B **469** (1999) 287–302,
arXiv:hep-ex/9911003 [hep-ex].

[75] J. Abdallah et al., *ZZ production in* e^+e^- *interactions at* $\sqrt{s} = 183$ *GeV to* 209 *GeV*,
Eur. Phys. J. C **30** (2003) 447–466, arXiv:hep-ex/0307050 [hep-ex].

[76] M. Acciarri et al., *Study of Z boson pair production in* e^+e^- *collisions at LEP at* $\sqrt{s} = 189$ *GeV*,
Phys. Lett. B **465** (1999) 363–375, arXiv:hep-ex/9909043 [hep-ex].

[77] G. Abbiendi et al., *Study of Z pair production and anomalous couplings in* e^+e^- *collisions at* $\sqrt{s}$ *between 190 GeV and 209 GeV*, Eur. Phys. J. C **32** (2003) 303–322,
arXiv:hep-ex/0310013 [hep-ex].

[78] U. Baur and D. L. Rainwater,
Probing neutral gauge boson self interactions in ZZ production at hadron colliders,
Phys. Rev. D **62** (2000) 113011, arXiv:hep-ph/0011016 [hep-ph].

[79] G. J. Gounaris, J. Layssac and F. M. Renard,
Off-shell structure of the anomalous Z and γ *self-couplings*, Phys. Rev. D **62** (2000) 073012,
arXiv:hep-ph/0005269 [hep-ph].

[80] G. Bella, *Weighting di-boson Monte Carlo events in hadron colliders*, (2008),
arXiv:0803.3307 [hep-ph].

[81] U. Baur, T. Han and J. Ohnemus,
QCD corrections and anomalous couplings in $Z\gamma$ *production at hadron colliders*,
Phys.Rev. D **57** (1998) 2823, arXiv:hep-ph/9710416 [hep-ph].

[82] G. Cowan et al., *Asymptotic formulae for likelihood-based tests of new physics*,
Eur. Phys. J. C **71** (2011) 1554, [Erratum: Eur. Phys. J. C 73, 2501 (2013)],
arXiv:1007.1727 [physics.data-an].

[83] G. J. Feldman and R. D. Cousins,
A Unified approach to the classical statistical analysis of small signals,
Phys. Rev. D **57** (1998) 3873–3889, arXiv:physics/9711021 [physics.data-an].

[84] ATLAS Collaboration, *ATLAS Computing Acknowledgements 2016-2017*, ATL-GEN-PUB-2016-002, 2016, URL: http://cds.cern.ch/record/2202407.

The ATLAS Collaboration

M. Aaboud[136d], G. Aad[87], B. Abbott[114], J. Abdallah[8], O. Abdinov[12], B. Abeloos[118], R. Aben[108], O.S. AbouZeid[138], N.L. Abraham[152], H. Abramowicz[156], H. Abreu[155], R. Abreu[117], Y. Abulaiti[149a,149b], B.S. Acharya[168a,168b,a], S. Adachi[158], L. Adamczyk[40a], D.L. Adams[27], J. Adelman[109], S. Adomeit[101], T. Adye[132], A.A. Affolder[76], T. Agatonovic-Jovin[14], J.A. Aguilar-Saavedra[127a,127f], S.P. Ahlen[24], F. Ahmadov[67,b], G. Aielli[134a,134b], H. Akerstedt[149a,149b], T.P.A. Åkesson[83], A.V. Akimov[97], G.L. Alberghi[22a,22b], J. Albert[173], S. Albrand[57], M.J. Alconada Verzini[73], M. Aleksa[32], I.N. Aleksandrov[67], C. Alexa[28b], G. Alexander[156], T. Alexopoulos[10], M. Alhroob[114], B. Ali[129], M. Aliev[75a,75b], G. Alimonti[93a], J. Alison[33], S.P. Alkire[37], B.M.M. Allbrooke[152], B.W. Allen[117], P.P. Allport[19], A. Aloisio[105a,105b], A. Alonso[38], F. Alonso[73], C. Alpigiani[139], A.A. Alshehri[55], M. Alstaty[87], B. Alvarez Gonzalez[32], D. Álvarez Piqueras[171], M.G. Alviggi[105a,105b], B.T. Amadio[16], K. Amako[68], Y. Amaral Coutinho[26a], C. Amelung[25], D. Amidei[91], S.P. Amor Dos Santos[127a,127c], A. Amorim[127a,127b], S. Amoroso[32], G. Amundsen[25], C. Anastopoulos[142], L.S. Ancu[51], N. Andari[19], T. Andeen[11], C.F. Anders[60b], G. Anders[32], J.K. Anders[76], K.J. Anderson[33], A. Andreazza[93a,93b], V. Andrei[60a], S. Angelidakis[9], I. Angelozzi[108], A. Angerami[37], F. Anghinolfi[32], A.V. Anisenkov[110,c], N. Anjos[13], A. Annovi[125a,125b], C. Antel[60a], M. Antonelli[49], A. Antonov[99,*], F. Anulli[133a], M. Aoki[68], L. Aperio Bella[19], G. Arabidze[92], Y. Arai[68], J.P. Araque[127a], A.T.H. Arce[47], F.A. Arduh[73], J-F. Arguin[96], S. Argyropoulos[65], M. Arik[20a], A.J. Armbruster[146], L.J. Armitage[78], O. Arnaez[32], H. Arnold[50], M. Arratia[30], O. Arslan[23], A. Artamonov[98], G. Artoni[121], S. Artz[85], S. Asai[158], N. Asbah[44], A. Ashkenazi[156], B. Åsman[149a,149b], L. Asquith[152], K. Assamagan[27], R. Astalos[147a], M. Atkinson[170], N.B. Atlay[144], K. Augsten[129], G. Avolio[32], B. Axen[16], M.K. Ayoub[118], G. Azuelos[96,d], M.A. Baak[32], A.E. Baas[60a], M.J. Baca[19], H. Bachacou[137], K. Bachas[75a,75b], M. Backes[121], M. Backhaus[32], P. Bagiacchi[133a,133b], P. Bagnaia[133a,133b], Y. Bai[35a], J.T. Baines[132], O.K. Baker[180], E.M. Baldin[110,c], P. Balek[176], T. Balestri[151], F. Balli[137], W.K. Balunas[123], E. Banas[41], Sw. Banerjee[177,e], A.A.E. Bannoura[179], L. Barak[32], E.L. Barberio[90], D. Barberis[52a,52b], M. Barbero[87], T. Barillari[102], M-S Barisits[32], T. Barklow[146], N. Barlow[30], S.L. Barnes[86], B.M. Barnett[132], R.M. Barnett[16], Z. Barnovska-Blenessy[59], A. Baroncelli[135a], G. Barone[25], A.J. Barr[121], L. Barranco Navarro[171], F. Barreiro[84], J. Barreiro Guimarães da Costa[35a], R. Bartoldus[146], A.E. Barton[74], P. Bartos[147a], A. Basalaev[124], A. Bassalat[118,f], R.L. Bates[55], S.J. Batista[162], J.R. Batley[30], M. Battaglia[138], M. Bauce[133a,133b], F. Bauer[137], H.S. Bawa[146,g], J.B. Beacham[112], M.D. Beattie[74], T. Beau[82], P.H. Beauchemin[166], P. Bechtle[23], H.P. Beck[18,h], K. Becker[121], M. Becker[85], M. Beckingham[174], C. Becot[111], A.J. Beddall[20e], A. Beddall[20b], V.A. Bednyakov[67], M. Bedognetti[108], C.P. Bee[151], L.J. Beemster[108], T.A. Beermann[32], M. Begel[27], J.K. Behr[44], C. Belanger-Champagne[89], A.S. Bell[80], G. Bella[156], L. Bellagamba[22a], A. Bellerive[31], M. Bellomo[88], K. Belotskiy[99], O. Beltramello[32], N.L. Belyaev[99], O. Benary[156,*], D. Benchekroun[136a], M. Bender[101], K. Bendtz[149a,149b], N. Benekos[10], Y. Benhammou[156], E. Benhar Noccioli[180], J. Benitez[65], D.P. Benjamin[47], J.R. Bensinger[25], S. Bentvelsen[108], L. Beresford[121], M. Beretta[49], D. Berge[108], E. Bergeaas Kuutmann[169], N. Berger[5], J. Beringer[16], S. Berlendis[57], N.R. Bernard[88], C. Bernius[111], F.U. Bernlochner[23], T. Berry[79], P. Berta[130], C. Bertella[85], G. Bertoli[149a,149b], F. Bertolucci[125a,125b], I.A. Bertram[74], C. Bertsche[44], D. Bertsche[114], G.J. Besjes[38], O. Bessidskaia Bylund[149a,149b], M. Bessner[44], N. Besson[137], C. Betancourt[50], A. Bethani[57], S. Bethke[102], A.J. Bevan[78], R.M. Bianchi[126], L. Bianchini[25], M. Bianco[32], O. Biebel[101], D. Biedermann[17], R. Bielski[86], N.V. Biesuz[125a,125b], M. Biglietti[135a], J. Bilbao De Mendizabal[51], T.R.V. Billoud[96], H. Bilokon[49], M. Bindi[56], S. Binet[118], A. Bingul[20b], C. Bini[133a,133b], S. Biondi[22a,22b], T. Bisanz[56], D.M. Bjergaard[47], C.W. Black[153], J.E. Black[146], K.M. Black[24], D. Blackburn[139], R.E. Blair[6], J.-B. Blanchard[137], T. Blazek[147a], I. Bloch[44], C. Blocker[25], A. Blue[55], W. Blum[85,*],

U. Blumenschein[56], S. Blunier[34a], G.J. Bobbink[108], V.S. Bobrovnikov[110,c], S.S. Bocchetta[83], A. Bocci[47], C. Bock[101], M. Boehler[50], D. Boerner[179], J.A. Bogaerts[32], D. Bogavac[14], A.G. Bogdanchikov[110], C. Bohm[149a], V. Boisvert[79], P. Bokan[14], T. Bold[40a], A.S. Boldyrev[168a,168c], M. Bomben[82], M. Bona[78], M. Boonekamp[137], A. Borisov[131], G. Borissov[74], J. Bortfeldt[32], D. Bortoletto[121], V. Bortolotto[62a,62b,62c], K. Bos[108], D. Boscherini[22a], M. Bosman[13], J.D. Bossio Sola[29], J. Boudreau[126], J. Bouffard[2], E.V. Bouhova-Thacker[74], D. Boumediene[36], C. Bourdarios[118], S.K. Boutle[55], A. Boveia[32], J. Boyd[32], I.R. Boyko[67], J. Bracinik[19], A. Brandt[8], G. Brandt[56], O. Brandt[60a], U. Bratzler[159], B. Brau[88], J.E. Brau[117], W.D. Breaden Madden[55], K. Brendlinger[123], A.J. Brennan[90], L. Brenner[108], R. Brenner[169], S. Bressler[176], T.M. Bristow[48], D. Britton[55], D. Britzger[44], F.M. Brochu[30], I. Brock[23], R. Brock[92], G. Brooijmans[37], T. Brooks[79], W.K. Brooks[34b], J. Brosamer[16], E. Brost[109], J.H Broughton[19], P.A. Bruckman de Renstrom[41], D. Bruncko[147b], R. Bruneliere[50], A. Bruni[22a], G. Bruni[22a], L.S. Bruni[108], BH Brunt[30], M. Bruschi[22a], N. Bruscino[23], P. Bryant[33], L. Bryngemark[83], T. Buanes[15], Q. Buat[145], P. Buchholz[144], A.G. Buckley[55], I.A. Budagov[67], F. Buehrer[50], M.K. Bugge[120], O. Bulekov[99], D. Bullock[8], H. Burckhart[32], S. Burdin[76], C.D. Burgard[50], B. Burghgrave[109], K. Burka[41], S. Burke[132], I. Burmeister[45], J.T.P. Burr[121], E. Busato[36], D. Büscher[50], V. Büscher[85], P. Bussey[55], J.M. Butler[24], C.M. Buttar[55], J.M. Butterworth[80], P. Butti[108], W. Buttinger[27], A. Buzatu[55], A.R. Buzykaev[110,c], S. Cabrera Urbán[171], D. Caforio[129], V.M. Cairo[39a,39b], O. Cakir[4a], N. Calace[51], P. Calafiura[16], A. Calandri[87], G. Calderini[82], P. Calfayan[63], G. Callea[39a,39b], L.P. Caloba[26a], S. Calvente Lopez[84], D. Calvet[36], S. Calvet[36], T.P. Calvet[87], R. Camacho Toro[33], S. Camarda[32], P. Camarri[134a,134b], D. Cameron[120], R. Caminal Armadans[170], C. Camincher[57], S. Campana[32], M. Campanelli[80], A. Camplani[93a,93b], A. Campoverde[144], V. Canale[105a,105b], A. Canepa[164a], M. Cano Bret[141], J. Cantero[115], T. Cao[42], M.D.M. Capeans Garrido[32], I. Caprini[28b], M. Caprini[28b], M. Capua[39a,39b], R.M. Carbone[37], R. Cardarelli[134a], F. Cardillo[50], I. Carli[130], T. Carli[32], G. Carlino[105a], L. Carminati[93a,93b], R.M.D. Carney[149a,149b], S. Caron[107], E. Carquin[34b], G.D. Carrillo-Montoya[32], J.R. Carter[30], J. Carvalho[127a,127c], D. Casadei[19], M.P. Casado[13,i], M. Casolino[13], D.W. Casper[167], E. Castaneda-Miranda[148a], R. Castelijn[108], A. Castelli[108], V. Castillo Gimenez[171], N.F. Castro[127a,j], A. Catinaccio[32], J.R. Catmore[120], A. Cattai[32], J. Caudron[23], V. Cavaliere[170], E. Cavallaro[13], D. Cavalli[93a], M. Cavalli-Sforza[13], V. Cavasinni[125a,125b], F. Ceradini[135a,135b], L. Cerda Alberich[171], A.S. Cerqueira[26b], A. Cerri[152], L. Cerrito[134a,134b], F. Cerutti[16], M. Cerv[32], A. Cervelli[18], S.A. Cetin[20d], A. Chafaq[136a], D. Chakraborty[109], S.K. Chan[58], Y.L. Chan[62a], P. Chang[170], J.D. Chapman[30], D.G. Charlton[19], A. Chatterjee[51], C.C. Chau[162], C.A. Chavez Barajas[152], S. Che[112], S. Cheatham[168a,168c], A. Chegwidden[92], S. Chekanov[6], S.V. Chekulaev[164a], G.A. Chelkov[67,k], M.A. Chelstowska[91], C. Chen[66], H. Chen[27], K. Chen[151], S. Chen[35b], S. Chen[158], X. Chen[35c], Y. Chen[69], H.C. Cheng[91], H.J Cheng[35a], Y. Cheng[33], A. Cheplakov[67], E. Cheremushkina[131], R. Cherkaoui El Moursli[136e], V. Chernyatin[27,*], E. Cheu[7], L. Chevalier[137], V. Chiarella[49], G. Chiarelli[125a,125b], G. Chiodini[75a], A.S. Chisholm[32], A. Chitan[28b], M.V. Chizhov[67], K. Choi[63], A.R. Chomont[36], S. Chouridou[9], B.K.B. Chow[101], V. Christodoulou[80], D. Chromek-Burckhart[32], J. Chudoba[128], A.J. Chuinard[89], J.J. Chwastowski[41], L. Chytka[116], G. Ciapetti[133a,133b], A.K. Ciftci[4a], D. Cinca[45], V. Cindro[77], I.A. Cioara[23], C. Ciocca[22a,22b], A. Ciocio[16], F. Cirotto[105a,105b], Z.H. Citron[176], M. Citterio[93a], M. Ciubancan[28b], A. Clark[51], B.L. Clark[58], M.R. Clark[37], P.J. Clark[48], R.N. Clarke[16], C. Clement[149a,149b], Y. Coadou[87], M. Cobal[168a,168c], A. Coccaro[51], J. Cochran[66], L. Colasurdo[107], B. Cole[37], A.P. Colijn[108], J. Collot[57], T. Colombo[167], G. Compostella[102], P. Conde Muiño[127a,127b], E. Coniavitis[50], S.H. Connell[148b], I.A. Connelly[79], V. Consorti[50], S. Constantinescu[28b], G. Conti[32], F. Conventi[105a,l], M. Cooke[16], B.D. Cooper[80], A.M. Cooper-Sarkar[121], K.J.R. Cormier[162], T. Cornelissen[179], M. Corradi[133a,133b], F. Corriveau[89,m], A. Cortes-Gonzalez[32], G. Cortiana[102], G. Costa[93a], M.J. Costa[171], D. Costanzo[142], G. Cottin[30], G. Cowan[79], B.E. Cox[86], K. Cranmer[111], S.J. Crawley[55], G. Cree[31], S. Crépé-Renaudin[57], F. Crescioli[82], W.A. Cribbs[149a,149b],

M. Crispin Ortuzar[121], M. Cristinziani[23], V. Croft[107], G. Crosetti[39a,39b], A. Cueto[84], T. Cuhadar Donszelmann[142], J. Cummings[180], M. Curatolo[49], J. Cúth[85], H. Czirr[144], P. Czodrowski[3], G. D'amen[22a,22b], S. D'Auria[55], M. D'Onofrio[76], M.J. Da Cunha Sargedas De Sousa[127a,127b], C. Da Via[86], W. Dabrowski[40a], T. Dado[147a], T. Dai[91], O. Dale[15], F. Dallaire[96], C. Dallapiccola[88], M. Dam[38], J.R. Dandoy[33], N.P. Dang[50], A.C. Daniells[19], N.S. Dann[86], M. Danninger[172], M. Dano Hoffmann[137], V. Dao[50], G. Darbo[52a], S. Darmora[8], J. Dassoulas[3], A. Dattagupta[117], W. Davey[23], C. David[173], T. Davidek[130], M. Davies[156], P. Davison[80], E. Dawe[90], I. Dawson[142], K. De[8], R. de Asmundis[105a], A. De Benedetti[114], S. De Castro[22a,22b], S. De Cecco[82], N. De Groot[107], P. de Jong[108], H. De la Torre[92], F. De Lorenzi[66], A. De Maria[56], D. De Pedis[133a], A. De Salvo[133a], U. De Sanctis[152], A. De Santo[152], J.B. De Vivie De Regie[118], W.J. Dearnaley[74], R. Debbe[27], C. Debenedetti[138], D.V. Dedovich[67], N. Dehghanian[3], I. Deigaard[108], M. Del Gaudio[39a,39b], J. Del Peso[84], T. Del Prete[125a,125b], D. Delgove[118], F. Deliot[137], C.M. Delitzsch[51], A. Dell'Acqua[32], L. Dell'Asta[24], M. Dell'Orso[125a,125b], M. Della Pietra[105a,l], D. della Volpe[51], M. Delmastro[5], P.A. Delsart[57], D.A. DeMarco[162], S. Demers[180], M. Demichev[67], A. Demilly[82], S.P. Denisov[131], D. Denysiuk[137], D. Derendarz[41], J.E. Derkaoui[136d], F. Derue[82], P. Dervan[76], K. Desch[23], C. Deterre[44], K. Dette[45], P.O. Deviveiros[32], A. Dewhurst[132], S. Dhaliwal[25], A. Di Ciaccio[134a,134b], L. Di Ciaccio[5], W.K. Di Clemente[123], C. Di Donato[105a,105b], A. Di Girolamo[32], B. Di Girolamo[32], B. Di Micco[135a,135b], R. Di Nardo[32], A. Di Simone[50], R. Di Sipio[162], D. Di Valentino[31], C. Diaconu[87], M. Diamond[162], F.A. Dias[48], M.A. Diaz[34a], E.B. Diehl[91], J. Dietrich[17], S. Díez Cornell[44], A. Dimitrievska[14], J. Dingfelder[23], P. Dita[28b], S. Dita[28b], F. Dittus[32], F. Djama[87], T. Djobava[53b], J.I. Djuvsland[60a], M.A.B. do Vale[26c], D. Dobos[32], M. Dobre[28b], C. Doglioni[83], J. Dolejsi[130], Z. Dolezal[130], M. Donadelli[26d], S. Donati[125a,125b], P. Dondero[122a,122b], J. Donini[36], J. Dopke[132], A. Doria[105a], M.T. Dova[73], A.T. Doyle[55], E. Drechsler[56], M. Dris[10], Y. Du[140], J. Duarte-Campderros[156], E. Duchovni[176], G. Duckeck[101], O.A. Ducu[96,n], D. Duda[108], A. Dudarev[32], A.Chr. Dudder[85], E.M. Duffield[16], L. Duflot[118], M. Dührssen[32], M. Dumancic[176], M. Dunford[60a], H. Duran Yildiz[4a], M. Düren[54], A. Durglishvili[53b], D. Duschinger[46], B. Dutta[44], M. Dyndal[44], C. Eckardt[44], K.M. Ecker[102], R.C. Edgar[91], N.C. Edwards[48], T. Eifert[32], G. Eigen[15], K. Einsweiler[16], T. Ekelof[169], M. El Kacimi[136c], V. Ellajosyula[87], M. Ellert[169], S. Elles[5], F. Ellinghaus[179], A.A. Elliot[173], N. Ellis[32], J. Elmsheuser[27], M. Elsing[32], D. Emeliyanov[132], Y. Enari[158], O.C. Endner[85], J.S. Ennis[174], J. Erdmann[45], A. Ereditato[18], G. Ernis[179], J. Ernst[2], M. Ernst[27], S. Errede[170], E. Ertel[85], M. Escalier[118], H. Esch[45], C. Escobar[126], B. Esposito[49], A.I. Etienvre[137], E. Etzion[156], H. Evans[63], A. Ezhilov[124], M. Ezzi[136e], F. Fabbri[22a,22b], L. Fabbri[22a,22b], G. Facini[33], R.M. Fakhrutdinov[131], S. Falciano[133a], R.J. Falla[80], J. Faltova[32], Y. Fang[35a], M. Fanti[93a,93b], A. Farbin[8], A. Farilla[135a], C. Farina[126], E.M. Farina[122a,122b], T. Farooque[13], S. Farrell[16], S.M. Farrington[174], P. Farthouat[32], F. Fassi[136e], P. Fassnacht[32], D. Fassouliotis[9], M. Faucci Giannelli[79], A. Favareto[52a,52b], W.J. Fawcett[121], L. Fayard[118], O.L. Fedin[124,o], W. Fedorko[172], S. Feigl[120], L. Feligioni[87], C. Feng[140], E.J. Feng[32], H. Feng[91], A.B. Fenyuk[131], L. Feremenga[8], P. Fernandez Martinez[171], S. Fernandez Perez[13], J. Ferrando[44], A. Ferrari[169], P. Ferrari[108], R. Ferrari[122a], D.E. Ferreira de Lima[60b], A. Ferrer[171], D. Ferrere[51], C. Ferretti[91], A. Ferretto Parodi[52a,52b], F. Fiedler[85], A. Filipčič[77], M. Filipuzzi[44], F. Filthaut[107], M. Fincke-Keeler[173], K.D. Finelli[153], M.C.N. Fiolhais[127a,127c], L. Fiorini[171], A. Firan[42], A. Fischer[2], C. Fischer[13], J. Fischer[179], W.C. Fisher[92], N. Flaschel[44], I. Fleck[144], P. Fleischmann[91], G.T. Fletcher[142], R.R.M. Fletcher[123], T. Flick[179], L.R. Flores Castillo[62a], M.J. Flowerdew[102], G.T. Forcolin[86], A. Formica[137], A. Forti[86], A.G. Foster[19], D. Fournier[118], H. Fox[74], S. Fracchia[13], P. Francavilla[82], M. Franchini[22a,22b], D. Francis[32], L. Franconi[120], M. Franklin[58], M. Frate[167], M. Fraternali[122a,122b], D. Freeborn[80], S.M. Fressard-Batraneanu[32], F. Friedrich[46], D. Froidevaux[32], J.A. Frost[121], C. Fukunaga[159], E. Fullana Torregrosa[85], T. Fusayasu[103], J. Fuster[171], C. Gabaldon[57], O. Gabizon[155], A. Gabrielli[22a,22b], A. Gabrielli[16], G.P. Gach[40a], S. Gadatsch[32], S. Gadomski[79], G. Gagliardi[52a,52b], L.G. Gagnon[96],

P. Gagnon[63], C. Galea[107], B. Galhardo[127a,127c], E.J. Gallas[121], B.J. Gallop[132], P. Gallus[129], G. Galster[38], K.K. Gan[112], J. Gao[59], Y. Gao[48], Y.S. Gao[146,g], F.M. Garay Walls[48], C. García[171], J.E. García Navarro[171], M. Garcia-Sciveres[16], R.W. Gardner[33], N. Garelli[146], V. Garonne[120], A. Gascon Bravo[44], K. Gasnikova[44], C. Gatti[49], A. Gaudiello[52a,52b], G. Gaudio[122a], L. Gauthier[96], I.L. Gavrilenko[97], C. Gay[172], G. Gaycken[23], E.N. Gazis[10], Z. Gecse[172], C.N.P. Gee[132], Ch. Geich-Gimbel[23], M. Geisen[85], M.P. Geisler[60a], K. Gellerstedt[149a,149b], C. Gemme[52a], M.H. Genest[57], C. Geng[59,p], S. Gentile[133a,133b], C. Gentsos[157], S. George[79], D. Gerbaudo[13], A. Gershon[156], S. Ghasemi[144], M. Ghneimat[23], B. Giacobbe[22a], S. Giagu[133a,133b], P. Giannetti[125a,125b], B. Gibbard[27], S.M. Gibson[79], M. Gignac[172], M. Gilchriese[16], T.P.S. Gillam[30], D. Gillberg[31], G. Gilles[179], D.M. Gingrich[3,d], N. Giokaris[9], M.P. Giordani[168a,168c], F.M. Giorgi[22a], F.M. Giorgi[17], P.F. Giraud[137], P. Giromini[58], D. Giugni[93a], F. Giuli[121], C. Giuliani[102], M. Giulini[60b], B.K. Gjelsten[120], S. Gkaitatzis[157], I. Gkialas[157], E.L. Gkougkousis[118], L.K. Gladilin[100], C. Glasman[84], J. Glatzer[50], P.C.F. Glaysher[48], A. Glazov[44], M. Goblirsch-Kolb[25], J. Godlewski[41], S. Goldfarb[90], T. Golling[51], D. Golubkov[131], A. Gomes[127a,127b,127d], R. Gonçalo[127a], J. Goncalves Pinto Firmino Da Costa[137], G. Gonella[50], L. Gonella[19], A. Gongadze[67], S. González de la Hoz[171], S. Gonzalez-Sevilla[51], L. Goossens[32], P.A. Gorbounov[98], H.A. Gordon[27], I. Gorelov[106], B. Gorini[32], E. Gorini[75a,75b], A. Gorišek[77], E. Gornicki[41], A.T. Goshaw[47], C. Gössling[45], M.I. Gostkin[67], C.R. Goudet[118], D. Goujdami[136c], A.G. Goussiou[139], N. Govender[148b,q], E. Gozani[155], L. Graber[56], I. Grabowska-Bold[40a], P.O.J. Gradin[57], P. Grafström[22a,22b], J. Gramling[51], E. Gramstad[120], S. Grancagnolo[17], V. Gratchev[124], P.M. Gravila[28e], H.M. Gray[32], E. Graziani[135a], Z.D. Greenwood[81,r], C. Grefe[23], K. Gregersen[80], I.M. Gregor[44], P. Grenier[146], K. Grevtsov[5], J. Griffiths[8], A.A. Grillo[138], K. Grimm[74], S. Grinstein[13,s], Ph. Gris[36], J.-F. Grivaz[118], S. Groh[85], E. Gross[176], J. Grosse-Knetter[56], G.C. Grossi[81], Z.J. Grout[80], L. Guan[91], W. Guan[177], J. Guenther[64], F. Guescini[51], D. Guest[167], O. Gueta[156], B. Gui[112], E. Guido[52a,52b], T. Guillemin[5], S. Guindon[2], U. Gul[55], C. Gumpert[32], J. Guo[141], Y. Guo[59,p], R. Gupta[42], S. Gupta[121], G. Gustavino[133a,133b], P. Gutierrez[114], N.G. Gutierrez Ortiz[80], C. Gutschow[46], C. Guyot[137], C. Gwenlan[121], C.B. Gwilliam[76], A. Haas[111], C. Haber[16], H.K. Hadavand[8], N. Haddad[136e], A. Hadef[87], S. Hageböck[23], M. Hagihara[165], Z. Hajduk[41], H. Hakobyan[181,*], M. Haleem[44], J. Haley[115], G. Halladjian[92], G.D. Hallewell[87], K. Hamacher[179], P. Hamal[116], K. Hamano[173], A. Hamilton[148a], G.N. Hamity[142], P.G. Hamnett[44], L. Han[59], K. Hanagaki[68,t], K. Hanawa[158], M. Hance[138], B. Haney[123], P. Hanke[60a], R. Hanna[137], J.B. Hansen[38], J.D. Hansen[38], M.C. Hansen[23], P.H. Hansen[38], K. Hara[165], A.S. Hard[177], T. Harenberg[179], F. Hariri[118], S. Harkusha[94], R.D. Harrington[48], P.F. Harrison[174], F. Hartjes[108], N.M. Hartmann[101], M. Hasegawa[69], Y. Hasegawa[143], A. Hasib[114], S. Hassani[137], S. Haug[18], R. Hauser[92], L. Hauswald[46], M. Havranek[128], C.M. Hawkes[19], R.J. Hawkings[32], D. Hayakawa[160], D. Hayden[92], C.P. Hays[121], J.M. Hays[78], H.S. Hayward[76], S.J. Haywood[132], S.J. Head[19], T. Heck[85], V. Hedberg[83], L. Heelan[8], S. Heim[123], T. Heim[16], B. Heinemann[16], J.J. Heinrich[101], L. Heinrich[111], C. Heinz[54], J. Hejbal[128], L. Helary[32], S. Hellman[149a,149b], C. Helsens[32], J. Henderson[121], R.C.W. Henderson[74], Y. Heng[177], S. Henkelmann[172], A.M. Henriques Correia[32], S. Henrot-Versille[118], G.H. Herbert[17], H. Herde[25], V. Herget[178], Y. Hernández Jiménez[148c], G. Herten[50], R. Hertenberger[101], L. Hervas[32], G.G. Hesketh[80], N.P. Hessey[108], J.W. Hetherly[42], R. Hickling[78], E. Higón-Rodriguez[171], E. Hill[173], J.C. Hill[30], K.H. Hiller[44], S.J. Hillier[19], I. Hinchliffe[16], E. Hines[123], R.R. Hinman[16], M. Hirose[50], D. Hirschbuehl[179], J. Hobbs[151], N. Hod[164a], M.C. Hodgkinson[142], P. Hodgson[142], A. Hoecker[32], M.R. Hoeferkamp[106], F. Hoenig[101], D. Hohn[23], T.R. Holmes[16], M. Homann[45], T. Honda[68], T.M. Hong[126], B.H. Hooberman[170], W.H. Hopkins[117], Y. Horii[104], A.J. Horton[145], J-Y. Hostachy[57], S. Hou[154], A. Hoummada[136a], J. Howarth[44], J. Hoya[73], M. Hrabovsky[116], I. Hristova[17], J. Hrivnac[118], T. Hryn'ova[5], A. Hrynevich[95], C. Hsu[148c], P.J. Hsu[154,u], S.-C. Hsu[139], Q. Hu[59], S. Hu[141], Y. Huang[44], Z. Hubacek[129], F. Hubaut[87], F. Huegging[23], T.B. Huffman[121], E.W. Hughes[37], G. Hughes[74], M. Huhtinen[32], P. Huo[151], N. Huseynov[67,b], J. Huston[92],

J. Huth[58], G. Iacobucci[51], G. Iakovidis[27], I. Ibragimov[144], L. Iconomidou-Fayard[118], E. Ideal[180], Z. Idrissi[136e], P. Iengo[32], O. Igonkina[108,v], T. Iizawa[175], Y. Ikegami[68], M. Ikeno[68], Y. Ilchenko[11,w], D. Iliadis[157], N. Ilic[146], T. Ince[102], G. Introzzi[122a,122b], P. Ioannou[9,*], M. Iodice[135a], K. Iordanidou[37], V. Ippolito[58], N. Ishijima[119], M. Ishino[158], M. Ishitsuka[160], R. Ishmukhametov[112], C. Issever[121], S. Istin[20a], F. Ito[165], J.M. Iturbe Ponce[86], R. Iuppa[163a,163b], W. Iwanski[64], H. Iwasaki[68], J.M. Izen[43], V. Izzo[105a], S. Jabbar[3], B. Jackson[123], P. Jackson[1], V. Jain[2], K.B. Jakobi[85], K. Jakobs[50], S. Jakobsen[32], T. Jakoubek[128], D.O. Jamin[115], D.K. Jana[81], R. Jansky[64], J. Janssen[23], M. Janus[56], G. Jarlskog[83], N. Javadov[67,b], T. Javůrek[50], F. Jeanneau[137], L. Jeanty[16], G.-Y. Jeng[153], D. Jennens[90], P. Jenni[50,x], C. Jeske[174], S. Jézéquel[5], H. Ji[177], J. Jia[151], H. Jiang[66], Y. Jiang[59], Z. Jiang[146], S. Jiggins[80], J. Jimenez Pena[171], S. Jin[35a], A. Jinaru[28b], O. Jinnouchi[160], H. Jivan[148c], P. Johansson[142], K.A. Johns[7], W.J. Johnson[139], K. Jon-And[149a,149b], G. Jones[174], R.W.L. Jones[74], S. Jones[7], T.J. Jones[76], J. Jongmanns[60a], P.M. Jorge[127a,127b], J. Jovicevic[164a], X. Ju[177], A. Juste Rozas[13,s], M.K. Köhler[176], A. Kaczmarska[41], M. Kado[118], H. Kagan[112], M. Kagan[146], S.J. Kahn[87], T. Kaji[175], E. Kajomovitz[47], C.W. Kalderon[121], A. Kaluza[85], S. Kama[42], A. Kamenshchikov[131], N. Kanaya[158], S. Kaneti[30], L. Kanjir[77], V.A. Kantserov[99], J. Kanzaki[68], B. Kaplan[111], L.S. Kaplan[177], A. Kapliy[33], D. Kar[148c], K. Karakostas[10], A. Karamaoun[3], N. Karastathis[10], M.J. Kareem[56], E. Karentzos[10], M. Karnevskiy[85], S.N. Karpov[67], Z.M. Karpova[67], K. Karthik[111], V. Kartvelishvili[74], A.N. Karyukhin[131], K. Kasahara[165], L. Kashif[177], R.D. Kass[112], A. Kastanas[150], Y. Kataoka[158], C. Kato[158], A. Katre[51], J. Katzy[44], K. Kawade[104], K. Kawagoe[72], T. Kawamoto[158], G. Kawamura[56], V.F. Kazanin[110,c], R. Keeler[173], R. Kehoe[42], J.S. Keller[44], J.J. Kempster[79], H. Keoshkerian[162], O. Kepka[128], B.P. Kerševan[77], S. Kersten[179], R.A. Keyes[89], M. Khader[170], F. Khalil-zada[12], A. Khanov[115], A.G. Kharlamov[110,c], T. Kharlamova[110], T.J. Khoo[51], V. Khovanskiy[98], E. Khramov[67], J. Khubua[53b,y], S. Kido[69], C.R. Kilby[79], H.Y. Kim[8], S.H. Kim[165], Y.K. Kim[33], N. Kimura[157], O.M. Kind[17], B.T. King[76], M. King[171], J. Kirk[132], A.E. Kiryunin[102], T. Kishimoto[158], D. Kisielewska[40a], F. Kiss[50], K. Kiuchi[165], O. Kivernyk[137], E. Kladiva[147b], M.H. Klein[37], M. Klein[76], U. Klein[76], K. Kleinknecht[85], P. Klimek[109], A. Klimentov[27], R. Klingenberg[45], J.A. Klinger[142], T. Klioutchnikova[32], E.-E. Kluge[60a], P. Kluit[108], S. Kluth[102], J. Knapik[41], E. Kneringer[64], E.B.F.G. Knoops[87], A. Knue[55], A. Kobayashi[158], D. Kobayashi[160], T. Kobayashi[158], M. Kobel[46], M. Kocian[146], P. Kodys[130], N.M. Koehler[102], T. Koffas[31], E. Koffeman[108], T. Koi[146], H. Kolanoski[17], M. Kolb[60b], I. Koletsou[5], A.A. Komar[97,*], Y. Komori[158], T. Kondo[68], N. Kondrashova[44], K. Köneke[50], A.C. König[107], T. Kono[68,z], R. Konoplich[111,aa], N. Konstantinidis[80], R. Kopeliansky[63], S. Koperny[40a], L. Köpke[85], A.K. Kopp[50], K. Korcyl[41], K. Kordas[157], A. Korn[80], A.A. Korol[110,c], I. Korolkov[13], E.V. Korolkova[142], O. Kortner[102], S. Kortner[102], T. Kosek[130], V.V. Kostyukhin[23], A. Kotwal[47], A. Koulouris[10], A. Kourkoumeli-Charalampidi[122a,122b], C. Kourkoumelis[9], V. Kouskoura[27], A.B. Kowalewska[41], R. Kowalewski[173], T.Z. Kowalski[40a], C. Kozakai[158], W. Kozanecki[137], A.S. Kozhin[131], V.A. Kramarenko[100], G. Kramberger[77], D. Krasnopevtsev[99], M.W. Krasny[82], A. Krasznahorkay[32], A. Kravchenko[27], M. Kretz[60c], J. Kretzschmar[76], K. Kreutzfeldt[54], P. Krieger[162], K. Krizka[33], K. Kroeninger[45], H. Kroha[102], J. Kroll[123], J. Kroseberg[23], J. Krstic[14], U. Kruchonak[67], H. Krüger[23], N. Krumnack[66], M.C. Kruse[47], M. Kruskal[24], T. Kubota[90], H. Kucuk[80], S. Kuday[4b], J.T. Kuechler[179], S. Kuehn[50], A. Kugel[60c], F. Kuger[178], A. Kuhl[138], T. Kuhl[44], V. Kukhtin[67], R. Kukla[137], Y. Kulchitsky[94], S. Kuleshov[34b], M. Kuna[133a,133b], T. Kunigo[70], A. Kupco[128], H. Kurashige[69], Y.A. Kurochkin[94], V. Kus[128], E.S. Kuwertz[173], M. Kuze[160], J. Kvita[116], T. Kwan[173], D. Kyriazopoulos[142], A. La Rosa[102], J.L. La Rosa Navarro[26d], L. La Rotonda[39a,39b], C. Lacasta[171], F. Lacava[133a,133b], J. Lacey[31], H. Lacker[17], D. Lacour[82], V.R. Lacuesta[171], E. Ladygin[67], R. Lafaye[5], B. Laforge[82], T. Lagouri[180], S. Lai[56], S. Lammers[63], W. Lampl[7], E. Lançon[137], U. Landgraf[50], M.P.J. Landon[78], M.C. Lanfermann[51], V.S. Lang[60a], J.C. Lange[13], A.J. Lankford[167], F. Lanni[27], K. Lantzsch[23], A. Lanza[122a], S. Laplace[82], C. Lapoire[32], J.F. Laporte[137], T. Lari[93a], F. Lasagni Manghi[22a,22b], M. Lassnig[32], P. Laurelli[49],

W. Lavrijsen[16], A.T. Law[138], P. Laycock[76], T. Lazovich[58], M. Lazzaroni[93a,93b], B. Le[90], O. Le Dortz[82], E. Le Guirriec[87], E.P. Le Quilleuc[137], M. LeBlanc[173], T. LeCompte[6], F. Ledroit-Guillon[57], C.A. Lee[27], S.C. Lee[154], L. Lee[1], B. Lefebvre[89], G. Lefebvre[82], M. Lefebvre[173], F. Legger[101], C. Leggett[16], A. Lehan[76], G. Lehmann Miotto[32], X. Lei[7], W.A. Leight[31], A.G. Leister[180], M.A.L. Leite[26d], R. Leitner[130], D. Lellouch[176], B. Lemmer[56], K.J.C. Leney[80], T. Lenz[23], B. Lenzi[32], R. Leone[7], S. Leone[125a,125b], C. Leonidopoulos[48], S. Leontsinis[10], G. Lerner[152], C. Leroy[96], A.A.J. Lesage[137], C.G. Lester[30], M. Levchenko[124], J. Levêque[5], D. Levin[91], L.J. Levinson[176], M. Levy[19], D. Lewis[78], A.M. Leyko[23], M. Leyton[43], B. Li[59,p], C. Li[59], H. Li[151], H.L. Li[33], L. Li[47], L. Li[141], Q. Li[35a], S. Li[47], X. Li[86], Y. Li[144], Z. Liang[35a], B. Liberti[134a], A. Liblong[162], P. Lichard[32], K. Lie[170], J. Liebal[23], W. Liebig[15], A. Limosani[153], S.C. Lin[154,ab], T.H. Lin[85], B.E. Lindquist[151], A.E. Lionti[51], E. Lipeles[123], A. Lipniacka[15], M. Lisovyi[60b], T.M. Liss[170], A. Lister[172], A.M. Litke[138], B. Liu[154,ac], D. Liu[154], H. Liu[91], H. Liu[27], J. Liu[87], J.B. Liu[59], K. Liu[87], L. Liu[170], M. Liu[47], M. Liu[59], Y.L. Liu[59], Y. Liu[59], M. Livan[122a,122b], A. Lleres[57], J. Llorente Merino[35a], S.L. Lloyd[78], F. Lo Sterzo[154], E.M. Lobodzinska[44], P. Loch[7], F.K. Loebinger[86], K.M. Loew[25], A. Loginov[180,*], T. Lohse[17], K. Lohwasser[44], M. Lokajicek[128], B.A. Long[24], J.D. Long[170], R.E. Long[74], L. Longo[75a,75b], K.A. Looper[112], J.A. López[34b], D. Lopez Mateos[58], B. Lopez Paredes[142], I. Lopez Paz[13], A. Lopez Solis[82], J. Lorenz[101], N. Lorenzo Martinez[63], M. Losada[21], P.J. Lösel[101], X. Lou[35a], A. Lounis[118], J. Love[6], P.A. Love[74], H. Lu[62a], N. Lu[91], H.J. Lubatti[139], C. Luci[133a,133b], A. Lucotte[57], C. Luedtke[50], F. Luehring[63], W. Lukas[64], L. Luminari[133a], O. Lundberg[149a,149b], B. Lund-Jensen[150], P.M. Luzi[82], D. Lynn[27], R. Lysak[128], E. Lytken[83], V. Lyubushkin[67], H. Ma[27], L.L. Ma[140], Y. Ma[140], G. Maccarrone[49], A. Macchiolo[102], C.M. Macdonald[142], B. Maček[77], J. Machado Miguens[123,127b], D. Madaffari[87], R. Madar[36], H.J. Maddocks[169], W.F. Mader[46], A. Madsen[44], J. Maeda[69], S. Maeland[15], T. Maeno[27], A. Maevskiy[100], E. Magradze[56], J. Mahlstedt[108], C. Maiani[118], C. Maidantchik[26a], A.A. Maier[102], T. Maier[101], A. Maio[127a,127b,127d], S. Majewski[117], Y. Makida[68], N. Makovec[118], B. Malaescu[82], Pa. Malecki[41], V.P. Maleev[124], F. Malek[57], U. Mallik[65], D. Malon[6], C. Malone[146], C. Malone[30], S. Maltezos[10], S. Malyukov[32], J. Mamuzic[171], G. Mancini[49], L. Mandelli[93a], I. Mandić[77], J. Maneira[127a,127b], L. Manhaes de Andrade Filho[26b], J. Manjarres Ramos[164b], A. Mann[101], A. Manousos[32], B. Mansoulie[137], J.D. Mansour[35a], R. Mantifel[89], M. Mantoani[56], S. Manzoni[93a,93b], L. Mapelli[32], G. Marceca[29], L. March[51], G. Marchiori[82], M. Marcisovsky[128], M. Marjanovic[14], D.E. Marley[91], F. Marroquim[26a], S.P. Marsden[86], Z. Marshall[16], S. Marti-Garcia[171], B. Martin[92], T.A. Martin[174], V.J. Martin[48], B. Martin dit Latour[15], M. Martinez[13,s], V.I. Martinez Outschoorn[170], S. Martin-Haugh[132], V.S. Martoiu[28b], A.C. Martyniuk[80], A. Marzin[32], L. Masetti[85], T. Mashimo[158], R. Mashinistov[97], J. Masik[86], A.L. Maslennikov[110,c], I. Massa[22a,22b], L. Massa[22a,22b], P. Mastrandrea[5], A. Mastroberardino[39a,39b], T. Masubuchi[158], P. Mättig[179], J. Mattmann[85], J. Maurer[28b], S.J. Maxfield[76], D.A. Maximov[110,c], R. Mazini[154], I. Maznas[157], S.M. Mazza[93a,93b], N.C. Mc Fadden[106], G. Mc Goldrick[162], S.P. Mc Kee[91], A. McCarn[91], R.L. McCarthy[151], T.G. McCarthy[102], L.I. McClymont[80], E.F. McDonald[90], J.A. Mcfayden[80], G. Mchedlidze[56], S.J. McMahon[132], R.A. McPherson[173,m], M. Medinnis[44], S. Meehan[139], S. Mehlhase[101], A. Mehta[76], K. Meier[60a], C. Meineck[101], B. Meirose[43], D. Melini[171], B.R. Mellado Garcia[148c], M. Melo[147a], F. Meloni[18], X. Meng[91], A. Mengarelli[22a,22b], S. Menke[102], E. Meoni[166], S. Mergelmeyer[17], P. Mermod[51], L. Merola[105a,105b], C. Meroni[93a], F.S. Merritt[33], A. Messina[133a,133b], J. Metcalfe[6], A.S. Mete[167], C. Meyer[85], C. Meyer[123], J-P. Meyer[137], J. Meyer[108], H. Meyer Zu Theenhausen[60a], F. Miano[152], R.P. Middleton[132], S. Miglioranzi[52a,52b], L. Mijović[48], G. Mikenberg[176], M. Mikestikova[128], M. Mikuž[77], M. Milesi[90], A. Milic[64], D.W. Miller[33], C. Mills[48], A. Milov[176], D.A. Milstead[149a,149b], A.A. Minaenko[131], Y. Minami[158], I.A. Minashvili[67], A.I. Mincer[111], B. Mindur[40a], M. Mineev[67], Y. Minegishi[158], Y. Ming[177], L.M. Mir[13], K.P. Mistry[123], T. Mitani[175], J. Mitrevski[101], V.A. Mitsou[171], A. Miucci[18], P.S. Miyagawa[142], J.U. Mjörnmark[83], M. Mlynarikova[130], T. Moa[149a,149b], K. Mochizuki[96],

S. Mohapatra[37], S. Molander[149a,149b], R. Moles-Valls[23], R. Monden[70], M.C. Mondragon[92], K. Mönig[44], J. Monk[38], E. Monnier[87], A. Montalbano[151], J. Montejo Berlingen[32], F. Monticelli[73], S. Monzani[93a,93b], R.W. Moore[3], N. Morange[118], D. Moreno[21], M. Moreno Llácer[56], P. Morettini[52a], S. Morgenstern[32], D. Mori[145], T. Mori[158], M. Morii[58], M. Morinaga[158], V. Morisbak[120], S. Moritz[85], A.K. Morley[153], G. Mornacchi[32], J.D. Morris[78], S.S. Mortensen[38], L. Morvaj[151], M. Mosidze[53b], J. Moss[146,ad], K. Motohashi[160], R. Mount[146], E. Mountricha[27], E.J.W. Moyse[88], S. Muanza[87], R.D. Mudd[19], F. Mueller[102], J. Mueller[126], R.S.P. Mueller[101], T. Mueller[30], D. Muenstermann[74], P. Mullen[55], G.A. Mullier[18], F.J. Munoz Sanchez[86], J.A. Murillo Quijada[19], W.J. Murray[174,132], H. Musheghyan[56], M. Muškinja[77], A.G. Myagkov[131,ae], M. Myska[129], B.P. Nachman[146], O. Nackenhorst[51], K. Nagai[121], R. Nagai[68,z], K. Nagano[68], Y. Nagasaka[61], K. Nagata[165], M. Nagel[50], E. Nagy[87], A.M. Nairz[32], Y. Nakahama[104], K. Nakamura[68], T. Nakamura[158], I. Nakano[113], R.F. Naranjo Garcia[44], R. Narayan[11], D.I. Narrias Villar[60a], I. Naryshkin[124], T. Naumann[44], G. Navarro[21], R. Nayyar[7], H.A. Neal[91], P.Yu. Nechaeva[97], T.J. Neep[86], A. Negri[122a,122b], M. Negrini[22a], S. Nektarijevic[107], C. Nellist[118], A. Nelson[167], S. Nemecek[128], P. Nemethy[111], A.A. Nepomuceno[26a], M. Nessi[32,af], M.S. Neubauer[170], M. Neumann[179], R.M. Neves[111], P. Nevski[27], P.R. Newman[19], D.H. Nguyen[6], T. Nguyen Manh[96], R.B. Nickerson[121], R. Nicolaidou[137], J. Nielsen[138], A. Nikiforov[17], V. Nikolaenko[131,ae], I. Nikolic-Audit[82], K. Nikolopoulos[19], J.K. Nilsen[120], P. Nilsson[27], Y. Ninomiya[158], A. Nisati[133a], R. Nisius[102], T. Nobe[158], M. Nomachi[119], I. Nomidis[31], T. Nooney[78], S. Norberg[114], M. Nordberg[32], N. Norjoharuddeen[121], O. Novgorodova[46], S. Nowak[102], M. Nozaki[68], L. Nozka[116], K. Ntekas[167], E. Nurse[80], F. Nuti[90], F. O'grady[7], D.C. O'Neil[145], A.A. O'Rourke[44], V. O'Shea[55], F.G. Oakham[31,d], H. Oberlack[102], T. Obermann[23], J. Ocariz[82], A. Ochi[69], I. Ochoa[37], J.P. Ochoa-Ricoux[34a], S. Oda[72], S. Odaka[68], H. Ogren[63], A. Oh[86], S.H. Oh[47], C.C. Ohm[16], H. Ohman[169], H. Oide[52a,52b], H. Okawa[165], Y. Okumura[158], T. Okuyama[68], A. Olariu[28b], L.F. Oleiro Seabra[127a], S.A. Olivares Pino[48], D. Oliveira Damazio[27], A. Olszewski[41], J. Olszowska[41], A. Onofre[127a,127e], K. Onogi[104], P.U.E. Onyisi[11,w], M.J. Oreglia[33], Y. Oren[156], D. Orestano[135a,135b], N. Orlando[62b], R.S. Orr[162], B. Osculati[52a,52b,*], R. Ospanov[86], G. Otero y Garzon[29], H. Otono[72], M. Ouchrif[136d], F. Ould-Saada[120], A. Ouraou[137], K.P. Oussoren[108], Q. Ouyang[35a], M. Owen[55], R.E. Owen[19], V.E. Ozcan[20a], N. Ozturk[8], K. Pachal[145], A. Pacheco Pages[13], L. Pacheco Rodriguez[137], C. Padilla Aranda[13], M. Pagáčová[50], S. Pagan Griso[16], M. Paganini[180], F. Paige[27], P. Pais[88], K. Pajchel[120], G. Palacino[164b], S. Palazzo[39a,39b], S. Palestini[32], M. Palka[40b], D. Pallin[36], E.St. Panagiotopoulou[10], C.E. Pandini[82], J.G. Panduro Vazquez[79], P. Pani[149a,149b], S. Panitkin[27], D. Pantea[28b], L. Paolozzi[51], Th.D. Papadopoulou[10], K. Papageorgiou[157], A. Paramonov[6], D. Paredes Hernandez[180], A.J. Parker[74], M.A. Parker[30], K.A. Parker[142], F. Parodi[52a,52b], J.A. Parsons[37], U. Parzefall[50], V.R. Pascuzzi[162], E. Pasqualucci[133a], S. Passaggio[52a], Fr. Pastore[79], G. Pásztor[31,ag], S. Pataraia[179], J.R. Pater[86], T. Pauly[32], J. Pearce[173], B. Pearson[114], L.E. Pedersen[38], M. Pedersen[120], S. Pedraza Lopez[171], R. Pedro[127a,127b], S.V. Peleganchuk[110,c], O. Penc[128], C. Peng[35a], H. Peng[59], J. Penwell[63], B.S. Peralva[26b], M.M. Perego[137], D.V. Perepelitsa[27], E. Perez Codina[164a], L. Perini[93a,93b], H. Pernegger[32], S. Perrella[105a,105b], R. Peschke[44], V.D. Peshekhonov[67], K. Peters[44], R.F.Y. Peters[86], B.A. Petersen[32], T.C. Petersen[38], E. Petit[57], A. Petridis[1], C. Petridou[157], P. Petroff[118], E. Petrolo[133a], M. Petrov[121], F. Petrucci[135a,135b], N.E. Pettersson[88], A. Peyaud[137], R. Pezoa[34b], P.W. Phillips[132], G. Piacquadio[146,ah], E. Pianori[174], A. Picazio[88], E. Piccaro[78], M. Piccinini[22a,22b], M.A. Pickering[121], R. Piegaia[29], J.E. Pilcher[33], A.D. Pilkington[86], A.W.J. Pin[86], M. Pinamonti[168a,168c,ai], J.L. Pinfold[3], A. Pingel[38], S. Pires[82], H. Pirumov[44], M. Pitt[176], L. Plazak[147a], M.-A. Pleier[27], V. Pleskot[85], E. Plotnikova[67], P. Plucinski[92], D. Pluth[66], R. Poettgen[149a,149b], L. Poggioli[118], D. Pohl[23], G. Polesello[122a], A. Poley[44], A. Policicchio[39a,39b], R. Polifka[162], A. Polini[22a], C.S. Pollard[55], V. Polychronakos[27], K. Pommès[32], L. Pontecorvo[133a], B.G. Pope[92], G.A. Popeneciu[28c], A. Poppleton[32], S. Pospisil[129], K. Potamianos[16], I.N. Potrap[67], C.J. Potter[30], C.T. Potter[117], G. Poulard[32], J. Poveda[32], V. Pozdnyakov[67],

M.E. Pozo Astigarraga[32], P. Pralavorio[87], A. Pranko[16], S. Prell[66], D. Price[86], L.E. Price[6], M. Primavera[75a], S. Prince[89], K. Prokofiev[62c], F. Prokoshin[34b], S. Protopopescu[27], J. Proudfoot[6], M. Przybycien[40a], D. Puddu[135a,135b], M. Purohit[27,aj], P. Puzo[118], J. Qian[91], G. Qin[55], Y. Qin[86], A. Quadt[56], W.B. Quayle[168a,168b], M. Queitsch-Maitland[44], D. Quilty[55], S. Raddum[120], V. Radeka[27], V. Radescu[121], S.K. Radhakrishnan[151], P. Radloff[117], P. Rados[90], F. Ragusa[93a,93b], G. Rahal[182], J.A. Raine[86], S. Rajagopalan[27], M. Rammensee[32], C. Rangel-Smith[169], M.G. Ratti[93a,93b], D.M. Rauch[44], F. Rauscher[101], S. Rave[85], T. Ravenscroft[55], I. Ravinovich[176], M. Raymond[32], A.L. Read[120], N.P. Readioff[76], M. Reale[75a,75b], D.M. Rebuzzi[122a,122b], A. Redelbach[178], G. Redlinger[27], R. Reece[138], R.G. Reed[148c], K. Reeves[43], L. Rehnisch[17], J. Reichert[123], A. Reiss[85], C. Rembser[32], H. Ren[35a], M. Rescigno[133a], S. Resconi[93a], O.L. Rezanova[110,c], P. Reznicek[130], R. Rezvani[96], R. Richter[102], S. Richter[80], E. Richter-Was[40b], O. Ricken[23], M. Ridel[82], P. Rieck[17], C.J. Riegel[179], J. Rieger[56], O. Rifki[114], M. Rijssenbeek[151], A. Rimoldi[122a,122b], M. Rimoldi[18], L. Rinaldi[22a], B. Ristić[51], E. Ritsch[32], I. Riu[13], F. Rizatdinova[115], E. Rizvi[78], C. Rizzi[13], S.H. Robertson[89,m], A. Robichaud-Veronneau[89], D. Robinson[30], J.E.M. Robinson[44], A. Robson[55], C. Roda[125a,125b], Y. Rodina[87,ak], A. Rodriguez Perez[13], D. Rodriguez Rodriguez[171], S. Roe[32], C.S. Rogan[58], O. Røhne[120], J. Roloff[58], A. Romaniouk[99], M. Romano[22a,22b], S.M. Romano Saez[36], E. Romero Adam[171], N. Rompotis[139], M. Ronzani[50], L. Roos[82], E. Ros[171], S. Rosati[133a], K. Rosbach[50], P. Rose[138], N.-A. Rosien[56], V. Rossetti[149a,149b], E. Rossi[105a,105b], L.P. Rossi[52a], J.H.N. Rosten[30], R. Rosten[139], M. Rotaru[28b], I. Roth[176], J. Rothberg[139], D. Rousseau[118], A. Rozanov[87], Y. Rozen[155], X. Ruan[148c], F. Rubbo[146], M.S. Rudolph[162], F. Rühr[50], A. Ruiz-Martinez[31], Z. Rurikova[50], N.A. Rusakovich[67], A. Ruschke[101], H.L. Russell[139], J.P. Rutherfoord[7], N. Ruthmann[32], Y.F. Ryabov[124], M. Rybar[170], G. Rybkin[118], S. Ryu[6], A. Ryzhov[131], G.F. Rzehorz[56], A.F. Saavedra[153], G. Sabato[108], S. Sacerdoti[29], H.F-W. Sadrozinski[138], R. Sadykov[67], F. Safai Tehrani[133a], P. Saha[109], M. Sahinsoy[60a], M. Saimpert[137], T. Saito[158], H. Sakamoto[158], Y. Sakurai[175], G. Salamanna[135a,135b], A. Salamon[134a,134b], J.E. Salazar Loyola[34b], D. Salek[108], P.H. Sales De Bruin[139], D. Salihagic[102], A. Salnikov[146], J. Salt[171], D. Salvatore[39a,39b], F. Salvatore[152], A. Salvucci[62a,62b,62c], A. Salzburger[32], D. Sammel[50], D. Sampsonidis[157], J. Sánchez[171], V. Sanchez Martinez[171], A. Sanchez Pineda[105a,105b], H. Sandaker[120], R.L. Sandbach[78], M. Sandhoff[179], C. Sandoval[21], D.P.C. Sankey[132], M. Sannino[52a,52b], A. Sansoni[49], C. Santoni[36], R. Santonico[134a,134b], H. Santos[127a], I. Santoyo Castillo[152], K. Sapp[126], A. Sapronov[67], J.G. Saraiva[127a,127d], B. Sarrazin[23], O. Sasaki[68], K. Sato[165], E. Sauvan[5], G. Savage[79], P. Savard[162,d], N. Savic[102], C. Sawyer[132], L. Sawyer[81,r], J. Saxon[33], C. Sbarra[22a], A. Sbrizzi[22a,22b], T. Scanlon[80], D.A. Scannicchio[167], M. Scarcella[153], V. Scarfone[39a,39b], J. Schaarschmidt[176], P. Schacht[102], B.M. Schachtner[101], D. Schaefer[32], L. Schaefer[123], R. Schaefer[44], J. Schaeffer[85], S. Schaepe[23], S. Schaetzel[60b], U. Schäfer[85], A.C. Schaffer[118], D. Schaile[101], R.D. Schamberger[151], V. Scharf[60a], V.A. Schegelsky[124], D. Scheirich[130], M. Schernau[167], C. Schiavi[52a,52b], S. Schier[138], C. Schillo[50], M. Schioppa[39a,39b], S. Schlenker[32], K.R. Schmidt-Sommerfeld[102], K. Schmieden[32], C. Schmitt[85], S. Schmitt[44], S. Schmitz[85], B. Schneider[164a], U. Schnoor[50], L. Schoeffel[137], A. Schoening[60b], B.D. Schoenrock[92], E. Schopf[23], M. Schott[85], J.F.P. Schouwenberg[107], J. Schovancova[8], S. Schramm[51], M. Schreyer[178], N. Schuh[85], A. Schulte[85], M.J. Schultens[23], H.-C. Schultz-Coulon[60a], H. Schulz[17], M. Schumacher[50], B.A. Schumm[138], Ph. Schune[137], A. Schwartzman[146], T.A. Schwarz[91], H. Schweiger[86], Ph. Schwemling[137], R. Schwienhorst[92], J. Schwindling[137], T. Schwindt[23], G. Sciolla[25], F. Scuri[125a,125b], F. Scutti[90], J. Searcy[91], P. Seema[23], S.C. Seidel[106], A. Seiden[138], F. Seifert[129], J.M. Seixas[26a], G. Sekhniaidze[105a], K. Sekhon[91], S.J. Sekula[42], D.M. Seliverstov[124,*], N. Semprini-Cesari[22a,22b], C. Serfon[120], L. Serin[118], L. Serkin[168a,168b], M. Sessa[135a,135b], R. Seuster[173], H. Severini[114], T. Sfiligoj[77], F. Sforza[32], A. Sfyrla[51], E. Shabalina[56], N.W. Shaikh[149a,149b], L.Y. Shan[35a], R. Shang[170], J.T. Shank[24], M. Shapiro[16], P.B. Shatalov[98], K. Shaw[168a,168b], S.M. Shaw[86], A. Shcherbakova[149a,149b], C.Y. Shehu[152], P. Sherwood[80], L. Shi[154,al], S. Shimizu[69], C.O. Shimmin[167], M. Shimojima[103], S. Shirabe[72],

M. Shiyakova[67,am], A. Shmeleva[97], D. Shoaleh Saadi[96], M.J. Shochet[33], S. Shojaii[93a,93b], D.R. Shope[114], S. Shrestha[112], E. Shulga[99], M.A. Shupe[7], P. Sicho[128], A.M. Sickles[170], P.E. Sidebo[150], O. Sidiropoulou[178], D. Sidorov[115], A. Sidoti[22a,22b], F. Siegert[46], Dj. Sijacki[14], J. Silva[127a,127d], S.B. Silverstein[149a], V. Simak[129], Lj. Simic[14], S. Simion[118], E. Simioni[85], B. Simmons[80], D. Simon[36], M. Simon[85], P. Sinervo[162], N.B. Sinev[117], M. Sioli[22a,22b], G. Siragusa[178], S.Yu. Sivoklokov[100], J. Sjölin[149a,149b], M.B. Skinner[74], H.P. Skottowe[58], P. Skubic[114], M. Slater[19], T. Slavicek[129], M. Slawinska[108], K. Sliwa[166], R. Slovak[130], V. Smakhtin[176], B.H. Smart[5], L. Smestad[15], J. Smiesko[147a], S.Yu. Smirnov[99], Y. Smirnov[99], L.N. Smirnova[100,an], O. Smirnova[83], M.N.K. Smith[37], R.W. Smith[37], M. Smizanska[74], K. Smolek[129], A.A. Snesarev[97], I.M. Snyder[117], S. Snyder[27], R. Sobie[173,m], F. Socher[46], A. Soffer[156], D.A. Soh[154], G. Sokhrannyi[77], C.A. Solans Sanchez[32], M. Solar[129], E.Yu. Soldatov[99], U. Soldevila[171], A.A. Solodkov[131], A. Soloshenko[67], O.V. Solovyanov[131], V. Solovyev[124], P. Sommer[50], H. Son[166], H.Y. Song[59,ao], A. Sood[16], A. Sopczak[129], V. Sopko[129], V. Sorin[13], D. Sosa[60b], C.L. Sotiropoulou[125a,125b], R. Soualah[168a,168c], A.M. Soukharev[110,c], D. South[44], B.C. Sowden[79], S. Spagnolo[75a,75b], M. Spalla[125a,125b], M. Spangenberg[174], F. Spanò[79], D. Sperlich[17], F. Spettel[102], R. Spighi[22a], G. Spigo[32], L.A. Spiller[90], M. Spousta[130], R.D. St. Denis[55,*], A. Stabile[93a], R. Stamen[60a], S. Stamm[17], E. Stanecka[41], R.W. Stanek[6], C. Stanescu[135a], M. Stanescu-Bellu[44], M.M. Stanitzki[44], S. Stapnes[120], E.A. Starchenko[131], G.H. Stark[33], J. Stark[57], P. Staroba[128], P. Starovoitov[60a], S. Stärz[32], R. Staszewski[41], P. Steinberg[27], B. Stelzer[145], H.J. Stelzer[32], O. Stelzer-Chilton[164a], H. Stenzel[54], G.A. Stewart[55], J.A. Stillings[23], M.C. Stockton[89], M. Stoebe[89], G. Stoicea[28b], P. Stolte[56], S. Stonjek[102], A.R. Stradling[8], A. Straessner[46], M.E. Stramaglia[18], J. Strandberg[150], S. Strandberg[149a,149b], A. Strandlie[120], M. Strauss[114], P. Strizenec[147b], R. Ströhmer[178], D.M. Strom[117], R. Stroynowski[42], A. Strubig[107], S.A. Stucci[27], B. Stugu[15], N.A. Styles[44], D. Su[146], J. Su[126], S. Suchek[60a], Y. Sugaya[119], M. Suk[129], V.V. Sulin[97], S. Sultansoy[4c], T. Sumida[70], S. Sun[58], X. Sun[35a], J.E. Sundermann[50], K. Suruliz[152], G. Susinno[39a,39b], M.R. Sutton[152], S. Suzuki[68], M. Svatos[128], M. Swiatlowski[33], I. Sykora[147a], T. Sykora[130], D. Ta[50], C. Taccini[135a,135b], K. Tackmann[44], J. Taenzer[162], A. Taffard[167], R. Tafirout[164a], N. Taiblum[156], H. Takai[27], R. Takashima[71], T. Takeshita[143], Y. Takubo[68], M. Talby[87], A.A. Talyshev[110,c], K.G. Tan[90], J. Tanaka[158], M. Tanaka[160], R. Tanaka[118], S. Tanaka[68], R. Tanioka[69], B.B. Tannenwald[112], S. Tapia Araya[34b], S. Tapprogge[85], S. Tarem[155], G.F. Tartarelli[93a], P. Tas[130], M. Tasevsky[128], T. Tashiro[70], E. Tassi[39a,39b], A. Tavares Delgado[127a,127b], Y. Tayalati[136e], A.C. Taylor[106], G.N. Taylor[90], P.T.E. Taylor[90], W. Taylor[164b], F.A. Teischinger[32], P. Teixeira-Dias[79], K.K. Temming[50], D. Temple[145], H. Ten Kate[32], P.K. Teng[154], J.J. Teoh[119], F. Tepel[179], S. Terada[68], K. Terashi[158], J. Terron[84], S. Terzo[13], M. Testa[49], R.J. Teuscher[162,m], T. Theveneaux-Pelzer[87], J.P. Thomas[19], J. Thomas-Wilsker[79], P.D. Thompson[19], A.S. Thompson[55], L.A. Thomsen[180], E. Thomson[123], M.J. Tibbetts[16], R.E. Ticse Torres[87], V.O. Tikhomirov[97,ap], Yu.A. Tikhonov[110,c], S. Timoshenko[99], P. Tipton[180], S. Tisserant[87], K. Todome[160], T. Todorov[5,*], S. Todorova-Nova[130], J. Tojo[72], S. Tokár[147a], K. Tokushuku[68], E. Tolley[58], L. Tomlinson[86], M. Tomoto[104], L. Tompkins[146,aq], K. Toms[106], B. Tong[58], P. Tornambe[50], E. Torrence[117], H. Torres[145], E. Torró Pastor[139], J. Toth[87,ar], F. Touchard[87], D.R. Tovey[142], T. Trefzger[178], A. Tricoli[27], I.M. Trigger[164a], S. Trincaz-Duvoid[82], M.F. Tripiana[13], W. Trischuk[162], B. Trocmé[57], A. Trofymov[44], C. Troncon[93a], M. Trottier-McDonald[16], M. Trovatelli[173], L. Truong[168a,168c], M. Trzebinski[41], A. Trzupek[41], J.C-L. Tseng[121], P.V. Tsiareshka[94], G. Tsipolitis[10], N. Tsirintanis[9], S. Tsiskaridze[13], V. Tsiskaridze[50], E.G. Tskhadadze[53a], K.M. Tsui[62a], I.I. Tsukerman[98], V. Tsulaia[16], S. Tsuno[68], D. Tsybychev[151], Y. Tu[62b], A. Tudorache[28b], V. Tudorache[28b], A.N. Tuna[58], S.A. Tupputi[22a,22b], S. Turchikhin[67], D. Turecek[129], D. Turgeman[176], R. Turra[93a,93b], P.M. Tuts[37], M. Tyndel[132], G. Ucchielli[22a,22b], I. Ueda[158], M. Ughetto[149a,149b], F. Ukegawa[165], G. Unal[32], A. Undrus[27], G. Unel[167], F.C. Ungaro[90], Y. Unno[68], C. Unverdorben[101], J. Urban[147b], P. Urquijo[90], P. Urrejola[85], G. Usai[8], J. Usui[68], L. Vacavant[87], V. Vacek[129], B. Vachon[89], C. Valderanis[101], E. Valdes Santurio[149a,149b],

N. Valencic[108], S. Valentinetti[22a,22b], A. Valero[171], L. Valery[13], S. Valkar[130], J.A. Valls Ferrer[171], W. Van Den Wollenberg[108], P.C. Van Der Deijl[108], H. van der Graaf[108], N. van Eldik[155], P. van Gemmeren[6], J. Van Nieuwkoop[145], I. van Vulpen[108], M.C. van Woerden[108], M. Vanadia[133a,133b], W. Vandelli[32], R. Vanguri[123], A. Vaniachine[161], P. Vankov[108], G. Vardanyan[181], R. Vari[133a], E.W. Varnes[7], T. Varol[42], D. Varouchas[82], A. Vartapetian[8], K.E. Varvell[153], J.G. Vasquez[180], G.A. Vasquez[34b], F. Vazeille[36], T. Vazquez Schroeder[89], J. Veatch[56], V. Veeraraghavan[7], L.M. Veloce[162], F. Veloso[127a,127c], S. Veneziano[133a], A. Ventura[75a,75b], M. Venturi[173], N. Venturi[162], A. Venturini[25], V. Vercesi[122a], M. Verducci[133a,133b], W. Verkerke[108], J.C. Vermeulen[108], A. Vest[46,as], M.C. Vetterli[145,d], O. Viazlo[83], I. Vichou[170,*], T. Vickey[142], O.E. Vickey Boeriu[142], G.H.A. Viehhauser[121], S. Viel[16], L. Vigani[121], M. Villa[22a,22b], M. Villaplana Perez[93a,93b], E. Vilucchi[49], M.G. Vincter[31], V.B. Vinogradov[67], C. Vittori[22a,22b], I. Vivarelli[152], S. Vlachos[10], M. Vlasak[129], M. Vogel[179], P. Vokac[129], G. Volpi[125a,125b], M. Volpi[90], H. von der Schmitt[102], E. von Toerne[23], V. Vorobel[130], K. Vorobev[99], M. Vos[171], R. Voss[32], J.H. Vossebeld[76], N. Vranjes[14], M. Vranjes Milosavljevic[14], V. Vrba[128], M. Vreeswijk[108], R. Vuillermet[32], I. Vukotic[33], Z. Vykydal[129], P. Wagner[23], W. Wagner[179], H. Wahlberg[73], S. Wahrmund[46], J. Wakabayashi[104], J. Walder[74], R. Walker[101], W. Walkowiak[144], V. Wallangen[149a,149b], C. Wang[35b], C. Wang[140,87], F. Wang[177], H. Wang[16], H. Wang[42], J. Wang[44], J. Wang[153], K. Wang[89], R. Wang[6], S.M. Wang[154], T. Wang[23], T. Wang[37], W. Wang[59], C. Wanotayaroj[117], A. Warburton[89], C.P. Ward[30], D.R. Wardrope[80], A. Washbrook[48], P.M. Watkins[19], A.T. Watson[19], M.F. Watson[19], G. Watts[139], S. Watts[86], B.M. Waugh[80], S. Webb[85], M.S. Weber[18], S.W. Weber[178], S.A. Weber[31], J.S. Webster[6], A.R. Weidberg[121], B. Weinert[63], J. Weingarten[56], C. Weiser[50], H. Weits[108], P.S. Wells[32], T. Wenaus[27], T. Wengler[32], S. Wenig[32], N. Wermes[23], M. Werner[50], M.D. Werner[66], P. Werner[32], M. Wessels[60a], J. Wetter[166], K. Whalen[117], N.L. Whallon[139], A.M. Wharton[74], A. White[8], M.J. White[1], R. White[34b], D. Whiteson[167], F.J. Wickens[132], W. Wiedenmann[177], M. Wielers[132], C. Wiglesworth[38], L.A.M. Wiik-Fuchs[23], A. Wildauer[102], F. Wilk[86], H.G. Wilkens[32], H.H. Williams[123], S. Williams[108], C. Willis[92], S. Willocq[88], J.A. Wilson[19], I. Wingerter-Seez[5], F. Winklmeier[117], O.J. Winston[152], B.T. Winter[23], M. Wittgen[146], J. Wittkowski[101], T.M.H. Wolf[108], M.W. Wolter[41], H. Wolters[127a,127c], S.D. Worm[132], B.K. Wosiek[41], J. Wotschack[32], M.J. Woudstra[86], K.W. Wozniak[41], M. Wu[57], M. Wu[33], S.L. Wu[177], X. Wu[51], Y. Wu[91], T.R. Wyatt[86], B.M. Wynne[48], S. Xella[38], D. Xu[35a], L. Xu[27], B. Yabsley[153], S. Yacoob[148a], D. Yamaguchi[160], Y. Yamaguchi[119], A. Yamamoto[68], S. Yamamoto[158], T. Yamanaka[158], K. Yamauchi[104], Y. Yamazaki[69], Z. Yan[24], H. Yang[141], H. Yang[177], Y. Yang[154], Z. Yang[15], W-M. Yao[16], Y.C. Yap[82], Y. Yasu[68], E. Yatsenko[5], K.H. Yau Wong[23], J. Ye[42], S. Ye[27], I. Yeletskikh[67], E. Yildirim[85], K. Yorita[175], R. Yoshida[6], K. Yoshihara[123], C. Young[146], C.J.S. Young[32], S. Youssef[24], D.R. Yu[16], J. Yu[8], J.M. Yu[91], J. Yu[66], L. Yuan[69], S.P.Y. Yuen[23], I. Yusuff[30,at], B. Zabinski[41], R. Zaidan[65], A.M. Zaitsev[131,ae], N. Zakharchuk[44], J. Zalieckas[15], A. Zaman[151], S. Zambito[58], L. Zanello[133a,133b], D. Zanzi[90], C. Zeitnitz[179], M. Zeman[129], A. Zemla[40a], J.C. Zeng[170], Q. Zeng[146], O. Zenin[131], T. Ženiš[147a], D. Zerwas[118], D. Zhang[91], F. Zhang[177], G. Zhang[59,ao], H. Zhang[35b], J. Zhang[6], L. Zhang[50], M. Zhang[170], R. Zhang[23], R. Zhang[59,au], X. Zhang[140], Z. Zhang[118], X. Zhao[42], Y. Zhao[140], Z. Zhao[59], A. Zhemchugov[67], J. Zhong[121], B. Zhou[91], C. Zhou[177], L. Zhou[37], L. Zhou[42], M. Zhou[151], N. Zhou[35c], C.G. Zhu[140], H. Zhu[35a], J. Zhu[91], Y. Zhu[59], X. Zhuang[35a], K. Zhukov[97], A. Zibell[178], D. Zieminska[63], N.I. Zimine[67], C. Zimmermann[85], S. Zimmermann[50], Z. Zinonos[56], M. Zinser[85], M. Ziolkowski[144], L. Živković[14], G. Zobernig[177], A. Zoccoli[22a,22b], M. zur Nedden[17], L. Zwalinski[32].

[1] Department of Physics, University of Adelaide, Adelaide, Australia

[2] Physics Department, SUNY Albany, Albany NY, United States of America

[3] Department of Physics, University of Alberta, Edmonton AB, Canada

[4] [(a)] Department of Physics, Ankara University, Ankara; [(b)] Istanbul Aydin University, Istanbul; [(c)]

Division of Physics, TOBB University of Economics and Technology, Ankara, Turkey
[5] LAPP, CNRS/IN2P3 and Université Savoie Mont Blanc, Annecy-le-Vieux, France
[6] High Energy Physics Division, Argonne National Laboratory, Argonne IL, United States of America
[7] Department of Physics, University of Arizona, Tucson AZ, United States of America
[8] Department of Physics, The University of Texas at Arlington, Arlington TX, United States of America
[9] Physics Department, University of Athens, Athens, Greece
[10] Physics Department, National Technical University of Athens, Zografou, Greece
[11] Department of Physics, The University of Texas at Austin, Austin TX, United States of America
[12] Institute of Physics, Azerbaijan Academy of Sciences, Baku, Azerbaijan
[13] Institut de Física d'Altes Energies (IFAE), The Barcelona Institute of Science and Technology, Barcelona, Spain
[14] Institute of Physics, University of Belgrade, Belgrade, Serbia
[15] Department for Physics and Technology, University of Bergen, Bergen, Norway
[16] Physics Division, Lawrence Berkeley National Laboratory and University of California, Berkeley CA, United States of America
[17] Department of Physics, Humboldt University, Berlin, Germany
[18] Albert Einstein Center for Fundamental Physics and Laboratory for High Energy Physics, University of Bern, Bern, Switzerland
[19] School of Physics and Astronomy, University of Birmingham, Birmingham, United Kingdom
[20] [(a)] Department of Physics, Bogazici University, Istanbul; [(b)] Department of Physics Engineering, Gaziantep University, Gaziantep; [(d)] Istanbul Bilgi University, Faculty of Engineering and Natural Sciences, Istanbul,Turkey; [(e)] Bahcesehir University, Faculty of Engineering and Natural Sciences, Istanbul, Turkey, Turkey
[21] Centro de Investigaciones, Universidad Antonio Narino, Bogota, Colombia
[22] [(a)] INFN Sezione di Bologna; [(b)] Dipartimento di Fisica e Astronomia, Università di Bologna, Bologna, Italy
[23] Physikalisches Institut, University of Bonn, Bonn, Germany
[24] Department of Physics, Boston University, Boston MA, United States of America
[25] Department of Physics, Brandeis University, Waltham MA, United States of America
[26] [(a)] Universidade Federal do Rio De Janeiro COPPE/EE/IF, Rio de Janeiro; [(b)] Electrical Circuits Department, Federal University of Juiz de Fora (UFJF), Juiz de Fora; [(c)] Federal University of Sao Joao del Rei (UFSJ), Sao Joao del Rei; [(d)] Instituto de Fisica, Universidade de Sao Paulo, Sao Paulo, Brazil
[27] Physics Department, Brookhaven National Laboratory, Upton NY, United States of America
[28] [(a)] Transilvania University of Brasov, Brasov, Romania; [(b)] National Institute of Physics and Nuclear Engineering, Bucharest; [(c)] National Institute for Research and Development of Isotopic and Molecular Technologies, Physics Department, Cluj Napoca; [(d)] University Politehnica Bucharest, Bucharest; [(e)] West University in Timisoara, Timisoara, Romania
[29] Departamento de Física, Universidad de Buenos Aires, Buenos Aires, Argentina
[30] Cavendish Laboratory, University of Cambridge, Cambridge, United Kingdom
[31] Department of Physics, Carleton University, Ottawa ON, Canada
[32] CERN, Geneva, Switzerland
[33] Enrico Fermi Institute, University of Chicago, Chicago IL, United States of America
[34] [(a)] Departamento de Física, Pontificia Universidad Católica de Chile, Santiago; [(b)] Departamento de Física, Universidad Técnica Federico Santa María, Valparaíso, Chile
[35] [(a)] Institute of High Energy Physics, Chinese Academy of Sciences, Beijing; [(b)] Department of Physics, Nanjing University, Jiangsu; [(c)] Physics Department, Tsinghua University, Beijing 100084, China

[36] Laboratoire de Physique Corpusculaire, Clermont Université and Université Blaise Pascal and CNRS/IN2P3, Clermont-Ferrand, France
[37] Nevis Laboratory, Columbia University, Irvington NY, United States of America
[38] Niels Bohr Institute, University of Copenhagen, Kobenhavn, Denmark
[39] [(a)] INFN Gruppo Collegato di Cosenza, Laboratori Nazionali di Frascati; [(b)] Dipartimento di Fisica, Università della Calabria, Rende, Italy
[40] [(a)] AGH University of Science and Technology, Faculty of Physics and Applied Computer Science, Krakow; [(b)] Marian Smoluchowski Institute of Physics, Jagiellonian University, Krakow, Poland
[41] Institute of Nuclear Physics Polish Academy of Sciences, Krakow, Poland
[42] Physics Department, Southern Methodist University, Dallas TX, United States of America
[43] Physics Department, University of Texas at Dallas, Richardson TX, United States of America
[44] DESY, Hamburg and Zeuthen, Germany
[45] Lehrstuhl für Experimentelle Physik IV, Technische Universität Dortmund, Dortmund, Germany
[46] Institut für Kern- und Teilchenphysik, Technische Universität Dresden, Dresden, Germany
[47] Department of Physics, Duke University, Durham NC, United States of America
[48] SUPA - School of Physics and Astronomy, University of Edinburgh, Edinburgh, United Kingdom
[49] INFN Laboratori Nazionali di Frascati, Frascati, Italy
[50] Fakultät für Mathematik und Physik, Albert-Ludwigs-Universität, Freiburg, Germany
[51] Section de Physique, Université de Genève, Geneva, Switzerland
[52] [(a)] INFN Sezione di Genova; [(b)] Dipartimento di Fisica, Università di Genova, Genova, Italy
[53] [(a)] E. Andronikashvili Institute of Physics, Iv. Javakhishvili Tbilisi State University, Tbilisi; [(b)] High Energy Physics Institute, Tbilisi State University, Tbilisi, Georgia
[54] II Physikalisches Institut, Justus-Liebig-Universität Giessen, Giessen, Germany
[55] SUPA - School of Physics and Astronomy, University of Glasgow, Glasgow, United Kingdom
[56] II Physikalisches Institut, Georg-August-Universität, Göttingen, Germany
[57] Laboratoire de Physique Subatomique et de Cosmologie, Université Grenoble-Alpes, CNRS/IN2P3, Grenoble, France
[58] Laboratory for Particle Physics and Cosmology, Harvard University, Cambridge MA, United States of America
[59] Department of Modern Physics, University of Science and Technology of China, Anhui, China
[60] [(a)] Kirchhoff-Institut für Physik, Ruprecht-Karls-Universität Heidelberg, Heidelberg; [(b)] Physikalisches Institut, Ruprecht-Karls-Universität Heidelberg, Heidelberg; [(c)] ZITI Institut für technische Informatik, Ruprecht-Karls-Universität Heidelberg, Mannheim, Germany
[61] Faculty of Applied Information Science, Hiroshima Institute of Technology, Hiroshima, Japan
[62] [(a)] Department of Physics, The Chinese University of Hong Kong, Shatin, N.T., Hong Kong; [(b)] Department of Physics, The University of Hong Kong, Hong Kong; [(c)] Department of Physics and Institute for Advanced Study, The Hong Kong University of Science and Technology, Clear Water Bay, Kowloon, Hong Kong, China
[63] Department of Physics, Indiana University, Bloomington IN, United States of America
[64] Institut für Astro- und Teilchenphysik, Leopold-Franzens-Universität, Innsbruck, Austria
[65] University of Iowa, Iowa City IA, United States of America
[66] Department of Physics and Astronomy, Iowa State University, Ames IA, United States of America
[67] Joint Institute for Nuclear Research, JINR Dubna, Dubna, Russia
[68] KEK, High Energy Accelerator Research Organization, Tsukuba, Japan
[69] Graduate School of Science, Kobe University, Kobe, Japan
[70] Faculty of Science, Kyoto University, Kyoto, Japan
[71] Kyoto University of Education, Kyoto, Japan

[72] Department of Physics, Kyushu University, Fukuoka, Japan
[73] Instituto de Física La Plata, Universidad Nacional de La Plata and CONICET, La Plata, Argentina
[74] Physics Department, Lancaster University, Lancaster, United Kingdom
[75] [(a)] INFN Sezione di Lecce; [(b)] Dipartimento di Matematica e Fisica, Università del Salento, Lecce, Italy
[76] Oliver Lodge Laboratory, University of Liverpool, Liverpool, United Kingdom
[77] Department of Physics, Jožef Stefan Institute and University of Ljubljana, Ljubljana, Slovenia
[78] School of Physics and Astronomy, Queen Mary University of London, London, United Kingdom
[79] Department of Physics, Royal Holloway University of London, Surrey, United Kingdom
[80] Department of Physics and Astronomy, University College London, London, United Kingdom
[81] Louisiana Tech University, Ruston LA, United States of America
[82] Laboratoire de Physique Nucléaire et de Hautes Energies, UPMC and Université Paris-Diderot and CNRS/IN2P3, Paris, France
[83] Fysiska institutionen, Lunds universitet, Lund, Sweden
[84] Departamento de Fisica Teorica C-15, Universidad Autonoma de Madrid, Madrid, Spain
[85] Institut für Physik, Universität Mainz, Mainz, Germany
[86] School of Physics and Astronomy, University of Manchester, Manchester, United Kingdom
[87] CPPM, Aix-Marseille Université and CNRS/IN2P3, Marseille, France
[88] Department of Physics, University of Massachusetts, Amherst MA, United States of America
[89] Department of Physics, McGill University, Montreal QC, Canada
[90] School of Physics, University of Melbourne, Victoria, Australia
[91] Department of Physics, The University of Michigan, Ann Arbor MI, United States of America
[92] Department of Physics and Astronomy, Michigan State University, East Lansing MI, United States of America
[93] [(a)] INFN Sezione di Milano; [(b)] Dipartimento di Fisica, Università di Milano, Milano, Italy
[94] B.I. Stepanov Institute of Physics, National Academy of Sciences of Belarus, Minsk, Republic of Belarus
[95] National Scientific and Educational Centre for Particle and High Energy Physics, Minsk, Republic of Belarus
[96] Group of Particle Physics, University of Montreal, Montreal QC, Canada
[97] P.N. Lebedev Physical Institute of the Russian Academy of Sciences, Moscow, Russia
[98] Institute for Theoretical and Experimental Physics (ITEP), Moscow, Russia
[99] National Research Nuclear University MEPhI, Moscow, Russia
[100] D.V. Skobeltsyn Institute of Nuclear Physics, M.V. Lomonosov Moscow State University, Moscow, Russia
[101] Fakultät für Physik, Ludwig-Maximilians-Universität München, München, Germany
[102] Max-Planck-Institut für Physik (Werner-Heisenberg-Institut), München, Germany
[103] Nagasaki Institute of Applied Science, Nagasaki, Japan
[104] Graduate School of Science and Kobayashi-Maskawa Institute, Nagoya University, Nagoya, Japan
[105] [(a)] INFN Sezione di Napoli; [(b)] Dipartimento di Fisica, Università di Napoli, Napoli, Italy
[106] Department of Physics and Astronomy, University of New Mexico, Albuquerque NM, United States of America
[107] Institute for Mathematics, Astrophysics and Particle Physics, Radboud University Nijmegen/Nikhef, Nijmegen, Netherlands
[108] Nikhef National Institute for Subatomic Physics and University of Amsterdam, Amsterdam, Netherlands
[109] Department of Physics, Northern Illinois University, DeKalb IL, United States of America

[110] Budker Institute of Nuclear Physics, SB RAS, Novosibirsk, Russia
[111] Department of Physics, New York University, New York NY, United States of America
[112] Ohio State University, Columbus OH, United States of America
[113] Faculty of Science, Okayama University, Okayama, Japan
[114] Homer L. Dodge Department of Physics and Astronomy, University of Oklahoma, Norman OK, United States of America
[115] Department of Physics, Oklahoma State University, Stillwater OK, United States of America
[116] Palacký University, RCPTM, Olomouc, Czech Republic
[117] Center for High Energy Physics, University of Oregon, Eugene OR, United States of America
[118] LAL, Univ. Paris-Sud, CNRS/IN2P3, Université Paris-Saclay, Orsay, France
[119] Graduate School of Science, Osaka University, Osaka, Japan
[120] Department of Physics, University of Oslo, Oslo, Norway
[121] Department of Physics, Oxford University, Oxford, United Kingdom
[122] [(a)] INFN Sezione di Pavia; [(b)] Dipartimento di Fisica, Università di Pavia, Pavia, Italy
[123] Department of Physics, University of Pennsylvania, Philadelphia PA, United States of America
[124] National Research Centre "Kurchatov Institute" B.P.Konstantinov Petersburg Nuclear Physics Institute, St. Petersburg, Russia
[125] [(a)] INFN Sezione di Pisa; [(b)] Dipartimento di Fisica E. Fermi, Università di Pisa, Pisa, Italy
[126] Department of Physics and Astronomy, University of Pittsburgh, Pittsburgh PA, United States of America
[127] [(a)] Laboratório de Instrumentação e Física Experimental de Partículas - LIP, Lisboa; [(b)] Faculdade de Ciências, Universidade de Lisboa, Lisboa; [(c)] Department of Physics, University of Coimbra, Coimbra; [(d)] Centro de Física Nuclear da Universidade de Lisboa, Lisboa; [(e)] Departamento de Fisica, Universidade do Minho, Braga; [(f)] Departamento de Fisica Teorica y del Cosmos and CAFPE, Universidad de Granada, Granada (Spain); [(g)] Dep Fisica and CEFITEC of Faculdade de Ciencias e Tecnologia, Universidade Nova de Lisboa, Caparica, Portugal
[128] Institute of Physics, Academy of Sciences of the Czech Republic, Praha, Czech Republic
[129] Czech Technical University in Prague, Praha, Czech Republic
[130] Faculty of Mathematics and Physics, Charles University in Prague, Praha, Czech Republic
[131] State Research Center Institute for High Energy Physics (Protvino), NRC KI, Russia
[132] Particle Physics Department, Rutherford Appleton Laboratory, Didcot, United Kingdom
[133] [(a)] INFN Sezione di Roma; [(b)] Dipartimento di Fisica, Sapienza Università di Roma, Roma, Italy
[134] [(a)] INFN Sezione di Roma Tor Vergata; [(b)] Dipartimento di Fisica, Università di Roma Tor Vergata, Roma, Italy
[135] [(a)] INFN Sezione di Roma Tre; [(b)] Dipartimento di Matematica e Fisica, Università Roma Tre, Roma, Italy
[136] [(a)] Faculté des Sciences Ain Chock, Réseau Universitaire de Physique des Hautes Energies - Université Hassan II, Casablanca; [(b)] Centre National de l'Energie des Sciences Techniques Nucleaires, Rabat; [(c)] Faculté des Sciences Semlalia, Université Cadi Ayyad, LPHEA-Marrakech; [(d)] Faculté des Sciences, Université Mohamed Premier and LPTPM, Oujda; [(e)] Faculté des sciences, Université Mohammed V, Rabat, Morocco
[137] DSM/IRFU (Institut de Recherches sur les Lois Fondamentales de l'Univers), CEA Saclay (Commissariat à l'Energie Atomique et aux Energies Alternatives), Gif-sur-Yvette, France
[138] Santa Cruz Institute for Particle Physics, University of California Santa Cruz, Santa Cruz CA, United States of America
[139] Department of Physics, University of Washington, Seattle WA, United States of America
[140] School of Physics, Shandong University, Shandong, China

[141] Department of Physics and Astronomy, Shanghai Key Laboratory for Particle Physics and Cosmology, Shanghai Jiao Tong University, Shanghai; (also affiliated with PKU-CHEP), China
[142] Department of Physics and Astronomy, University of Sheffield, Sheffield, United Kingdom
[143] Department of Physics, Shinshu University, Nagano, Japan
[144] Fachbereich Physik, Universität Siegen, Siegen, Germany
[145] Department of Physics, Simon Fraser University, Burnaby BC, Canada
[146] SLAC National Accelerator Laboratory, Stanford CA, United States of America
[147] [(a)] Faculty of Mathematics, Physics & Informatics, Comenius University, Bratislava; [(b)] Department of Subnuclear Physics, Institute of Experimental Physics of the Slovak Academy of Sciences, Kosice, Slovak Republic
[148] [(a)] Department of Physics, University of Cape Town, Cape Town; [(b)] Department of Physics, University of Johannesburg, Johannesburg; [(c)] School of Physics, University of the Witwatersrand, Johannesburg, South Africa
[149] [(a)] Department of Physics, Stockholm University; [(b)] The Oskar Klein Centre, Stockholm, Sweden
[150] Physics Department, Royal Institute of Technology, Stockholm, Sweden
[151] Departments of Physics & Astronomy and Chemistry, Stony Brook University, Stony Brook NY, United States of America
[152] Department of Physics and Astronomy, University of Sussex, Brighton, United Kingdom
[153] School of Physics, University of Sydney, Sydney, Australia
[154] Institute of Physics, Academia Sinica, Taipei, Taiwan
[155] Department of Physics, Technion: Israel Institute of Technology, Haifa, Israel
[156] Raymond and Beverly Sackler School of Physics and Astronomy, Tel Aviv University, Tel Aviv, Israel
[157] Department of Physics, Aristotle University of Thessaloniki, Thessaloniki, Greece
[158] International Center for Elementary Particle Physics and Department of Physics, The University of Tokyo, Tokyo, Japan
[159] Graduate School of Science and Technology, Tokyo Metropolitan University, Tokyo, Japan
[160] Department of Physics, Tokyo Institute of Technology, Tokyo, Japan
[161] Tomsk State University, Tomsk, Russia, Russia
[162] Department of Physics, University of Toronto, Toronto ON, Canada
[163] [(a)] INFN-TIFPA; [(b)] University of Trento, Trento, Italy, Italy
[164] [(a)] TRIUMF, Vancouver BC; [(b)] Department of Physics and Astronomy, York University, Toronto ON, Canada
[165] Faculty of Pure and Applied Sciences, and Center for Integrated Research in Fundamental Science and Engineering, University of Tsukuba, Tsukuba, Japan
[166] Department of Physics and Astronomy, Tufts University, Medford MA, United States of America
[167] Department of Physics and Astronomy, University of California Irvine, Irvine CA, United States of America
[168] [(a)] INFN Gruppo Collegato di Udine, Sezione di Trieste, Udine; [(b)] ICTP, Trieste; [(c)] Dipartimento di Chimica, Fisica e Ambiente, Università di Udine, Udine, Italy
[169] Department of Physics and Astronomy, University of Uppsala, Uppsala, Sweden
[170] Department of Physics, University of Illinois, Urbana IL, United States of America
[171] Instituto de Fisica Corpuscular (IFIC) and Departamento de Fisica Atomica, Molecular y Nuclear and Departamento de Ingeniería Electrónica and Instituto de Microelectrónica de Barcelona (IMB-CNM), University of Valencia and CSIC, Valencia, Spain
[172] Department of Physics, University of British Columbia, Vancouver BC, Canada
[173] Department of Physics and Astronomy, University of Victoria, Victoria BC, Canada

[174] Department of Physics, University of Warwick, Coventry, United Kingdom
[175] Waseda University, Tokyo, Japan
[176] Department of Particle Physics, The Weizmann Institute of Science, Rehovot, Israel
[177] Department of Physics, University of Wisconsin, Madison WI, United States of America
[178] Fakultät für Physik und Astronomie, Julius-Maximilians-Universität, Würzburg, Germany
[179] Fakultät für Mathematik und Naturwissenschaften, Fachgruppe Physik, Bergische Universität Wuppertal, Wuppertal, Germany
[180] Department of Physics, Yale University, New Haven CT, United States of America
[181] Yerevan Physics Institute, Yerevan, Armenia
[182] Centre de Calcul de l'Institut National de Physique Nucléaire et de Physique des Particules (IN2P3), Villeurbanne, France
[a] Also at Department of Physics, King's College London, London, United Kingdom
[b] Also at Institute of Physics, Azerbaijan Academy of Sciences, Baku, Azerbaijan
[c] Also at Novosibirsk State University, Novosibirsk, Russia
[d] Also at TRIUMF, Vancouver BC, Canada
[e] Also at Department of Physics & Astronomy, University of Louisville, Louisville, KY, United States of America
[f] Also at Physics Department, An-Najah National University, Nablus, Palestine
[g] Also at Department of Physics, California State University, Fresno CA, United States of America
[h] Also at Department of Physics, University of Fribourg, Fribourg, Switzerland
[i] Also at Departament de Fisica de la Universitat Autonoma de Barcelona, Barcelona, Spain
[j] Also at Departamento de Fisica e Astronomia, Faculdade de Ciencias, Universidade do Porto, Portugal
[k] Also at Tomsk State University, Tomsk, Russia, Russia
[l] Also at Universita di Napoli Parthenope, Napoli, Italy
[m] Also at Institute of Particle Physics (IPP), Canada
[n] Also at National Institute of Physics and Nuclear Engineering, Bucharest, Romania
[o] Also at Department of Physics, St. Petersburg State Polytechnical University, St. Petersburg, Russia
[p] Also at Department of Physics, The University of Michigan, Ann Arbor MI, United States of America
[q] Also at Centre for High Performance Computing, CSIR Campus, Rosebank, Cape Town, South Africa
[r] Also at Louisiana Tech University, Ruston LA, United States of America
[s] Also at Institucio Catalana de Recerca i Estudis Avancats, ICREA, Barcelona, Spain
[t] Also at Graduate School of Science, Osaka University, Osaka, Japan
[u] Also at Department of Physics, National Tsing Hua University, Taiwan
[v] Also at Institute for Mathematics, Astrophysics and Particle Physics, Radboud University Nijmegen/Nikhef, Nijmegen, Netherlands
[w] Also at Department of Physics, The University of Texas at Austin, Austin TX, United States of America
[x] Also at CERN, Geneva, Switzerland
[y] Also at Georgian Technical University (GTU),Tbilisi, Georgia
[z] Also at Ochadai Academic Production, Ochanomizu University, Tokyo, Japan
[aa] Also at Manhattan College, New York NY, United States of America
[ab] Also at Academia Sinica Grid Computing, Institute of Physics, Academia Sinica, Taipei, Taiwan
[ac] Also at School of Physics, Shandong University, Shandong, China
[ad] Also at Department of Physics, California State University, Sacramento CA, United States of America
[ae] Also at Moscow Institute of Physics and Technology State University, Dolgoprudny, Russia
[af] Also at Section de Physique, Université de Genève, Geneva, Switzerland
[ag] Also at Eotvos Lorand University, Budapest, Hungary

[ah] Also at Departments of Physics & Astronomy and Chemistry, Stony Brook University, Stony Brook NY, United States of America
[ai] Also at International School for Advanced Studies (SISSA), Trieste, Italy
[aj] Also at Department of Physics and Astronomy, University of South Carolina, Columbia SC, United States of America
[ak] Also at Institut de Física d'Altes Energies (IFAE), The Barcelona Institute of Science and Technology, Barcelona, Spain
[al] Also at School of Physics and Engineering, Sun Yat-sen University, Guangzhou, China
[am] Also at Institute for Nuclear Research and Nuclear Energy (INRNE) of the Bulgarian Academy of Sciences, Sofia, Bulgaria
[an] Also at Faculty of Physics, M.V.Lomonosov Moscow State University, Moscow, Russia
[ao] Also at Institute of Physics, Academia Sinica, Taipei, Taiwan
[ap] Also at National Research Nuclear University MEPhI, Moscow, Russia
[aq] Also at Department of Physics, Stanford University, Stanford CA, United States of America
[ar] Also at Institute for Particle and Nuclear Physics, Wigner Research Centre for Physics, Budapest, Hungary
[as] Also at Flensburg University of Applied Sciences, Flensburg, Germany
[at] Also at University of Malaya, Department of Physics, Kuala Lumpur, Malaysia
[au] Also at CPPM, Aix-Marseille Université and CNRS/IN2P3, Marseille, France
[*] Deceased